BIO-INSPIRED CATECHOL CHEMISTRY FOR MATERIAL FUNCTIONALIZATION

LAM YIN TUNG

PhD

The Hong Kong Polytechnic University

2023

The Hong Kong Polytechnic University

School of Fashion and Textiles

Bio-inspired Catechol Chemistry for Material Functionalization

LAM Yin Tung

A Thesis Submitted in Partial Fulfilment of the Requirements for the Degree of Doctor of Philosophy

Dec 2022

CERTIFICATE OF ORIGINALITY

I hereby declare that this thesis is my own work and that, to the best of my knowledge and belief, it reproduces no material previously published or written, nor material that has been accepted for the award of any other degree or diploma, except where due acknowledgement has been made in the text.

_____(Signed)

LAM Yin Tung (Name of student)

In Memory of my caring mother

ABSTRACT

Sustainable approaches for material functionalization based on catechol chemistry are proposed. In this thesis, three studies related to catechol-based pigmentation, catechol-induced tunable surface charges for wastewater treatment and catechol-enhanced functional material for energy generation will be discussed. These studies have demonstrated the versatile functionalities of the catechol moiety and its potential for a wide range of applications.

For the study of catechol-based pigmentation, the heteromolecular pigmentations using naturally derived catechol and amino acids were developed for sustainable textile coloration through the inspiration of the strong adhesion feature of DOPA discovered in mussel adhesive proteins. A diverse range of colour could be generated via biomimicking pigmentation with different combinations of catechol and amino at room temperature. The pigmentation could be finely tuned to form various attractive coatings on textile materials. The findings showed that a gram of material could be dyed with milligrams of reactants, and the heteromolecular pigmentations could endow fabrics a wider colour gamut ranging from brown to blue. The catechol-amino acid pigments demonstrated good fastness properties, low toxicity, and highly reproducible colours on textile substrates. This catechol-based pigmentation can also be realized in a more environmentally friendly way with cold pad-batch method, which further minimizes both water and energy consumption. The results of the study open a novel sustainable direction for coloration of textile materials.

For the study of catechol-induced tunable surface charges, magnetic polydopamine (PDA) nanocomposites were prepared with a facile and sustainable synthetic method. The as-synthesized polymer-based hybrid composites inherited the intrinsic adhesiveness contributed by catechol and amino moieties of PDA as well as the magnetic property of Fe_3O_4. With the unique properties of PDA, the surface charges of Fe_3O_4@PDA could be easily tuned by pH for smart adsorption-desorption behaviors. Four commercially available dyestuffs including crystal violet, rhodamine B, direct blue 71 and orange G with different structures and surface charges in solution were selected to investigate the adsorption ability and universality of Fe_3O_4@PDA in wastewater treatment. It was found that the nanocomposites could successfully adsorb these cationic and anionic dyes under suitable pH conditions. This confirmed the ability of these nanoadsorbents for the removal of common textile dyes. The dispersed magnetic nanoadsorbents also demonstrated the ease of collection from dye mixtures, and the possibility in reusing them for several cycles. Selective dye separation was found to be achievable via simple charge control without large consumption of organic solvent and energy. These bio-inspired nanocomposite adsorbents have shown high potential in wastewater treatment and selective recovery of dye waste, especially for wastewater containing ionic dyes.

For the study of catechol-enhanced functional material, polylactic acid (PLA) film with catechol-coated zeolitic imidazolate framework-8 (ZIF-8) composite material was fabricated as a tribopositive layer for sustainable triboelectric energy application. Catechol coating served as an interfacial layer between the ZIF-8 filler and PLA polymer matrix, yielding a composite material in a more homogeneous state. It was found that the presence of catechol layer on fillers could endow the PLA composite film with enhanced electrical performance of the polymer materials, more uniform distribution of nanofillers, improved tensile property, and antibacterial effect. The catechol-enhanced film could effectively power electronic devices. The

effectiveness of catechols for the modulation of interfacial interaction between fillers and substrate was preliminary confirmed. This work gives an idea of employing interfacial coupling effect of catechols for the improvement of doping metal-organic framework nanoparticles into polymer matrix, facilitating the development of multifunctional dielectric materials for triboelectric applications.

LIST OF PUBLICATIONS

Related journal publications

1. **Y. Lam**, P. Yao, S. Fan, B. Fei, and J. H. Xin, "Catechol-enhanced interfacial modulation between ZIF-8 nanofillers and polymer for material performance enhancement in energy application" (In preparation)

2. **Y. Lam**, S. Fan, L. He, Y. Ho, B. Fei, and J. H. Xin, "Charge-controllable mussel-inspired magnetic nanocomposites for selective dye adsorption and separation," *Chemosphere (Oxford)*, vol. 300, pp. 134404–134404, 2022, doi: 10.1016/j.chemosphere.2022.134404.

3. **Y. Lam**, S. Fan, Y. Chae, L. Wong, L. He, Y. Ho, B. Fei, and J. H. Xin, "Heteromolecular pigmentations of plant-derived catechol and their application on textiles," *Journal of cleaner production*, vol. 332, p. 130010–, 2022, doi: 10.1016/j.jclepro.2021.130010.

4. **Y. Lam**, Y. Ho, L. He, X. Wang, and J. H. Xin, "Laccase-catalyzed biomimetic colouration of wool fabrics with phenols," *AATCC Journal of Research*, vol. 6, no. 3, pp. 41-44, 2019.

Other journal publications

1. J. Xu, **Y. Lam,** H. Liu, J. Luo, B. Tawiah, G. Liu and H. Jia., "Highly stable and low-temperature-tolerant zinc ion storage enabled by carbitol electrolyte additive engineering," *Journal of colloid and interface science*, vol. 631, pp. 17–24, 2023, doi: 10.1016/j.jcis.2022.10.127.

2. S. Fan, **Y. Lam**, J. Yang, X. Bian, and J. H. Xin, "Development of photochromic poly(azobenzene)/PVDF fibers by wet spinning for intelligent textile engineering," *Surfaces and interfaces*, vol. 34, 2022, doi: 10.1016/j.surfin.2022.102383.

3. H. Jia†, K. Liu†, **Y. Lam**†, B. Tawiah, J. H. Xin, W. Nie, and S. X. Jiang, "Fiber-Based Materials for Aqueous Zinc Ion Batteries," *Advanced Fiber Materials*, 1-23, 2022, doi: 10.1007/s42765-022-00215-x. († equal contribution)

4. S. Fan, **Y. Lam**, L. He, and J. H. Xin, "Synthesis and photochromism of catechol-containing symmetrical azobenzene compounds," *Royal Society open science*, vol. 9, no. 6, pp. 211894–211894, 2022, doi: 10.1098/rsos.211894.

5. Y. Xiao, B. Xu, Q. Bao and **Y. Lam**, "Wearable Triboelectric Nanogenerators Based on Polyamide Composites Doped with 2D Graphitic Carbon Nitride," *Polymers*, vol. 14, no. 3029, p. 3029–, 2022, doi: 10.3390/polym14153029.

6. S. Fan, **Y. Lam**, L. He, and J. H. Xin, "Novel and Sustainable Colorants Developed via Incorporating Azo Chromophores into Dopamine Molecules," *ACS omega*, vol. 7, no. 13, pp. 11082–11091, 2022, doi: 10.1021/acsomega.1c07084.

Conferences

1. **Y. Lam**, S. Fan and J. H. Xin, "Heteromolecular pigmentations of plant-derived catechol with amino acids for textile coloration" in Future Textiles, University of the West of England Bristol, Bristol, United Kingdom, 2023.

2. **Y. Lam**, S. Fan and J. H. Xin, "Catechol-based UV shield for photochromic electrospun materials," in Asian Textile Conference 16, Japan (Online), 2022.

3. **Y. Lam**, L. He and J. H. Xin, "Bionic coloration with plant-derived phenols" in Asia and Africa Sci. Platform Progr., The Hong Kong Polytechnic University, Hong Kong SAR, China, 2019.

ACKNOWLEDGEMENTS

First and foremost, I would like to express my sincere gratitude to The Hong Kong Polytechnic University and School of Fashion & Textiles for granting me the financial support. I particularly would like to extend my courtesy to Prof John H. Xin and Dr Bin Fei, who have given me this valuable opportunity to pursue my academic journey and offered a flexible work environment for me to explore various research areas. I would also like to acknowledge the financial assistance from the National Natural Science Foundation of China (Grant No. 21776235, No. 21376197).

More importantly, I would like to convey my deepest gratitude and apology to my family which unconditionally takes great care of me, especially my late mother Manyee Mandy Chow. She suffered twice from terminal cancer and bravely strove her best to adapt to the substantial changes in life. Nevertheless, she gave it her all for the sake of staying with me as long as she could. Even with all the pain and desperation, she still constantly encouraged me to accomplish anything that I wanted to and gave me unlimited courage to go on until her final moment. Despite the fact that I feel deep remorse for past wrongs and truly wish I could make amends, I am relieved that she can now rest peacefully in another dimension as she hoped.

In addition, I would take this opportunity to show my appreciation to all my friends and colleagues, particularly Miss Suju Fan, Dr Chang Liu, Dr Yidi Wang, Miss Simmy Chan, Miss Yuanyuan Zhao, Dr Alan Tang, Miss Xueyan Biao, Miss Jing Yang, Dr Pengpeng Yao, Mr Xia Gang, Dr Hao Jia, Dr Kaikai Ma, Dr Zhihua Li, Dr Su Yang, Dr Ziqi Li, Dr Shuping Lin, Dr Tian Xiao, Mr Heng Luo, Miss Linlin Ma, Mr Anson Chan, Miss Yanki Ho, Dr Liang He,

Miss Kalina Lui, and all the other colleagues from Prof John H. Xin's and Dr Bin Fei's group. They have accompanied and supported me through the hardships encountered during the time of my research journey, existential crisis, pandemic, and social unrest. I am also grateful to all the scientific officers and technicians including Dr Siukwong Patrick Pang, Dr Chenghao Lee, Dr Hardy Lui, Miss Pendy Ho, Mr Kwanon Choi, Miss Rise Choi, and the colleagues from Prof Xiaoming Tao's and Dr Tao Hua's group for their technical support. Besides, I express my greatest thank you to all the counselors and medical consultants, particularly Dr Sumyin Ruth Wong, Dr Chunyu Wu, Dr Yeeki Yiu, Miss Amy Sze, Miss Heidi Tang and Miss Salina Chan, who have monitored my conditions and shared their insightful opinions with me. Furthermore, I deliver my thanks to all those who have once offered me any forms of kind assistance, genuine support, or even malicious criticism. I have really learnt so much from them all.

Finally, I would like to thank myself for not giving up until today, even though I struggle a lot with all that happened and find that this study becomes nearly meaningless to me. This work is dedicated to my brave mother and all those who are enduring their own difficulties.

TABLE OF CONTENTS

LIST OF FIGURES

LIST OF TABLES

ABBREVIATIONS

Ala	Alanine
Arg	Arginine
Asn	Asparagine
Asp	Aspartic acid
BET	Brunauer-Emmett-Teller
CA	Caffeic acid
CV	Crystal violet
Cys	Cysteine
DA	Dopamine
DB	Direct blue 71
DMF	N,N-dimethylformamide
DSC	Differential scanning calorimetry
EDX	Energy-dispersive X-ray spectroscopy
FESEM	Field Emission Scanning Electron Microscope
FTIR	Fourier transform infrared
Gln	Glutamine
Glu	Glutamic acid
Gly	Glycine
His	Histidine
Hmim	2-methylimidazole
Ile	Isoleucine

K/S	Kubelka-Munk
L-DOPA	3,4-dihydroxyphenylalanine
Leu	Leucine
Lys	Lysine
Met	Methionine
MOF	Metal-organic framework
OG	Orange G
PDA	Polydopamine
PDMS	Polydimethylsiloxane
Phe	Phenylalanine
PLA	Polylactic acid
Pro	Proline
RhB	Rhodamine B
SEM	Scanning electron microscopy
Ser	Serine
STEM	Scanning transmission electron microscope
TEM	Transmission electron microscopy
TENG	Triboelectric nanogenerator
TGA	Thermogravimetric analysis
Thr	Threonine
Tris	Tris (hydroxymethyl) aminomethane
Trp	Trytophan
Tyr	Tyrosine
UV-Vis	Ultraviolet-visible
Val	Valine

XRD	X-ray diffraction
ZIF-8	Zeolitic imidazolate framework-8

1 INTRODUCTION

1.1 Research Background

Bio-inspiration has become one of the key innovative ideas for the future technology and advanced material development. Enlightened by the fascinating phenomena found in wide nature, many researchers from various fields have started investigating the capabilities of catechol chemistry and its integration in multidisciplinary applications. It is worth noting that marine organisms like mussels and barnacles have been highlighted as a potential candidate for diverse material functionalization in recent studies. They are well known for their secretion of liquid adhesive proteins for the purposes of firm attachment on substrates under changing tidal conditions. The solidification of liquid secretion results in the formation of waterproof adhesive plaque which has a strong adhesion on various materials [1]. It is widely believed that the adhesion mechanism of mussel adhesive proteins is attributed to the presence of large quantities of 3,4-dihydroxyphenylalanine (L-DOPA) displaying adsorptive or cohesive features [2]. The adhesiveness is closely related to the oxidative formation of moisture-resistant quinone and the intermolecular cross-linking of catecholic contents mainly via aryl-aryl coupling and Michael-type addition [3, 4]. In addition, other physical and chemical interactions like hydrogen bonding, ionic bonding, covalent bonding, coordination and π–π interaction contribute to the persistent adsorption and attachment [5]. Apart from this remarkable adhesiveness, the proteins possess other versatile functionalities, and they can demonstrate their ability well even in wet conditions [6]. The presence of abundant functional moieties in catechol-based structures endows themselves with promising chemical modifiability. A

considerable number of catechol derivatives, especially dopamine (DA), resembled the structure of L-DOPA catechol and ethylamino groups. Similarly, their polymerized forms generally have the ability to serve as an adhesive layer, provide a versatile platform for subsequent surface-mediated reactions and impart their inherent properties to materials [7, 8]. Catechol derivations including naturally occurring catecholamines and plant-derived o-diphenolic compounds can generally self-polymerize under mild conditions to form coloured bio-adhesive layers with potential multifunctionalities onto or into substrates, having great prospective in high-level functionalization and integration. Hence, polycatechols can be employed as a key component in fabricating multidisciplinary or interdisciplinary materials for applications such as biomedical engineering (antifouling coating, tissue engineering, drug delivery, phototherapy), energy generation and storage, filtration and separation, catalytic degradation and textiles [9-11]. It is worth noting that novel functional materials based on the inspiration of polycatechols continues to emerge.

Textile materials are essential materials in everyday life, varying from garments to infrastructure components. These take up a large proportion of global resource consumption, and the textile wet processing involved is known to be a major contributor to water and air pollution in the entire textile production. The severe pollution caused has posed risks to environment, wildlife, and also humans. The consequences arose from the textile production activities have driven the development in sustainable production. The integration of green chemistry into textile technology has already been proposed. The main ideas of green chemistry are to lessen the use of hazardous materials and organic solvents, enhance the efficiency of chemical synthesis and modification reactions, minimize toxic waste production, adopt mild reaction conditions, and reduce energy consumption [12, 13]. Textile coloration has been brought to the fore as a severe water pollution contributor, much effort has thus been devoted

by numerous textile scientists for the development of more sustainable processes like novel dyeing methods and substrate material modification. To diminish the negative impact of synthetic colorants and dyeing auxiliaries, natural-occurring colorants and the extraction of natural components for green synthesis of colorants may be adopted instead [14]. However, inferior affinity of natural colorants to substrates and limited colour range are some of the main obstacles, preventing them from being widely employed. The bio-inspiration opens a novel way to develop sustainable textile processing methods. Catechol-based pigmentation has potential to be employed as a more environmentally benign substitution for conventional coloration.

In addition to sustainable coloration methods, advanced wastewater treatment is another aspect being given emphasis to. The efficiency and universality of wastewater treatment methods for various unused colorants in textile effluents are highlighted with the intention to simplify the subsequent handling process and utilize the reusable resources. Nanotechnology provides diverse routes for the exploration of highly efficient and specific adsorbents for easy physical separation of dyestuffs from wastewater. The recyclability of natural-based adsorbent, the reusability of the collected colorants, and environmental impacts of the separation methods are worth being explored. In virtue of bio-inspiration techniques, the performance of sustainable wastewater treatment can possibly be enhanced with the use of catechol-coated nanocomposites. The tuneable surface charges of catechol-based coating are highlighted as it can endow the adsorbents with higher specificity, promoting selective adsorption of components in mixture.

With the gaining attention of smart materials in multidisciplinary fields, their advancement has been extended to textile context. Smart materials have shown opportunities in future innovation

for various daily necessities, especially in wearable applications. In the light of global energy crisis, scientists have been conducting substantial research studies in the exploration of sustainable energy sources. Some smart materials have specific responses to mechanical stimuli, which allow them to convert mechanical motions into electrical energy for powering electronic devices or sensors. Among different mechanical energy harvesters, triboelectric energy has been highlighted to be one of the most prosperous alternatives to non-renewable energy sources. Wang has proposed the development trend of energy research, and his group has spotlighted the variety of triboelectric-based harvesters especially triboelectric nanogenerator (TENG) on wearable electronics. These novel harvesters provide a way to utilize the wasted mechanical energy generated during the daily activities and wave energy from the oceans. It is well noted that TENGs offer relatively higher output power, abundant choices of material combinations, sustainable and simple fabrication process, and flexibility to be integrated in various working modes for specialized applications [15].

The development of high-performance and multifunctional triboelectric materials is likely to involve chemical doping, but the addition of dopants generally induces some undesirable drawbacks on the properties of host materials. To address these imminent problems, the catechol derivatives may be introduced to buffer the adverse effects arising from interfacial incompatibility. Intrinsic properties of catechol derivatives can be a latent dopant for functionalization of polymeric host materials. It can also serve as a remarkable interfacial layer for bridging the foreign rigid fillers and the polymer matrix. This interfacial buffer between two distinct materials increases the degree of compatibility of foreign fillers in the host substrate material of different chemical nature, benefitting the energy generation processes and enhancing other functional performances. Therefore, catechols can be investigated for their capabilities in improving the energy-generating materials for combating global energy crisis.

Catechol derivatives are an ideal candidate for the development of multifunctional applications in interdisciplinary fields. This is because they are flexible to be fabricated into diverse morphologies for achieving multiple functionalities, and they have shown high compatibility with different types of materials as well as structures for seamless integration. This integration between materials with distinct properties favourably shows synergistic effect and improves applicability, benefiting the fabrication of advanced composite materials. Catechol materials and responsive materials are the candidates to be integrated for producing smart functional materials. Many studies have elucidated that catechol contents can endow host materials new functionalities with their intrinsic properties, yet they can retain or promote the existing properties of the host. This is an intriguing area to be explored across different scientific fields.

1.2 Research Objectives

This study attempts to tackle some of the current challenges encountered in textile coloration, wastewater treatment and energy material based upon the bio-inspired catechol chemistry. Catechol derivatives are investigated as an active component to functionalize different materials to achieve corresponding purposes. Specifically, the objectives are stated as follows:

1. To develop a catechol-based pigmentation method for sustainable coloration of textile materials.
2. To synthesize a nanocomposite with catechol-induced tunable surface charges for selective adsorption in wastewater treatment.

3. To fabricate a catechol-enhanced composite dielectric material for energy-generating purpose.
4. To demonstrate the diverse functionalities of catechol derivatives in fabricating materials and their potentials to be integrated in multidisciplinary research.

1.3 Significance and Values

The studies have revealed that catechol derivatives can be utilized for natural pigmentation, selective adsorption via tunable surface charges and enhancement of energy material. It has demonstrated that catechol derivatives are capable of taking up the main or auxiliary role for sustainable material functionalization in multiple applications. The chemical tailorability of catechol derivatives also open a way for improvement and subsequent modification in future studies.

For the study of catechol-based pigmentation, the heteromolecular pigmentations of catechol and amino acids were investigated for sustainable textile coloration. Compared with other natural dyeing studies, a more diverse colour gamut with better performances could be attained via the proposed biomimicking pigmentation method. The colour formation of pigmentation could be finely tuned with different concentration and combinations of catechol and amino acid at room temperature. The textile materials coloured with these catechol-amino acid pigments have demonstrated to have good fastness properties, low toxicity, and highly reproducible colours on textile substrates. This catechol-based pigmentation have showed potential in the integration with other sustainable coloration techniques, widening the applications in textile coloration.

For the study of catechol-induced tunable surface charges, magnetic catechol-based nanoadsorbents were synthesized with polydopamine (PDA) and Fe_3O_4 via a simple method. The hybrid nanocomposites retained the adhesive property of PDA and magnetic feature of Fe_3O_4. Smart adsorption-desorption behaviors of this nanoadsorbents were predominantly contributed by the pH-tunable surface charges of PDA layers. Common textile cationic and anionic dyestuffs were found to be adsorbed by Fe_3O_4@PDA selectively and efficiently under appropriate pH conditions. Their magnetic properties have allowed them to be collected easily for subsequent reuse. The selectivity and universality of Fe_3O_4@PDA nanocomposites for different ionic dyestuffs has broadened their applicability in wastewater treatment.

For the study of catechol-enhanced functional material, PDA-coated zeolitic imidazolate framework-8 (ZIF-8) filler was prepared for doping polylactic acid (PLA) to form a composite dielectric layer for sustainable triboelectric energy application. It was found that PLA composite film with fillers having catechol-based interfacial layer displayed better electrical performance in triboelectric nanogenerator (TENG), more uniform distribution of nanofillers and improved tensile properties than that with pristine fillers. The synergistic effect of ZIF-8 and PDA also endowed the film with enhanced antibacterial effect. The interfacial coupling effect of catechols between filler ZIF-8 and polymer matrix PLA on the performances of the dielectric composite material in TENG was preliminarily confirmed. Catechols have shown prospect in facilitating the fabrication of multifunctional heterogenous materials by integrating two materials of different characteristics.

1.4 Outline of the Thesis

This thesis mainly consists of 7 chapters:

In Chapter 1, the overview of catechol chemistry and their potentials in advanced material functionalization in multiple areas is introduced. The objectives and significance of the research studies are briefly summarized.

In Chapter 2, the detailed research background of the catechol-related applications is illustrated and the position of catechol derivatives in multidisciplinary research is explored. The emerging technologies for advanced material functionalization used in sustainable textile coloration, wastewater treatment and energy material fabrication are particularly depicted.

In Chapter 3, the experimental design of each study and the general characterization of specimens involved is comprehensively presented.

In Chapter 4, the study of catechol-based pigmentation is elucidated. The effect of various parameters on the pigmentation of catechol derivatives with amino acids have been investigated, and their application and performances on textile materials are examined.

In Chapter 5, the study of catechol-induced tunable surface charges is elucidated. The as-synthesized magnetic catechol-based nanocomposites are carefully characterized and their adsorption behaviors towards different ionic dyestuffs is evaluated.

In Chapter 6, the study of catechol-enhanced functional material is elucidated. Catechol-coated metal-organic framework was synthesized for doping polymer to fabricate tribopositive material. The effect of catechol coating on the performances of the polymer composite film is assessed.

In Chapter 7, all the research findings are summarized, and the outlook of catechol-related applications is discussed.

2 LITERATURE REVIEW

2.1 Bio-Inspired Catechol Chemistry for Multifunctional Applications

2.1.1 Bio-inspiration

Nature has shown numerous fascinating biological, chemical and physical phenomena with perfectly optimized characteristics [16-18]. Nature does not only provide an abundant source of materials, but also enlightens us with the ideas of fabricating multifunctional materials from submicron units. Different from biomimicry which generally imitates the structures and phenomena from nature, bio-inspiration, on the other hand, takes the ideas from nature and expand them for predetermined purposes with the use of other technologies [19]. When facing the gap in advanced functional materials, material engineers start creating new materials and bio-inspiration can be an attractive approach for meeting the challenges. As shown in Figure 2.1, the bio-inspiration approach in material design begins with the analysis of required material functions, further breakdown of the requirements, and finally the identification and selection of appropriate materials and fabrication process [20]. With the vast inspiration from nature, the number of successful constructions of bio-inspired functional materials continues to increase. Besides, many of these natural phenomena have undergone after long evolution process, offering highly eco-benignant and efficient ideas that can be utilized for the sustainable development of materials and fabrication methods.

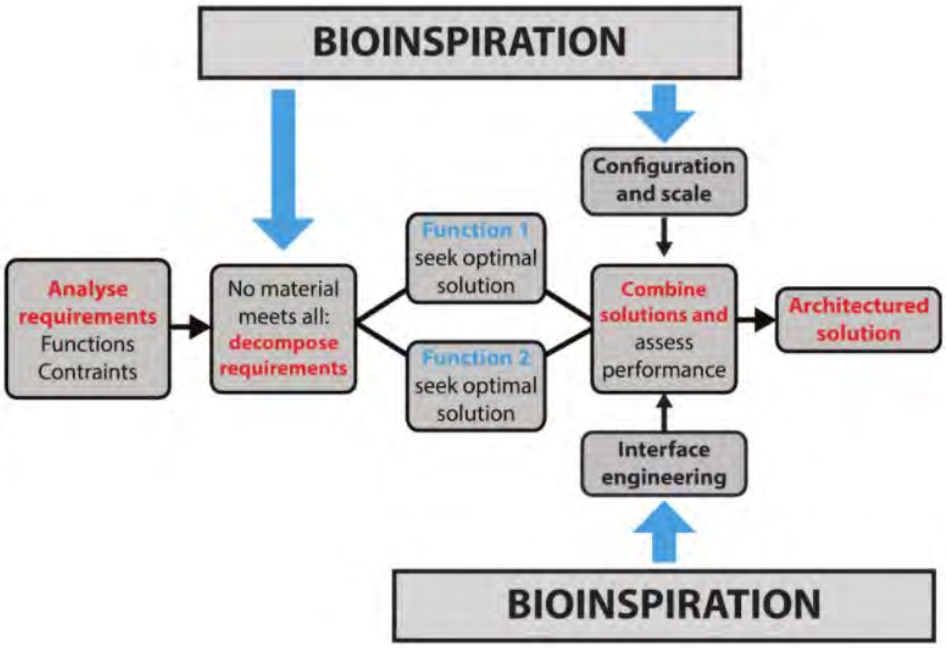

Figure 2.1 The approach of bio-inspiration in material design [7]

2.1.2 Catechol and phenolic chemistry

Abundant sources of catechols and phenolic compounds can be found in numerous natural organisms from bacteria, plants to animals [21]. These types of compounds demonstrate powerful capacities to attain various physiologies and other adaptative functionalities [22]. These catechols and phenolic compounds possess diverse intrinsic reactivities and properties including polymerization, hydrogen bonding, redox potential differences, radical scavenging activity, antioxidant activity, pH sensitivity, and light absorptivity [23, 24].

Bio-inspired adhesives and coatings found in many marine organisms have currently received much interest for their wet adhesion among the scientific community. Mussels and barnacles are the representative examples that can demonstrate the fascinating adhesive mechanism in the nature [25, 26]. Both mussel adhesive proteins and barnacle adhesive proteins contributes

to their intriguing adhesion on the surface of various substrates, and these proteins mainly consist of 3,4-dihydroxyphenyl-L-alanine (L-DOPA) [27]. Dopamine (DA) can be an analogue to L-DOPA as it likewise contains both catechol and amino group in the structure [8, 28]. DA can demonstrate the ability to self-polymerize to form coating or film that can adhere on both organic and inorganic substrates. The presence of these polycatechol materials can add functional values to the substrates or even serve as an interfacial modifier between different materials with distinct characteristics. The recent growth of research study on catechols are ascribed to their versatile adsorption capacities, excellent stability, and intrinsic functionalities like bioactivity, pH sensitivity and light absorptivity [8, 29].

Polydopamine (PDA), as a commonly found catechol, has been extensively studied in a variety of research areas. The formation, modification, features and applications of this typical polycatcholamine are comprehensively summarized in Figure 2.2 [9]. DA and its derivatives can simply undergo self-assembly under suitable pH, light, thermal or oxidative conditions to form polycatechols. They may also be modified chemically or physically to facilitate their incorporation in the other substrates and functional materials. Diverse morphologies existing in polycatechols in conjunction with their versatile properties give the possibility to their employment in sensing, electrical conducting, separating, catalytic, and medical applications [30-34].

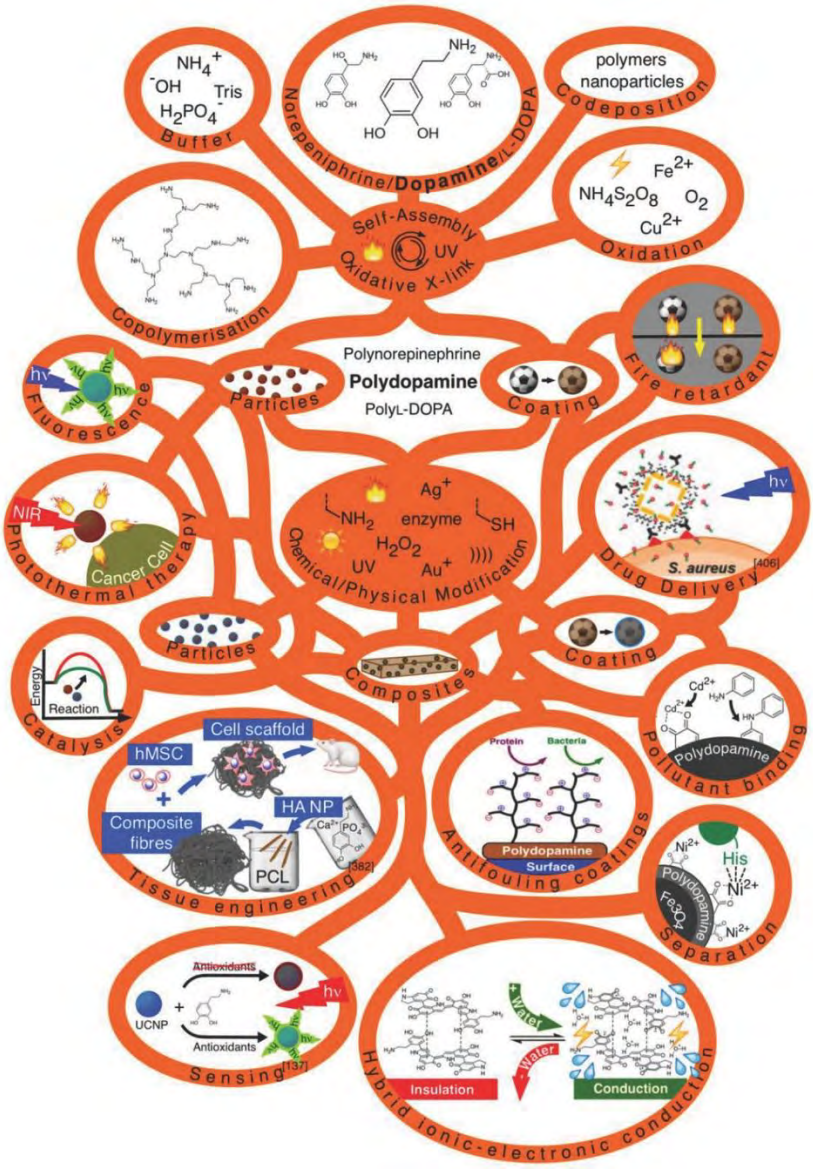

Figure 2.2 A general overview of the formation, features, modification and applications of polycatcholamine [9]

2.1.2.1 Mechanisms and properties

Catechol structure bears a phenyl ring and two hydroxyl groups in ortho position. It is an amphiphilic moiety with both hydrophobic and hydrophilic characters, originating from its non-polar aromatic and polar hydroxyl components. The diversity of interactive paths of

phenolic functional group (Figure 2.3) especially enhances the reactivities of catechol moieties with other materials.

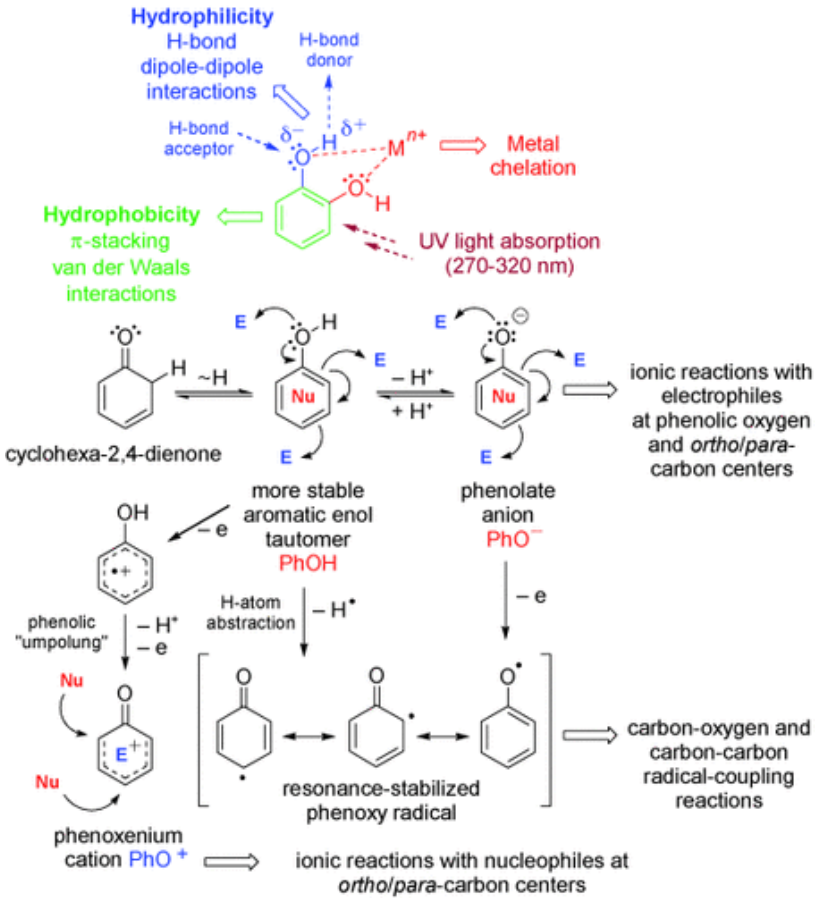

Figure 2.3 Scheme in reactivities and properties of phenolic functional group [21]

Catechol moieties basically can have three oxidation states including catechol (reduced form), semiquinone (semi-oxidized form) and quinone (oxidized form), as shown in Figure 2.4. Catechol moieties are susceptible to undergo oxidation with the presence of oxygen, oxidants or under alkaline conditions. Quinones are a highly electrophilic species, therefore having relatively high reactivity with nucleophiles like amino or thiol moieties. Hence, catechols have great potential to react via inter- or intramolecular interactions. It is important to be noted that four main catechol-surface interactions, namely hydrogen bonding, π–π stacking, coordination,

and covalent bonding with nucleophiles through Michael-type addition, have been deduced through a considerable number of investigations [7, 35].

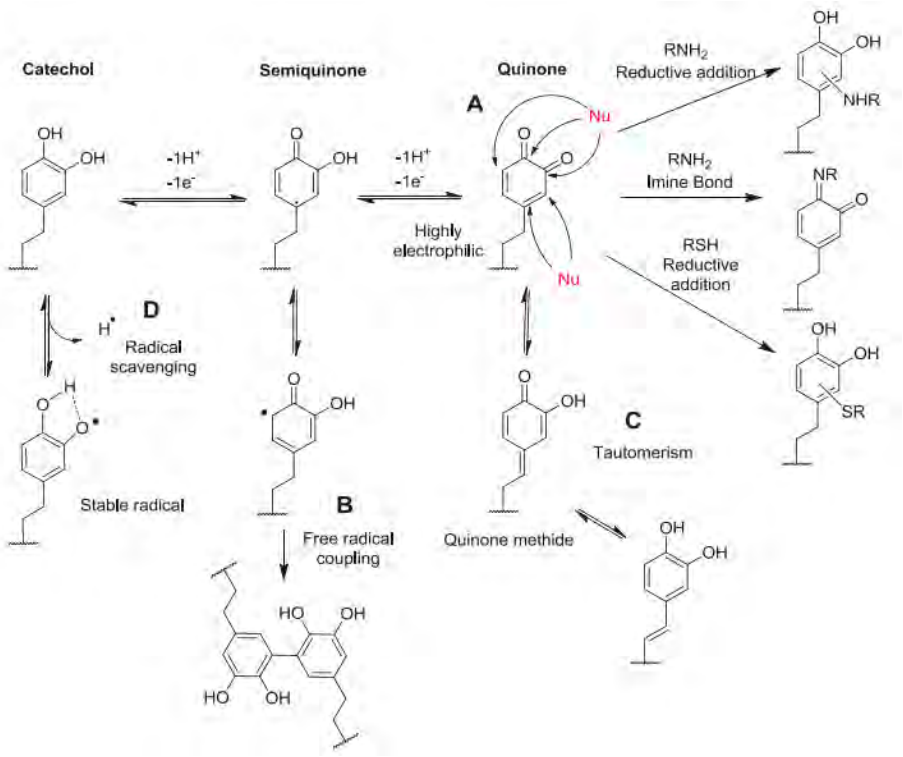

Figure 2.4 Scheme in possible reactions of catechol moieties [35]

The conjugated double bonds and nitrogen atoms in the polycatechols contribute to the visible light region absorption, resulting in the fascinating colours observed. In addition to visible light absorption, the presence of hydroxyl groups and other electron-withdrawing groups like carbonyl and ester on the aromatic ring promotes the shift of absorption maximum to a wider UV region, endowing them with UV protection properties [36, 37]. Radical scavenging property is another attractive feature of polycatechols. The radical scavenging mechanism involves the dissipation of radiation energy preventing the formation of free radicals and the quenching of reactive radical species, based on Compton scattering and electron delocalization within the microstructures [38, 39]. Some studies have already shown that catechol groups resemble the catalytical site of enzyme or nanomaterials in specific reactions [40, 41].

For the highlighted adhesive properties, DA can be selected for exemplifying the self-polymerization of catechol moieties involved in the adhesive formation process. In fact, the structural formation of PDA is known to be resulted from a series of complicated reactions, and therefore, it is unlikely to establish a single mechanism to explain all the reactions and interactions involved [42]. From the illustration in Figure 2.5, it is suggested that dopamine hydrochloric is reacted in aqueous medium under oxidative conditions to form resultant polymers, consisting of intra- and interchain hydrogen bonding, π-stacking and charge transfer [43]. These reactions contribute to the anchoring of PDA on the material surfaces. On top of adhesiveness, the electrical properties of conductive materials can also be enhanced through the incorporation of catechols. This is because adhesive catechols can adhere the conductive components closely together for a denser package. In addition, catechols may act as a dopant and provides more charges on the materials for electrical conduction [44].

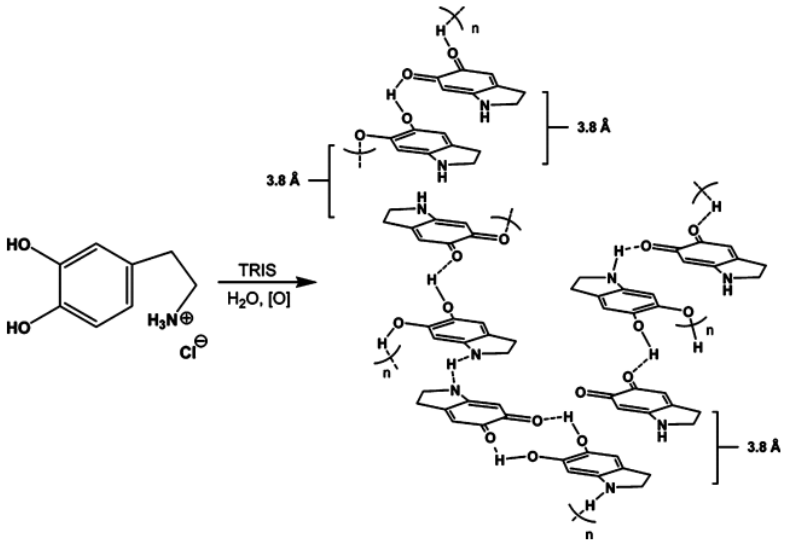

Figure 2.5 Proposed structure of PDA synthesized in tris buffer [43]

2.1.2.2 Applications

Catechols possess versatile reactivities for intra and intermolecular interactions, which allows them to act as a promising main or auxiliary component in material functionalization. Catechol chemistry promotes the formation of diverse structures, the introduction of unique physicochemical properties and the tunability of functions in materials for a broad scope of advanced applications including UV light absorber, medical usages, and energy [45].

UV light absorber

The intrinsic structure of naturally occurring catechol moieties facilitates the light absorption. For instance, plant-derived phenols like caffeic acid (CA), ferulic acid and gallic acid are natural UV absorbers that can be used as photo-stabilization [46]. Similarly, animals have natural protection mechanism like melanin pigments for shielding UV irradiation [47]. PDA can mimic the behaviors of natural melananosomes, and they are known to be non-phototoxic and non-irritating. Hence, the applications of catechols in the sustainable development of radiation protection materials are promising [48].

Medical usages

Catechols have been regarded as a safe and compatible material for biomedical applications such as antimicrobial treatment, bioimaging, drug delivery, smart hydrogels and photothermal therapy. Polycatechols, especially PDA, have been highlighted to be a latent medical material [49]. They may exhibit antimicrobial activities based on contact-active antibacterial effect, photothermal conversion and reactive oxygen species [50-52]. These mechanisms can interfere

the physiological properties of bacteria by destroying the bacterial cell wall and cell membrane. The antimicrobial behaviors of materials can be enhanced with the incorporation of catechols, gaining the synergistic effect. The chemical structure of catechols is also highly tailorable for antimicrobial modification. In addition, they can be used as injectable and implantable materials since most of the polycatechols are natural antioxidants, easy to manipulate, and have similar viscoelasticity as extracellular matrices, which reduce the risk of tissue irritation [53, 54]. Furthermore, PDA nanomaterials can be employed in photothermal therapy to transform near-infrared energy into heat for killing cancer cells in selective region [55].

Energy

PDA exhibits reactive redox activities and excellent adhesive properties, thus it is suitable to produce energy materials. The catechol chemistry promotes the advanced development of electrochemical energy storage devices like organic electrodes [56]. The versatility and flexibility of catechols enable themselves to synergistically incorporate with other conductive materials to fabricate potential biomass-based supercapacitors [57]. The abundant charged components on polycatecholamines also enable their hybrid electronic-ionic conductivity.

Other applications

Catechol-containing molecules can also be employed for the functionalization of metal-organic framework (MOF) based on metal-phenolic coordination chemistry [58]. Phenolic compounds may act as organic ligand building units for the formation of crystalline structures. Besides, polycatechols may be integrated into MOF as a polymer guest via post-synthetic modification. For instance, PDA serves to preserve the porosity of the internal structure (Figure 2.6) and also

provides a platform for the adhesion of other functional molecules on the structure [59, 60]. Furthermore, the polymerization of catechols on the surface of MOF templates allows the fabrication of organic nanoparticles with defined nanostructures.

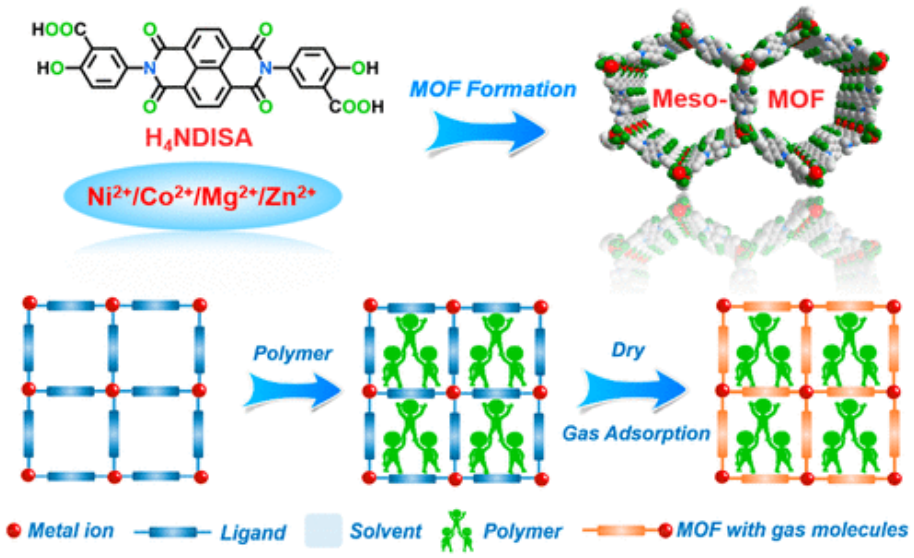

Figure 2.6 PDA as a polymer guest to support the porous structure of MOF [59]

2.2 Sustainable Developments

Sustainability can be referred to the scientific vision beneath implementing the measures in relation to the conservation of energy and environment [61]. Sustainable development has become an important research topic in different disciplines due to the overexploitation of resources and environmental degradation. Climate change, destruction of natural habitats and extinction of various species have given a warning signal to humans about the negative impacts of continuous large-scale industrial activities. To possibly alleviate or mitigate the current situation, scientists have been paying much attention to sustainability-oriented innovation including concepts and technologies. The number of terms related to sustainability continues

to grow, indicating the rapid development in this area. According to the classification shown in Figure 2.7, those terms can be categorized into different levels including principles, approaches, sub-systems, sustainable systems or sustainability policy with the dimension of ecology, economy, or society [62]. Among these sustainability terms, green chemistry is one of the most widely adopted approach in promoting the sustainability of industrial activities.

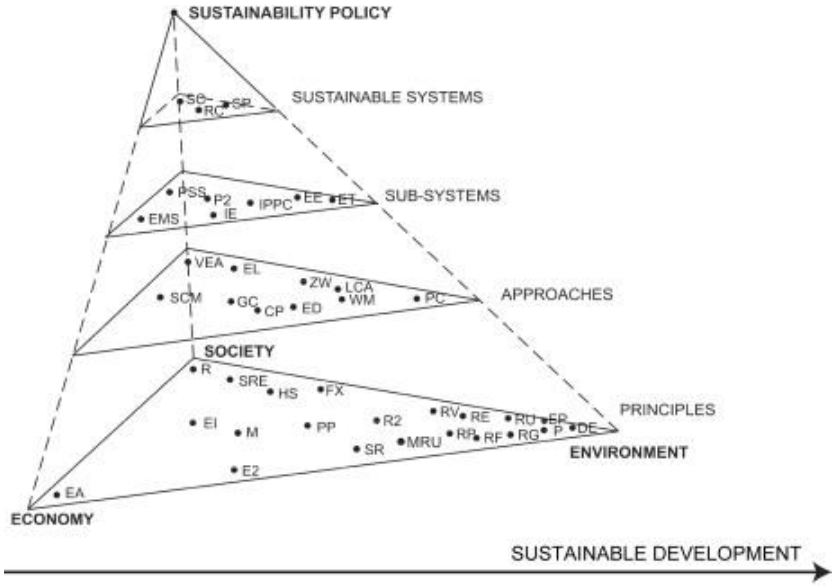

CP, cleaner production; DE, degradation; EA, environmental accounting; ED, eco-design; EE, environmental engineering; EI, ethical investment; EL, environmental legalisation; EMS, environmental management strategy; ET, environmental technology; E2, eco-efficiency; FX, factor *X*; GC, green chemistry; HS, health and safety; IE, industrial ecology; IPPC, integrated pollution prevention and control; LCA, life cycle assessment; M, mutualism; MRU, minimization of resource usage; P, purification; PC, pollution control; PO, policy; PP, "polluter pays" principle; PSS, product service system; P2, pollution prevention; RC, responsible care; R, reporting to the stakeholders; RE, recycling; RF, remanufacturing; RG, regeneration; RP, repair; RU, reuse; RV, recovery; R2, renewable resources; SC, sustainable consumption; SCM, supply chain management; SD, sustainable development; SP, sustainable production; SR, source reduction; SRE, social responsibility; VEA, voluntary environmental agreement; WM, waste minimization; and ZW, zero waste.

Figure 2.7 Terminologies of sustainability classified into different levels including principles, approaches, sub-systems, sustainable systems or sustainability policy with the dimension of ecology, economy, or society [62]

2.2.1 Green chemistry

The adoption of green chemistry in material development has been contributing to the future of sustainability. It emphasizes on the principles like eliminating hazardous materials and organic solvents, enhancing reaction efficiency, minimizing toxic waste production, and mild reaction conditions with lower temperature and pressure [12, 13]. Biomimetics is an attractive approach to achieve green chemistry development since nature demonstrates numerous fascinating biological phenomena with perfectly optimized characteristics [16-18]. These phenomena are highly eco-benignant after long evolution process, which can be utilized for the development of green technologies.

Scientists have proposed the concept of green chemistry for years, of which utilization of raw materials, elimination of the use of hazardous chemicals and reduction of waste generation are the key essences [63]. The 12 guiding concepts of Green Chemistry was proposed by Anastas and colleagues, as listed in Table 2.1 [64, 65]. The ultimate goal of green chemistry is to strike a balance between economic growth and environmental protection for sustainability. It is crucial to note that the first principle indicates the importance of 'prevention is better than cure'. In conjunction with the increasing public awareness of eco and health safety, greater number of environmentally friendly technologies and products are eagerly pursued in different fields for attaining sustainable development and pollution prevention in industrial activities. The strategies in addressing the current demands have started showing the characteristics of material, water and energy conservation [12, 13].

Designing less hazardous chemical synthesis method is another key green approach in industrial chemical synthetic process. This aims at creating less toxic and harmful substances

in order to minimize the negative impacts on the environment and human health. The practical solutions are to reduce the use of toxic reagents as raw materials, lessen the reaction stages and avoid the production of contaminants [66]. However, the practical feasibility of the concepts is the largest obstacle encountered in the study of practical green chemistry. In most cases, we lack comprehensive information and experience to develop sophisticated synthetic methods for promising yields and products with similar functionalities. Hence, more comprehensive investigation into this aspect is highly demanded.

Table 2.1 Twelves principles of green chemistry [64, 65]

Code	Principle of Green Chemistry
G1	Prevent waste
G2	Atom economy
G3	Less hazardous materials
G4	Design benign chemicals
G5	Safer solvents and auxiliaries
G6	Design for energy efficiency
G7	Use of renewable feedstocks
G8	Reduce derivatives
G9	Catalysis
G10	Design for degradation
G11	Real-time analysis for Pollution Prevention
G12	Inherently safer chemistry for accident prevention

2.2.2 Biomaterials

The concept of “from cradle to cradle” in product life cycle has widely been studied and emphasized in the modern development of material manufacturing. Therefore, environmentally benign materials have raised much attention from the manufactures of textiles, electronics and packaging. Among these materials, bio-based polymers are more extensively used since they are generally produced with renewable, non-toxic and biodegradable resources. Bio-based polymers are generally categorized into three distinct groups based on their raw material sources (polypeptides, polysaccharides and microorganisms) and production methods [67]. Naturally occurring biopolymers are more preferable to synthetic biopolymers, nevertheless, synthetic biomaterials are also gaining attention with their versatility. They often have higher possibility in synthetic modification, which can be a potential way for tailor-made functional purposes. Among these polymers, polylactic acid (PLA) is a highlighted biodegradable and biocompatible polymer that can be widely and safely used in multidisciplinary fields. Furthermore, the reinforcement or functionalization of these bio-based materials can be achieved easily with the introduction of natural fillers or additives containing catechol moiety. The emerging trend of biocomposites encourages the use of both green substrates and functional modifiers.

2.2.3 Textile coloration

The world production of textile fibres has been increasing with the growing demand in recent decades. The fibre production process is always accompanied with wet processing activities. Among different textile wet processing, dyeing of textile materials is one of the greatest

contributors to environmental pollution, especially in air and water. In conventional exhaust dyeing, it is relatively difficult to attain high fixation rate since the utilization of synthetic dyes particularly depends on the nature of fibres, substantivity of corresponding dyes and types of coloration methods used [68]. Thus, textile colouration processes usually produce an enormous volume of effluent containing high amount of non-biodegradable dye compounds, dyeing auxiliaries, and other heavy metals. On a conservative estimate, about 1.6×10^6 tonnes of dyes are produced globally every year, and approximately 0.96 to 1.2×10^6 tonnes of dyeing auxiliaries are consumed worldwide annually solely for textile coloration [69, 70]. The dye effluents discharged mostly contains commercial azo and anthraquinone-based dyes, of which azo dyes may be degraded into carcinogenic amines causing environmental pollution and health issues to the residents living in the vicinity of the dyeing plants [71]. In addition, the suspended particles in dye wastewater block the sunlight affecting the photosynthesis of microorganisms, and the presence of heavy metals damages the aquatic lives [72]. To reduce the harmful composition in the effluents, approaches including physical, chemical or biological and electrochemical methods for pollutant removal are adopted [73]. No single dye removal technology can effectively purify the effluents containing varieties of synthetic chemicals. On top of all those solutions, reducing waste at source is in fact the most effective approach.

In recent times, the concept of green chemistry has been introduced to textile technology, and thus the gradual increment of more biodegradable and reactive dyes have been synthesized for effective coloration [14]. In addition, more novel coloration methods have been proposed for reducing the consumption of water and energy. Some textile engineers have suggested a recent classification of sustainable textile coloration processes based on materials or methods used. These include natural materials, surface modification, enzyme-assisted dyeing, low water immersion technique and other advanced technologies such as supercritical fluid, ultrasonic

and laser [74]. To lessen the adverse effect caused by synthetic colorants, more sustainable colorants produced via green production methods and natural colorants extracted through an environmentally friendly processes are employed as the alternatives to the conventional colorants. For instance, cashew nut shells liquid consist of sixteen types of phenolic compounds, and these natural compounds therefore provide a abundant source of raw materials for manufacturing sustainable colorants [75]. These green approaches for colorant production and application have resolved some of the environmental and sustainable challenges encountered in colorant industry.

Natural pigmentation is another attractive approach to realize the formation of sustainable colorants. By mimicking the formation of natural melanin pigments, catechol-containing plant derivatives may be adopted to form a series of pigments. Different from other natural colorants, less dyeing auxiliary agent is needed for the fixation of catechol-based pigments on the substrates. Specifically, the affinity problems can be partly resolved by the adhesive nature of catechol derivatives. However, natural pigmentation of phenolic compounds usually gives less attractive colours like yellow and brown due to browning process. In addition, surface modification of substrate materials may be necessary for promoting the uptake of natural-based colorants. For the commercialization of natural-based pigments, the cost, availability of colour range, performance of colorants and simplicity of production process should be enhanced to the extent that is comparable to the competitive synthetic counterparts.

2.2.4 Water treatment

In the sector of wastewater treatment, adsorption process has been gaining more attention for their advantages in terms of cost, material choices and ease of installation. Most of the

advanced adsorbents are composites or hybrid materials, which compose of two or more distinct types of materials having different chemical and physical properties. The integration between materials with different properties usually endow the composite materials a new applicability, and the new combination may also gain synergistic effect of enhanced properties or performances. Composite materials generally outweigh the performance of pristine materials, therefore careful planning and investigation of material combinations can encourage the fabrication of materials tailored for specific purposes.

With the concept of sustainable development, a number of green materials are synthesized for the achievement of high-performance and specific adsorption activity. However, the adsorption of these green adsorbents often suffers from limited capacity, complicated fabrication and limited range of applications. It is also rare to have a universal adsorbent for different adsorbates in a wastewater mixture. With the goal of fabricating an efficient adsorbent, composite materials are preferred for their benefits of multiple properties. To attain more selective adsorption and desorption behaviors of adsorbents for advanced wastewater treatment, materials that can alter the adsorption specificity upon the change of certain parameter are desired.

2.3 Emerging Advanced Functional Materials

Advanced materials can be defined as the materials possess exceptional features and functionalities when compared with the conventional counterparts [61]. They may perform certain functions under predefined stimuli. The definitions of advanced materials continue to change with the present scientific discoveries of unprecedented properties found in materials.

Nanoengineered materials, smart materials, biomaterials and semiconductors are the common classes of materials that have been widely studying for their development of advanced functionalities. The advanced materials can be made of different varieties of materials including distinct material types like metals, ceramics, polymers and their composites.

The innovation of material science technologies potentially contributes to the current manufacturing processes and the development of novel products [76]. Hence, both consumers and manufacturers are anticipating more well-developed methodologies to fabricate high-performance materials for an extensive range of applications. Despite the emergence of smart materials have caught the attention from various parties, the adoptability and practicability of many of these advanced materials remains a challenge for different scientific fields. Thereby, numerous substantial research works have been devoted to the study of smart materials, composite materials and energy materials for practical use today. In particular, the performance, value, and recycling of these materials have to be considered thoroughly to enhance their viability in real-world contexts.

2.3.1 Smart materials

Smart materials are the materials designed to simulate the ‘respond to stimuli’ feature in nature. They have the ability to sense, react and adapt to the external changes. In recent decades, more experts from multidisciplinary fields have been exploring the possibility of smartness in different materials. Textile engineers have thus become more aware of the potential of advanced textiles, and the pioneer thinking of smart textile material has been proposed. However, smart textiles are generally an innovative idea and the realization of smart textiles is

impeded by the limited technological support. Assisted by the rapid growth of advanced material fabrication technologies, many ideas of smart textiles can be made into physical prototypes. This has signified the beginning of a deveopment revolution in textile industry.

More smart textiles start taking social factor into account and these textiles are specifically designed for addressing the problems encountered in daily lifes. In addition to the availability of technologies that meet the fabrication requirements, the feasibility of the products used in real-life applications is critical, especially for wearable smart textiles. The level of convenience and performance in usage of these smart textiles are important criteria to be fulfilled before achieving community-wide adoption. Therefore, enormous research efforts have been spent to build up fundamental technologies to support the advancement of smart textile materials. To date, smart textiles have been actively developed for more than twenty years. The progress of advancement can be divided into three stages, namely ‘from materials to devices’, ‘from devices to systems’ and ‘from systems to content’ [77]. Each transition in the development stage has contributed to the emergence of smart textiles for multiple functional and aesthetic applications.

Classification of smart textiles

Based on the widely accepted classification of smart textiles, the materials can be classified into three types, which are passive smart textiles, active smart textiles and very smart textiles. Passive textiles resemble sensors and are able to detect the changes of certain ambient parameter [78]. Active smart textiles can act as both sensors and actuators to give response to the detected ambient stimuli [79]. Very smart textiles not just have the capacity to sense and react, but also adapt upon the detection of external stimuli as units and systems [80]. The

responses can be realized by the textile-based components or the embedded miniaturized actuators [81]. In general, the type of sensitivity of smart textiles can be predetermined by the composition of specific building materials. Different natures and combinations of materials enable smart textile to sense, react or adapt under the constantly changing environment. The nature of detectable stimuli and environmental conditions range from optical, vibrational, thermal, chemical, electrical, magnetic to mechanical origins [82]. Some smart materials can be designed for medical purposes, ansome can even be implanted inside the human bodies. Nevertheless, these stimuli-responsive products also subject to the physiological microenvironment like the constantly changing pH, reduction and oxidation, temperature and, also the presence of enzymes [83]. Their reactivities to environmental stimuli need to be examined in detail before these materials can be used to construct a feasible product for predetermined applications.

Material and incorporation methods

The performance of smart textiles is predominantly determined by the materials and the types of incorporation methods used. Textiles can be interpreted as the materials that are formed by interlacing fibres or yarns, and the term broadly refers to the intermediate and final products in the textile industry [84]. Fibres or yarns as the building unit may individually carry functionalities serving as smart functional components in a unit, or act as a substrate for the incorporation with other functional materials. In addition, textile materials can be manufactured into different shapes, properties, and forms. The versatility, compatibility and robustness of textiles allow them to be fabricated into a wide variety of components in smart devices. In the developing process of wearable smart textiles, it is preferable to maintain the properties

including high flexibility, deformability, light weight, wearable comfort and cleanable found in conventional textiles.

Integration generally refers to the incorporation methods of smart materials to textiles. This incorporation varies from physisorption, chemisorption, encapsulation, embedment, and implantation into the human body in the level of fibre, yarn, fabric or other forms [81]. Some physical incorporation methods can be achieved with the use of existing textile techniques such as electrospinning, knitting, weaving, braiding and direct writing [85]. In addition, chemical incorporation methods may involve dyeing or finishing processes. Some delicate foreign materials are susceptible to damage or degradation with the exposure to water and oxygen, therefore encapsulation and surface mounting technology are usually needed for extra protection. Encapsulation is commonly adopted for improving the washability of these smart textiles and also preventing them from leaking harmful substances.

Smart textiles continue to evolve with the availability of novel smart materials. The degree of smartness and degree of integration are the indicators for the progress of development [86]. Conventional textiles provide the basic functionalities such as warmth, comfort and aesthetic. The emergence of passive smart textiles allows materials to sense the ambient changes. Moreover, active smart textiles are able to sense the stimuli and react as actuators. To date, very smart textiles even possess the ability to adapt to the environmental changes. The textile products can be regarded as very intelligent if they possess the functions of sensors, data processing, actuators, storage, and communication [87]. Very smart textiles always involve the use of electronics or microprocessors as their essential components, and this is because they are required to perform complicated operations. Electronic units can capture specific signals to be interpreted by machine-learning algorithm, and the processed data can be subsequently

transmitted to external devices for user to monitor the changes [81]. Smart textiles are flexible enough to be established into a vital sign or physiological monitoring system, mobile wearable information processing system and motion supervision system. Nowadays, smart textiles can generate electrical energy internally by converting energy from solar heat, body temperature and pressure, and this provides sufficient electrical energy to power up the whole devices. Besides, more green materials are involved in the sustainable development of smart textiles. With these benefits and potentials, researchers from the fields of medical and healthcare, energy-harvesting and storage, military protection and detoxification, sports, robotics, aerospace, architectures and other functional apparels have started investigating the fabrication of smart textiles.

To date, many existing textile manufacturers not only focus on the production of single-use products, but also the production of value-added multi-functional products for long-term usage [87]. Many small companies have tried to produce innovative smart textile prototypes. Nevertheless, the number of smart textiles available in the market is still limited. Even though extensive research studies and product development have been conducted, smart textiles remain a niche market in the textile industry. This is ascribed to the current level of maturity of smart textiles. Even textile engineers have concerns over the reliability and washability of the new applications, so it is expected that mass production and adoption of smart textile are impossible in this situation [88]. In addition, there are inadequate well-defined standards for consumers to assess the quality and the price of smart textiles, this may lower their willingness to purchase the products. Besides, smart textiles are yet to be an indispensable item in modern life, and the drivers for customers to purchase smart textiles are insufficient, particularly for civil uses.

Despite the unsolved limitations, contemporary development of high-performance smart textiles opens the door for textile materials to be employed in various sectors, widening the global textile market. This innovative application is undoubtedly creating a current trend in the textile industry. To further expand the market, bridging the gap between textile research and the damands of textile end-users are necessary. User involvement in the development of smart textiles can confer guidance to the researchers. Understanding, inspiration, involvement, motivation, engagement are the five approaches that can be employed to better analyze the needs of the end-users and find out the benefit–cost ratio (BCR) for end-users [89].

2.3.2 Triboelectric energy materials

With the urge of global energy crisis, there is an imminent need for the exploration of renewable energy sources. It is worth noting that smart material system can sense the changes of environmental stimuli including temperature, humidity and triboelectricity, and then react correspondingly for transducing energy. In 2012, the first triboelectric nanogenerator (TENG) was proposed from Wang's research group, and this discovery marked the new era of the development of mechanical energy harvester [90]. The emergence of this device has realized the utilization of wasted mechanical energy for generating electricity. As TENG has demonstrated itself a remarkable energy converter for the utilization of wasted mechanical energy, it has become fast-growing research direction in the multidisciplinary fields. Particularly, wearable TENG devices have been highlighted for their possibility in harvesting the mechanical energy procured from human daily activities. It was estimated that triboelectricity generated in daily physical activities can be more than 35000 V, and numerous TENG systems exhibit the energy conversion efficiency reaching above 85% [91]. The energy

harvesting ability of TENG systems outperform other existing devices, and the energy harvested is able to further power the electronic system or other functional devices for advanced applications.

Triboelectrification (also known as contact electrification) coupled with the electrostatic induction is the fundamental basis of TENG. Some studies have proposed that the triboelectrification between two distinct dielectric materials may involve electronic transfer, ionic transfer, and also material species transfer [15]. It is agreed that the triboelectrification is universal for different physical phases of triboelectric pairs variations, including interfaces between solid-solid interface, solid-liquid interface and solid-gas interface. For TENG applications, contact electrification at the solid-solid interface is mostly considered. As shown in Figure 2.8, overlapped electron-cloud model and electron cloud-potential well model were proposed for the schematic illustration of triboelectrification and charge transfer. When atoms of two distinct dielectric materials are in contact, their electron clouds are overlapped, resulting in the electron transfer [92]. It should be noted that this contact electrification effect efficiently occurs between atoms in a few layers at the interface [93]. Thus, the thickness of triboelectric materials should be carefully designed in order to maintain a high output performance.

Common operating modes in recent studies include contact-separation mode, single-electrode mode, relative-sliding mode, and free-standing mode. Basic working mechanism for the most common contact-separation operating mode of triboelectric system in double-electrode configuration involves the coupling of triboelectrification effect and electrostatic induction (Figure 2.9) [94]. A triboelectric pair generally consists of a tribopositive layer and a tribonegative layer in electrically neutral state. When a mechanical force is asserted onto the dielectric pair, one layer is forced to be in contact with another layer, causing friction. Due to

the difference in polarity between the two layers and the result of triboelectrification effect, positive charges are generated on the tribopositive layer, and the equal number of negative charges is also generated on the tribonegative layer. When the force is released, the two layers start separating from each other and a potential difference is generated between the two materials. The difference also induces the charge formation on the electrodes, and then electric charge can be transferred from one electrode to another via the arising electrostatic field. When the triboelectric pair comes into contact again, the electrostatic field vanishes, and the electrons flow back to the original position. Alternating current power can therefore be generated through the repetitive cyclic motion. Under this system, the mechanical energy can be harvested and successfully converted into high-voltage pulse output for powering the electronic devices. Furthermore, they are especially suitable for high-frequency applications.

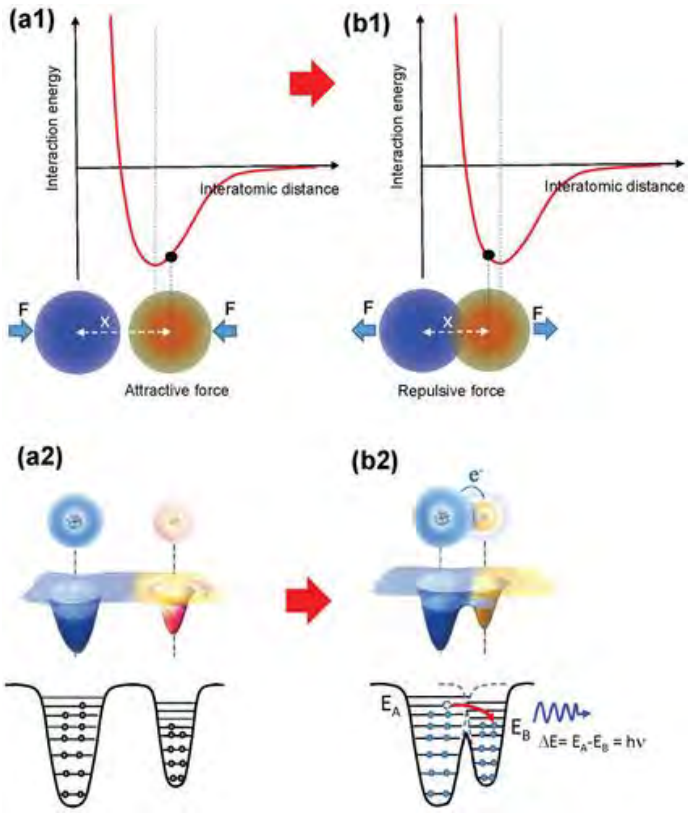

Figure 2.8 Overlapped electron-cloud model and electron cloud-potential well model for the schematic illustration of triboelectrification and charge transfer [95]

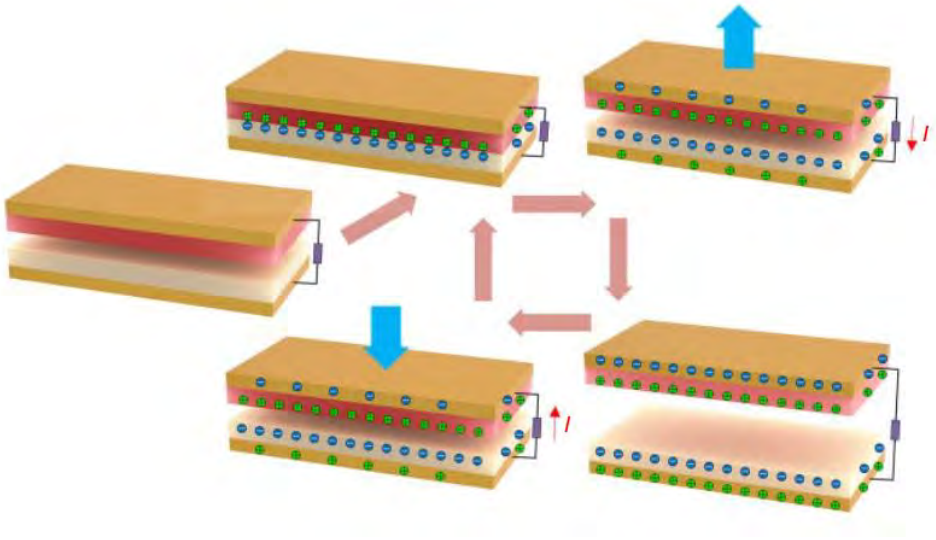

Figure 2.9 Working mechanism of contact-separation mode TENG [94]

TENG is generally composed of two separated dielectric materials attached with back electrode, and the two dielectric materials usually have distinct electron affinity, facilitating the generation of triboelectricity. Dielectric layers in the TENG system are not only the friction material, but also the charge storage material [96]. As such, material selection of dielectrics for TENG system is eminently a critical factor affecting the triboelectric performance of the system. To assist the design of triboelectric pair, the triboelectric series of various materials was established empirically through contact-charging experiments [97]. In addition, the performance of TENG could be preliminarily predicted according to the theoretical equations. With reference to the deconstructed equation derived from Maxwell equation, three components have deduced to have influences on the displacement current density of TENG. Three parts namely (σ_T), $\left(\frac{dH}{dt}\right)$ and $\left(\frac{d_1\,\varepsilon_0/\varepsilon_1 + d_2\,\varepsilon_0/\varepsilon_2}{(d_1\,\varepsilon_0/\varepsilon_1 + d_2\,\varepsilon_0/\varepsilon_2 + z)^2}\right)$ correspond to triboelectric effect, device, and electrostatic induction, respectively. The equation is shown below:

$$J_D \approx (\sigma_T)\left(\frac{dH}{dt}\right)\left(\frac{d_1\ \varepsilon_0/\varepsilon_1\ +\ d_2\ \varepsilon_0/\varepsilon_2}{(d_1\ \varepsilon_0/\varepsilon_1\ +\ d_2\ \varepsilon_0/\varepsilon_2\ +\ z)^2}\right)$$

, where σ_T represents the surface charge density, H represents the function of time when two dielectric materials are in contact, dH/dt is the speed at the contact/separation of the two dielectrics in TENG system, d_1 and d_2 are the thickness of the two dielectrics, ε_0 represents the vacuum permittivity, ε_1 and ε_2 represents the permittivity of the two dielectrics, and z is the distance between the two dielectric layers [98, 99].

For the selection and fabrication of polymeric dielectric materials, electronegativity of the functional groups, orientation of molecular chains, the polarizability, and traps between amorphous and crystalline regions play a critical role to determine the properties of the materials (Figure 2.10) [100]. First, the electronegativity of atoms determines the electron-capturing or electron-withdrawing nature of the materials. Second, the orientation of molecular chains affects the exposure of particular functional groups and atoms, which influence the interactions with that of counter triboelectric material. Third, higher crystallinity contributes to larger dipole moments, and the interface between amorphous and crystalline regions encourages charge storage.

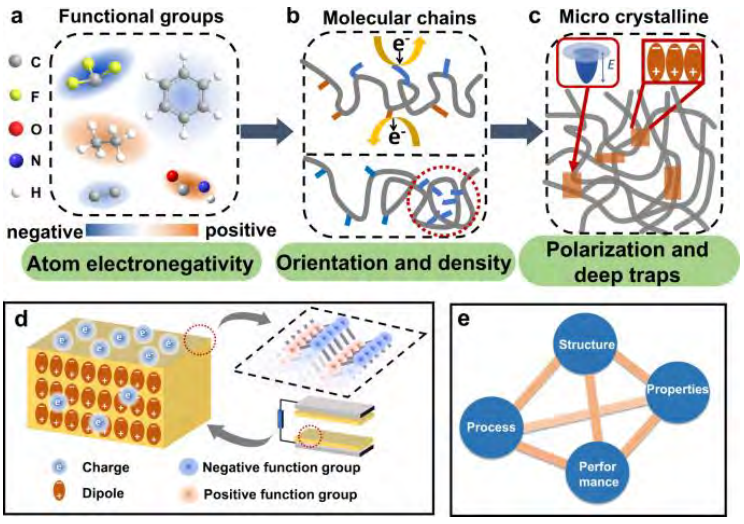

Figure 2.10 Summary of factors of polymeric chains influencing triboelectrification [100]

Material modification

The material structures can be tailored-made to enhance both energy harvesting efficiency and energy converting efficiency, which have great contribution to the power output of the triboelectric system. Physical modification with micro/nano- structures to increase the surface contact area and chemical modification to alter the electronegativity are two main approaches. Physical doping is a widely adopted method for increasing the performance and functionality of the dielectric materials. For instance, nanofillers have been extensively incorporated into polymers for the preparation of high-performance materials. Doping can synergize the benefits of both fillers and substrate matrices, yielding the favourable enhancement in the performance. The doped composites consist of two phases, namely fillers as the dispersed phase and substrate as continuous phase. The interconnectivity of dispersed phase in the continuous phase determines the percolation threshold, which is crucial for improving the performance of materials. It is worth mentioning that mechanical properties and surface morphologies of materials likely influence the percolation dynamic of fillers [101]. High loadings of nanofillers always induce agglomerations and interfacial defects, leading to non-uniform distribution of functional fillers in the matrix. It was proposed that the customized structural design of nanofillers could allow lower loadings to achieve percolation threshold, therefore reducing the possibility of agglomerations and interfacial defects [102].

Heterogeneous fillers as the dispersed phase may cause the formation of unwanted interfacial voids and rigidify the surrounding polymer, resulting in the loss of intrinsic properties and synergistic effect [103]. The incompatibility between fillers and matrices is another important issue to be tackled. This is because the modulus discrepancy and relatively poor interfacial

adhesion between the rigid nanofillers and flexible polymeric matrix can impede the mechanical-electrical conversion efficiency, having negative impacts on the performance of the doped materials [104]. Different surface and interface engineering approaches for the fabrication of organic-inorganic composites were summarized in Figure 2.11. Pre-modification of nanofillers is a popular strategy to promote the compatibility between fillers and host material. The application of coupling agent on fillers is one of the facile and low-cost methods to improve the interfacial compatibility and also the interfacial polarization [105].

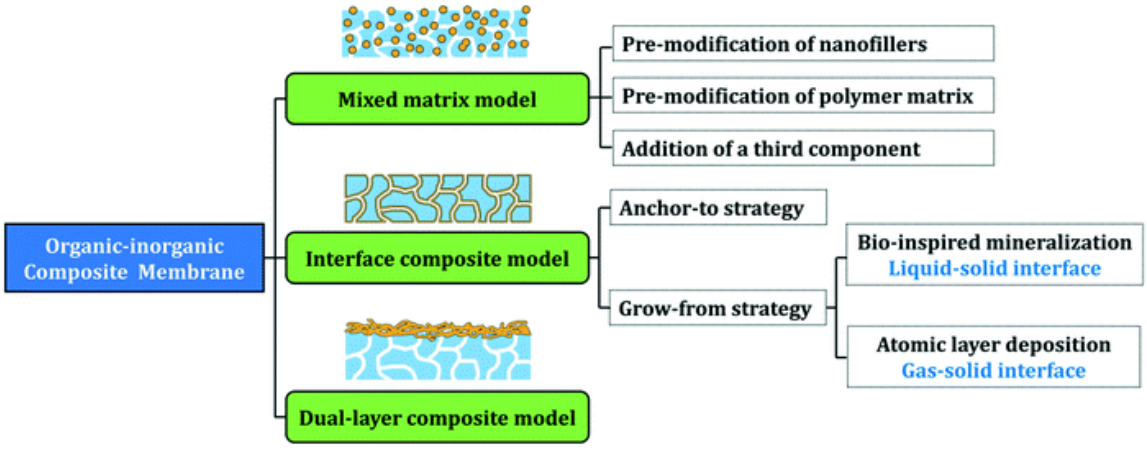

Figure 2.11 Approaches for the fabrication of organic-inorganic composite materials [106]

Metal-organic framework (MOF)

With the advent of MOF, researchers in various fields start developing new structures and investigating their novel properties and applicable ranges. MOF-based materials are ground-breaking porous materials possessing extraordinary designable characteristics, unique properties, modular flexibility and great application diversities. The scope of MOF applications ranges from adsorption, storage, catalysis to other specific functionalities. The most fascinating characteristic of MOF-based materials is that these materials can realize the concept of 'function-structure-synthesis' [107]. MOF technologies enable researchers to synthesize

customized materials by constructing the whole structure based on modular components. One of the modification strategies is to incorporate foreign functional molecules, and the incorporation of foreign molecules into MOF materials can generally be categorized into three approaches. For instance, foreign molecules are able to be incorporated as moieties in the framework backbone, on the side group of organic linker or a guest in the host structure (Figure 2.12). Rapid development of MOF-based materials with various porous dimensions and record-breaking surface area allow the emergence of high-performance materials with customized synthesis techniques and multiple functionalities. Besides, MOF is recognized as a scientific endeavour amid material science field in nanoscale, and this makes them a promising nanofiller for the modification of host materials.

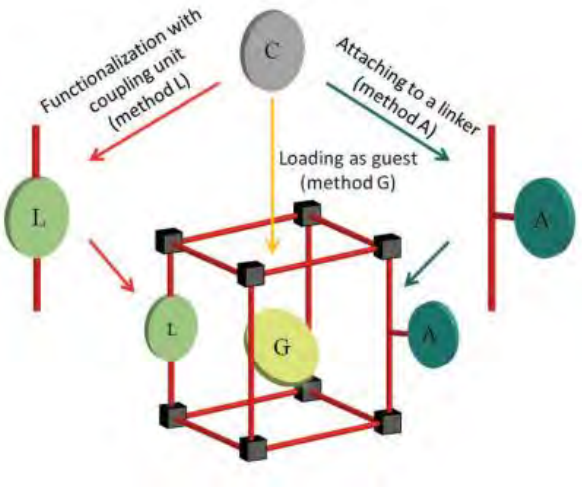

Figure 2.12 Three different approaches for the incorporating foreign molecules to metal-organic framework [108]

MOF-based TENG device was reported as a novel energy harvester with higher porosity, better chemical stability and wider functionality [109]. MOF architectures are highly tailorable with the selection of diverse range of metal nodes and organic linkers. The differences in natures of constituents can give multivariate crystalline structures, displaying various size, geometry,

porosity, chemical stability, thermal stability, as well as functionalities [110]. The porosity can reduce the effective thickness of the materials and increase the surface contact area for triboelectrification. Some studies have already pointed out that the relative permittivity and porosity of the triboelectric layers have certain association with the surface charge density and charge transfer quantity [93]. With their merits of high customization, specific MOF structures can also be synthesized to achieve multifunctional purposes.

To fabricate an advanced TENG system for a wider applicable range, researchers should focus on the power density, operational stability, mechanical flexibility, sustainability, and scalability of materials and integrated devices. In addition, TENG systems are a latent self-powered active sensors that can utilizes various mechanical energies for sensing different mechanical agitations and chemicals [111]. The structures of TENG system can also be easily integrated with other modules to realize more advanced applications including wireless sensing. Therefore, the prospects of triboelectric energy have driven the research trend of renewable energy and other related devices.

2.4 Summary of Current Research Potentials

With the discovery of diverse reactivities and versatile functionalities of catechol chemistry, scientists from multiple disciplines have engaged in exploring the potentials of catechols in a wide variety of applications. Limited studies have been dedicated to demonstrate the capabilities of catechol and their derivatives in developing coloration and functionalization technologies for textile materials. Three research potentials based on catechol-based inspiration are proposed as follows:

1. Catechol-based pigmentation for textile coloration

To alleviate the negative environmental and health impacts arising from the conventional coloration process, textile engineers have begun to investigate the bio-inspired synthesis of colorants for substituting the conventional synthetic colorants and auxiliaries. As reviewed before, some research studies have suggested the possibility of bio-adhesive coating using PDA as a sustainable colorant for substrate coloration. Nevertheless, they usually impart unattractive brown or black shades to the materials or mask other lighter colours. These intense colours restrict the range of colour selection for textile coloration. In contrast, the polymerization of plant-derived phenolic compounds like caffeic acid can form paler shades compared with other polycatecholamine compounds. The catechol-based compounds consist of conjugated double bonds for strong visible light absorbance, and they also have active groups to form a bio-adhesive coating on fibres. In addition to more attractive colour shades, plant-derived catechol may react with other small nucleophilic molecules like amino acids to undergo heteromolecular polymerization. This has given many opportunities to tune the colour formation. Therefore, the study of catechol-amino acids may expand the colour gamut of bio-adhesive colorants and widen the applicability of this novel type of textile coloration method. It is also significant to deduce a reliable system with optimum conditions for water and energy conserving purposes.

2. Catechol-induced tunable surface charges

The severe water pollution caused by high consumption of synthetic dyestuffs in textile dyeing is yet to be efficiently solved. The demands for advanced adsorbent have triggered more studies on the sustainable nanocomposites for wastewater treatment. However, most of the synthesis

methods of these advanced nanocomposites are complicated, and the universality of these adsorbents are limited. To broaden the adsorption range, catechol derivatives can be introduced as a tunable adsorption material. The presence of abundant chargeable functional groups on polycatecholamines can endow a layer with pH sensitivity. The distinct surface charges under specific pH condition can facilitate the efficient adsorption and desorption of various ionic dyestuffs. Furthermore, catechols are highly compatible with magnetic metal oxides, offering chances to establish organic-inorganic hybrid system. This yields synergistic effect of distinct materials, contributing to gaining better capacity, simpler handling process and potential reusability. It is crucial to investigate the characteristics and performance of magnetic catechol-coated adsorbent to deduce the optimum synthesis and application conditions.

3. Catechol-enhanced functional materials

Dielectric materials for producing high-performance TENG have become a widely investigated topic for sustainable energy development. To enhance the functionality and performance of dielectric materials, physical doping of fillers is a common approach. However, the foreign fillers with distinct features may cause adverse impacts on the host substrate. To minimize the effect arising from the undesirable interfacial interaction, catechols may be selected to form an interfacial layer intermediating two distinct material system. There is a lack of comprehensive study of catechols as the interfacial layers between fillers and polymer matrices. Polycatechols are natural materials exhibiting reactive redox activities and excellent adhesive properties, which are an ideal candidate for fabricating bio-based functional composite materials with better homogeneity and enhanced properties. Furthermore, the presence of different functional groups on the polycatecholamines allow themselves to fit into the host substrate. For fillers with inorganic nature, catechol coating may enhance the interfacial adhesion between fillers

and substrate. With better incorporation of fillers into the host matrix, the catechol-coated materials are likely to exhibit enhanced performances, and more types of fillers can also be utilized.

3 METHODOLOGY

3.1 Catechol-Based Pigmentation

3.1.1 Materials

The catechol-containing caffeic acid (CA) and amino acids (Figure 3.1) were purchased from Sigma-Aldrich and J&K Chemical Ltd., respectively. Tris(hydroxymethyl)aminomethane and potassium periodate (KIO_4) were from Alfa Aesar. 1-Ethyl-3-(3-dimethylaminopropyl)carbodiimide (EDC) was from Shenzhen Dieckmann Technology Co., Ltd. All chemicals and reagents were used as received without further purification. Woven wool fabrics with the weight of 274 g/m^2 employed were commercially available. The fabrics were first washed with 5‰ sodium dodecylbenzenesulfonate solution at 85°C to remove impurities on the surface. In the pretreatment process for activating carboxylic acids, each gram of wool fabric was immersed in the 100 mL solution of 0.04 M EDC and 1.25 M sodium chloride for 24 hours, followed by rinsing with deionized water [112, 113].

3.1.2 Pigmentation and coloration

The catechol-based pigments of CA with amino acids were first prepared in aqueous medium at room temperature. For comparison purposes, 6 μmol of CA and different amount of amino acids (25/50/100/150/200 μmol) were respectively dissolved in 3 mL of 10 mM Tris buffer at

different pH (pH 5/6/7/8/9) containing 1 mol of ethanol. Then, KIO_4 (1 equivalent to catechol) was added, and the solution was kept for 24 hours. The effect of tris concentration (1/10/100 mM) and EDC pretreatment on fabric on catechol-amino acid coloration were evaluated. For fabric coloration, wool specimens were immersed into 10 mM tris solution containing 2 mM CA with 50 mM amino acid at a liquor-to-good ratio of 25:1. The exhaustion solution was kept overnight without shaking under room conditions (c.a. 22°C, 65% relative humidity). The fabrics were rinsed with deionized water and subsequently dried for microscopic evaluation, colorimetric and spectroscopic analysis, and colour fastness measurement. Five set of wool samples were respectively dyed in five different batches under the same conditions for the investigation of reproducibility. To explore the possibility of cold pad-batch dyeing with catechol-based pigments, the blank fabrics were respectively padded with five-fold increase of catechol-amino acid and KIO4 concentration in 1 M tris buffer. The padded fabrics were then incubated in enclosed environment under the aforementioned room conditions for 24 hours.

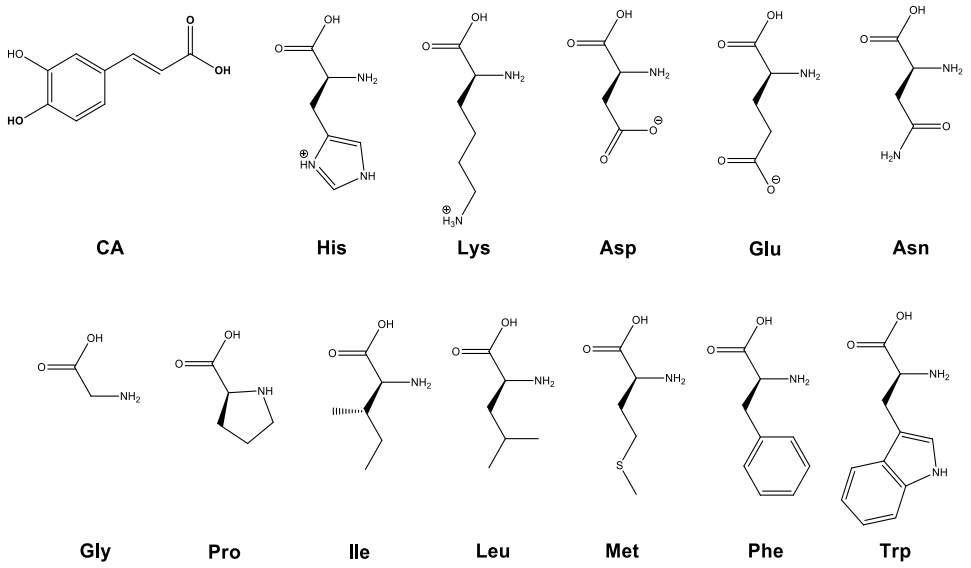

Figure 3.1 Chemical structures of CA, and amino acids, of which side chain charges carried at pH 7.4 [114]

3.2 Catechol-Induced Tunable Surface Charges

3.2.1 Materials

Anhydrous iron(III) chloride hexahydrate ($FeCl_3$) was purchased from International Laboratory USA. Iron(II) chloride tetrahydrate ($FeCl_2 \cdot 4H_2O$), Pluronic F-127 (F127) and 1,3,5-trimethylbenzene (TMB) were purchased from Sigma-Aldrich. Dopamine (DA) was from J&K Chemical Ltd. Tris (hydroxymethyl) aminomethane (Tris) was purchased from Tianjin Yong Da Chemical Reagent Development Center. Rhodamine B (RhB), direct blue 71 (DB), crystal violet (CV) and orange G (OG) was purchased from Shanghai Macklin Biochemical Co., Ltd. The dye structures were shown in Figure 3.2. All chemicals were used as received without further purification.

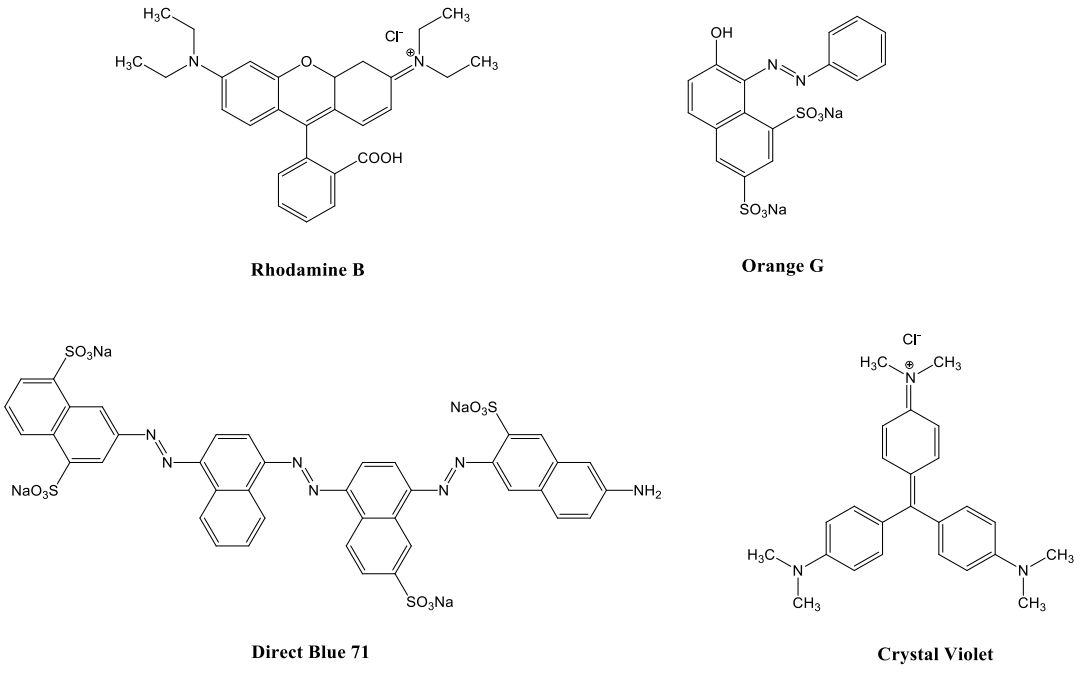

Figure 3.2 General chemical structures of the dyes used

3.2.2 Synthesis of composites

The magnetic Fe_3O_4@PDA was prepared through two-step synthesis, which was co-precipitation of metal oxides followed by simple polymerization of DA [115, 116]. Precisely, 1.63 g $FeCl_3$ and 1.0 g $FeCl_2 \cdot 4H_2O$ were dissolved into 50 mL degassed distilled water under N_2 protection with constant stirring. Diluted NH_3 solution (25%) was added dropwise to the solution until the pH reached 8, changing the colour from orange-brown to black. The chemical formation of magnetite nanoparticles is presented in *Equation (1)*. Then, the mixture was stirred for 1 h at room temperature. Magnetic particles were separated by a magnet and washed with distilled water until it became neutral. The obtained particles were stored in 50 mL distilled water and kept in the fridge. For the second step, 0.36 g TMB and 0.36 g F127 were dissolved into a mixture of 60 mL ethanol and 65 mL distilled water under constant stirring for 30 min, and these TMB/F127 emulsion micelles served as a nanoparticle coassembly template for enhanced loading capacity [116]. The collected magnetic particles and Tris solution (90 mg Tris in 10 mL deionized water) were added into the mixture in sequence. DA (20/40/60/80/100 mg) was finally added, and the system was kept stirring for 24 h to facilitate the growth of PDA. Fe_3O_4@PDA formed was separated by a magnet and washed with 2:1 ethanol and acetone under 30-min sonication for 3 times to remove the TMB template. The washed particles (ca. 1.11 g) were stored in 300 mL ethanol (adsorbent concentration: ~3.67 mg mL^{-1}) and kept in the fridge. The synthesis of the organic-inorganic hybrid system was summarized in Figure 3.3. The Fe_3O_4@PDA used in the following investigation was formed with 60 mg DA (Fe_3O_4@60mgDA), unless otherwise specified.

Chemical equation of Fe_3O_4 formation:

$$2FeCl_3 + FeCl_2 + 8NH_3 + 4H_2O \rightarrow Fe_3O_4 + 8NH_4Cl \quad (1)$$

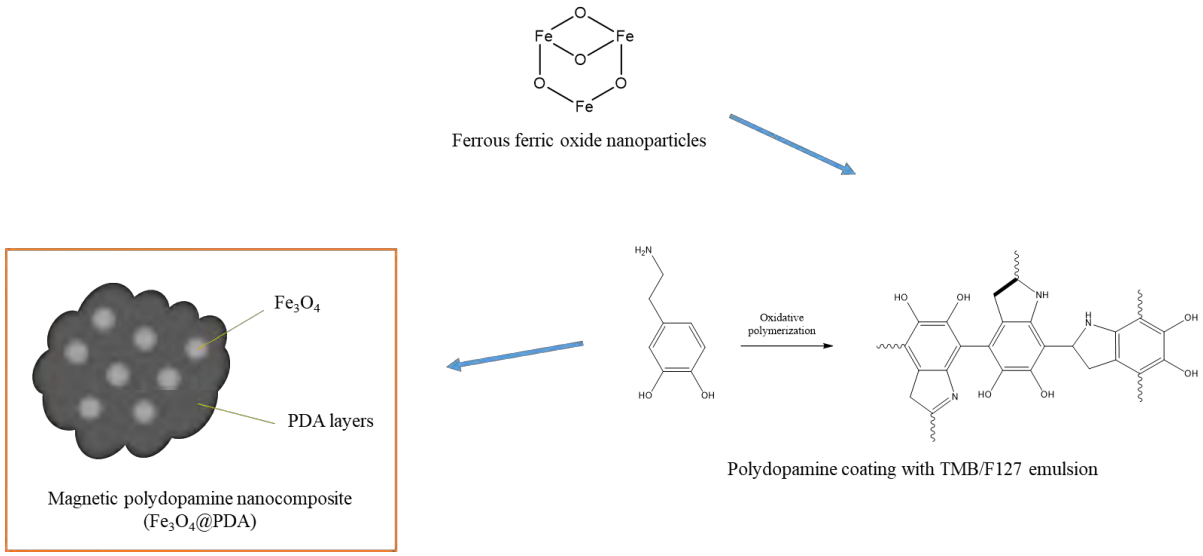

Figure 3.3 Synthesis of organic-inorganic hybrid system

3.2.3 Performance studies

Adsorption studies

The calibration curves of four different dyes (RhB, DB, CV and OG) were constructed with corresponding absorbance against dye solutions of known concentration (Figure S1). The curves were employed for subsequent determination of dye concentration changes in solution from sample absorbance. In general, the initial dye solutions contained 3 mL of the magnetic mesoporous nanoadsorbents, 20 mL Tris buffer and 2 mL of 1 mg mL^{-1} dye stock solution (dye concentration: 80 µg mL^{-1}), and they were kept under constant stirring. The adsorption ability

of the Fe_3O_4@PDA particles was assessed based on the change of solution absorbance, which was proportional to the dye concentration. The effect of initial dye concentration and pH from 4 to 9 on the adsorption behavior of Fe_3O_4@PDA were further studied. The adsorption capacity of different dyes on Fe_3O_4@PDA was evaluated according to the following Eq. 1:

$$q_e = \frac{(C_0 - C_e)V}{W} \quad (1)$$

, where q_e (μg mg^{-1}) is the amount of dyes adsorbed onto the adsorbents at equilibrium, C_0 (μg mL^{-1}) and C_e (μg mL^{-1}) are the initial and equilibrated dye concentrations, respectively, V (mL) is the volume of solution added, and W (mg) is the mass of the adsorbent.

Langmuir and Freundlich adsorption isotherm model at 298 K were adopted to study the equilibrium adsorption characteristics of the nanocomposites. The transformed linear equations of the two models, and also separation factor R_L for the determination of the degree of favourability were used for the evaluation [117].

In addition, pseudo-first order and pseudo-second order kinetic models were applied for analyzing the kinetic behaviors of the adsorption of ionic dyes onto the nanocomposites, and the linear forms of the two models were employed [118].

Reusability of Fe_3O_4@PDA

The magnetic property of Fe_3O_4@PDA nanoadsorbents allowed them to be easily collected by an external magnet for subsequent reuse. The Fe_3O_4@PDA nanoparticles saturated with different dyes could be regenerated by using solvent desorption method. The desorption solvent

was prepared by mixing *N*,*N*-dimethylformamide (DMF) and Tris buffer in the ratio of 1:4. The nanoadsorbents were first used for dye adsorption. Then, the dye-adsorbed adsorbents were separated by a magnet, and they were dispersed in the solvent (adsorbent/desorption solvent ratio: 1 mL/10 mL) for desorption under magnetic stirring for 6 h. The recovered adsorbents were separated again by a magnet and reused for the next dye adsorption. The adsorption-desorption process was repeated 5 times to investigate the reusability.

Separation of dyes in the mixture

A cationic dye and an anionic dye were mixed in both pH 4 and pH 7 Tris buffer solutions, respectively. 3 mL of Fe_3O_4@PDA was added into the mixture under magnetic stirring, and the solution further underwent dye adsorption for 24 h. Subsequently, the nanoparticles adsorbed with dye molecules were collected by a magnet and underwent desorption using Tris buffer of opposite pH, i.e. if pH 4 buffer was used for adsorption, pH 7 buffer was then used for desorption, and vice versa. The colour change of each stage was observed.

3.3 Catechol-Enhanced Functional Material

3.3.1 Materials

Zinc nitrate hexahydrate ($Zn(NO_3)_2 \cdot 6H_2O$, 98%) was purchased from Alfa Aesar Chemical Reagent Co., Ltd. 2-methylimidazole (Hmim, 98%), dopamine hydrochloride (DA, 98%) and Tris (hydroxymethyl) aminomethane (Tris, 97%) were from Shanghai Aladdin Bio-Chem

Technology Co., Ltd, respectively. Polylactic acid (MW=200,000) was supplied by Anhui Fengyuan Bio-Fiber Co., Ltd.

3.3.2 Fabrication of TENG with catechol-based dielectric composites

Synthesis of ZIF-8

ZIF-8 nanocrystals were first synthesized based on the method of the previous work with minor modifications [119]. 0.0336 M $Zn(NO_3)_2 \cdot 6H_2O$ and 1.10 M Hmim were respectively dissolved in aqueous solution. The distinct difference in the concentration of two reactants can effectively control the growth of ZIF-8 crystal, thus the size of ZIF-8 nanoparticles [120]. Two solutions containing the reactants were then mixed and stirred for 5 min. The mixture was transferred to 100 ml Teflon-lined autoclave for hydrothermal reaction at 120 °C for 6 h. The ZIF-8 nanocrystals were separated from the mother liquor by centrifugation and washed with methanol for few times to remove unreacted components. The nanocrystals were dried overnight under vacuum at room temperature.

Surface modification on ZIF-8 with PDA

Buffer at ca. pH 10.26 was prepared by dissolving 10 mM Tris in deionized water. 22 mM ZIF-8 nanocrystals were dispersed in the Tris buffer under ultrasonication for 30 min. 48 mM DA was then added to the solution with suspended ZIF-8, and the mixture was vigorously stirred for 24 h. The ZIF-8@PDA nanoparticles were collected by centrifugation, and they were washed with deionized water and ethanol for several times. The catechol-coated ZIF-8 nanoparticles were dried overnight under vacuum at room temperature. The synthesis of ZIF-

8@PDA was summarized in Figure 3.4. For comparison purpose, PDA nanoparticles were synthesized under the same conditions without the addition of ZIF-8. All the nanoparticles were grinded into fine powder before usage.

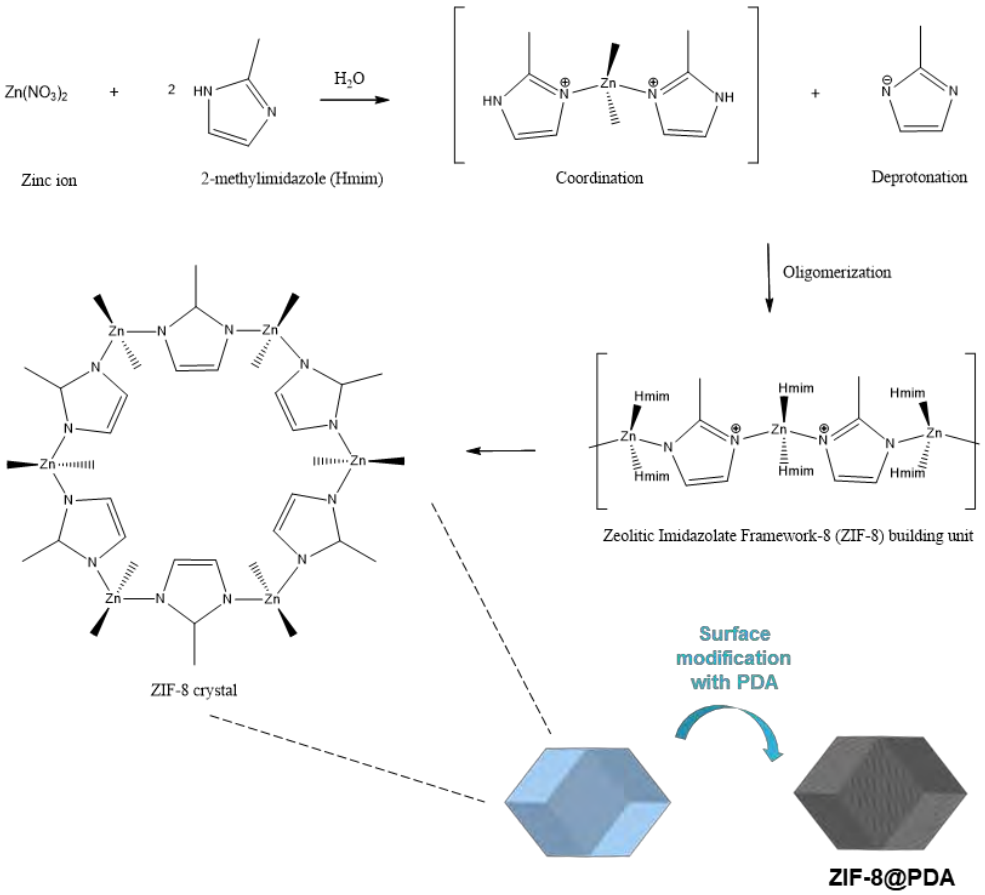

Figure 3.4 Synthesis of ZIF-8@PDA

Preparation of PLA composite thin film

12 wt% of PLA was firstly dissolved in pure dichloromethane. 1 wt% of ZIF-8@PDA and PDA were separately added to the polymer solutions under stirring. To allow time for uniform dispersion and hydrogen bonding formation between catechol-containing fillers (ZIF-8@PDA or PDA) and PLA polymer solution, the mixture underwent ultrasonic treatment and stirred vigorously overnight. The stable mixture was poured onto a glass plate and spread by a doctor

blade. 0.1 mm thick (30.7 gf/cm^2) composite film was therefore obtained via tape-casting method after drying at 70 °C for 30 min.

Fabrication of TENG structure

The prepared composite PLA film and Dow Corning® SYLGARD 184 Polydimethylsiloxane (PDMS) film were selected as the tribopositive layer and tribonegative layer, respectively. 3M™ conductive Cu/Ni fabric serving as the electrode was attached to the films. Two layers of materials were trimmed to the size of 2 × 2 cm^2. To facilitate the measurement of electric performance, the materials were separately adhered onto two different acrylic boards. The fabrication process of TENG with PLA/ZIF-8@PDA was summarized in Figure 3.5.

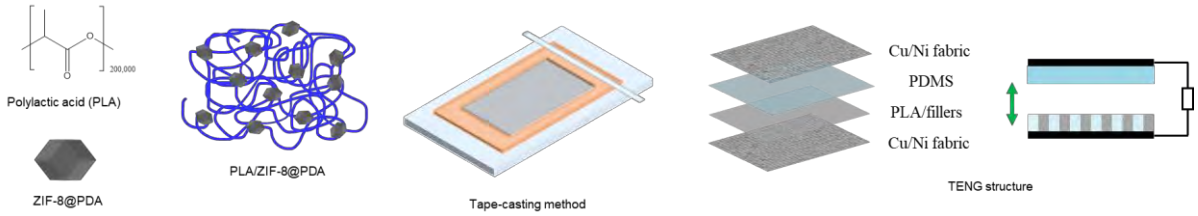

Figure 3.5 Fabrication of TENG with PLA/ZIF-8@PDA

3.4 General Characterization

The materials fabricated in the studies were generally characterized by microscopic analysis, spectroscopic analysis and thermal analysis.

3.4.1 Microscopy

(a) Optical microscopy

Optical microscope can magnify the microscale morphology of samples with visible light, and thus they are suitable to evaluate coloured samples. The cross-sectional images of sample yarns with the support of white nylon yarns were recorded by a Nikon Optiphot-POL optical microscope with a high-performance Leica LAS software. The degree of penetration of colorants into the interior part of substrate fibres could be observed via the optical micrographs.

(b) Scanning electron microscopy (SEM) with Energy-dispersive X-ray spectroscopy (EDX)

SEM employs electron beams to image the surfaces of specimens in microscale/nanoscale resolution and enables elemental microanalysis. The surface morphologies of the sample fibres, nanocomposites and films were evaluated using a Tescan VEGA3 scanning electron microscope operated at an accelerating voltage of 20.0 kV and a Tescan MAIA3 Field Emission Scanning Electron Microscope (FESEM) operated at an accelerating voltage of 5.0 kV. SEM coupled with EDX for the detection of elements and their distribution in specimens via elemental mapping.

(c) Transmission electron microscopy (TEM)

Transmission electron microscope offers high-resolution images and information of specimens based on mass-thickness contrast, diffraction contrast, and phase contrast. Since mass-density

contrast of amorphous and crystalline materials is obvious, catechol-based layer structure on the surface of nanocrystals can be differentiated easily. Scanning transmission electron microscope (STEM) micrographs of catechol-coated MOF nanocrystals and magnetic nanoparticles were taken by a FEI Tecnai G2 F20 S-TWIN transmission electron microscopy with an accelerating voltage of 200.0 kV and a JEOL Model JEM-2100F transmission electron microscope, respectively. TEM micrographs could reveal the formation of functional catechol coating on various materials.

3.4.2 Spectroscopy

Optical radiation

(a) Ultraviolet-visible (UV-vis) spectroscopy

UV-Vis is a common analytical technique to measure the light absorption, transmittance, and reflectance of the samples illuminated with 190 to 900 nm radiation. The absorption spectra of solutions of pigments and dyes were recorded on a Hitachi UH5300 UV-Visible Spectrophotometer.

(b) Fourier transform infrared (FTIR) spectroscopy

FTIR spectroscopy is a simple technique for detecting different functional groups of materials, and it can obtain infrared spectra of absorption of material in solid, liquid and gas state. The attenuated total reflection-Fourier transform infrared (ATR-FTIR) spectra of the textile

materials were recorded by PerKin Elmer Spectrum 100 FT-IR Spectrometer. The ATR-FTIR spectra of catechol layer on nanocrystals was evaluated by Thermo Scientific Nicolet IS50 FT-IR Spectrometer. In the catechol-related studies, the formation of new chemical bonding and the introduction of doping content in the substrate could be evaluated.

(c) Raman spectroscopy

Raman spectroscopy is a non-destructive analytical technique for detecting the vibrational and rotational energy occurred in a molecular system, and therefore it can probe the chemical structures of specimens by the principle of inelastic scattering. To evaluate the change of fibre after pigmentation, raman spectra of the dyed fibres were measured by a Renishaw inVia micro-Raman system with 785 nm laser source.

X-ray radiation

(a) X-ray Diffractometer

X-ray diffraction (XRD) is an analytical technique to identify the crystalline phases present in the specimens. XRD diffractogram was studied using a Rigaku SmartLab 9kW-Advanced X-ray diffractometer and a Rigaku SmartLab 9kW X-ray diffractometer with a rotating anode X-ray source ($\lambda \sim 1.54$Å) in theta/2-theta mode. The X-ray diffraction patterns of pristine and catechol-based magnetic nanoparticles as well as MOF nanocrystals could be analyzed.

3.4.3 Thermal analysis

(a) Thermogravimetric analysis (TGA)

TGA can be employed to analyze the thermal stability of specimens by monitoring the change of specimen weight at a constant rate of heating. TGA of catechol-containing composites was carried out from 50 to 800°C at a rate 10°C/min by Mettler Toledo TGA/DSC 1 Thermogravimetric Analyzer. The doped polymeric materials were evaluated from 30 to 800°C at a rate of 20°C/min by PerkinElmer Thermogravimetric Analyzer TGA 4000. The thermal decomposition of specimens can reveal their composition since materials of distinct components or structures usually decompose with different patterns. For instance, iron (II, III) oxides gradually decompose into smaller structures with increasing temperature ($Fe_3O_4 \rightarrow FeO + Fe_2O_3 \rightarrow 3Fe + 2O_2$). The differences in thermal decomposition pattern of catechol-modified layer and base materials could be used to estimate the content of catechols in the composites.

(b) Differential scanning calorimetry (DSC)

DSC is able to monitor the glass transition endotherm, crystallization exotherm, and melting endotherm as a function of temperature. Quantitative heat flow of pristine and composite polymeric materials was measured by Mettler Toledo DSC3 from 25 to 220°C under nitrogen atmosphere at a heating rate of 10°C/min. The effect of catechol-based interfacial layer between fillers and polymer substrates on the glass transition temperature (T_g), cold crystallization temperature (T_{cc}) and melting temperature (T_m) could be evaluated.

3.5 Property and Performance Measurements

(a) Colour measurement

The colour of an object generally is referred the spectral characteristics of the surface on the object. Colorimetric values of the dyed fabrics were measured using a Datacolor 650 spectrophotometer, and the results were recorded in the form of CIE L*a*b* color space, CIE L*C*h* color space and Kubelka-Munk (K/S) values. The colour difference between different batches of the dyed materials was assessed by CIE delta E76 equation [121, 122].

$$\Delta E^*_{ab} = \sqrt{(L^*_2 - L^*_1)^2 + (a^*_2 - a^*_1)^2 + (b^*_2 - b^*_1)^2}$$

, where L* represents lightness, a* represents the redness-greenness quality of the colour and b* represents the yellowness-blueness quality of the colour. 1 corresponds to the standard sample and 2 corresponds to the batch sample.

(b) Colour fastness

Coloured textile articles are subject to colour fading or running in daily use, and thus their colour resistance should be evaluated to confirm the durability for practical uses. The colour fastness to washing and rubbing of dyed fabrics were evaluated according to AATCC standards including AATCC 61-2010 2A (Test Method for Colorfastness to Laundering) and AATCC 8-2016 (Test Method for Colorfastness to Crocking), respectively. The colour change between two samples is rated according to the ISO standard grey scale with a range of 1 to 5, where 1 is the lowest score and 5 is the highest score. For dyed textile materials, scale between 3 to 5 is usually regarded as the acceptable range of colour change.

(c) Cytotoxicity

Cytotoxicity test was investigated using mouse embryonic fibroblasts and experienced according to GB/T 16886.5-2017 /ISO-10993-5:2009 (Biological evaluation of medical devices - Part 5: Tests for in vitro cytotoxicity). Culture media were prepared using DMEM/high glucose with 10% fetal bovine serum. The fibroblasts were cultured in a 24 microplate and incubated in a humidified atmosphere for 18 hours at 37 °C and 5% CO_2. Blank and treated materials were autoclave sterilized and subsequently cut into 0.2 cm^2. The samples were then saturated in 500 μL culture media, respectively. The cytotoxicity of the solutions was evaluated by using Cell Counting Kit (CCK-8) method. Cell survival was reported as the relative absorbance of the treated sample with respective to the absorbance of blank sample, measured at 450 nm with microplate reader. The experiment was performed six times independently. The percentage of cell viability was assessed by the following equation.

$$\text{Cell viability (\%)} = [\ (A_1 - A_0) / (A_2 - A_0)\ ] \times 100$$

, where A_0 is the average absorbance of culture medium with CCK-8, A_1 is the average absorbance of treated sample in the medium, A_2 is the average absorbance of blank sample in the medium.

(d) Antimicrobial assay

Bacterial glycerol stocks were purchased from Beijing Microbiological Culture Collection Center Limited. The antimicrobial activity of samples was determined on Escherichia coli (E. coli, CMCC 44102) and Staphylococcus aureus (S. aureus, ATCC 6538) under dynamic

contact conditions based on ASTM E2149-13a (Standard Test Method for Determining the Antimicrobial Activity of Antimicrobial Agents Under Dynamic Contact Conditions) with minor modifications. Two types of bacteria were respectively cultured in Luria-Bertani medium. Thin film samples in a dimension of 150 × 100 mm^2 were incubated with bacterial suspension in a concentration of 10^5 CFU/mL under moderate shaking conditions (200 rpm/min) for 18 hours. The bacterial suspensions were subsequently incubated on agar plates for quantitative analysis. The quantitative antibacterial performance can be evaluated with the following equations:

$$\text{Reduction, \% (CFU/mL)} = \frac{B-A}{B} \text{ x } 100$$

$$\log_{10} \text{ bacterial reduction} = \log_{10}(B) - \log_{10}(A)$$

, where A represents the CFU/mL in the flask with treated materials after 18 h, and B represents the CFU/mL in the flask with inoculum only after 18 hours.

(e) Tensile test

Tensile tester can examine the strength, deformation and fracture properties of specimen in response to load. Load-extension data was measured by an Instron 5544 mechanical tester with a setting of 10 mm gauge length and 50 N load cell with operating speed of 2 mm/min. The effect of different dopants on the physical properties of materials could be determined via the change of load-extension curve.

(f) Brunauer-Emmett-Teller (BET) surface area analysis

BET theory is based on the physical multilayer adsorption behaviors of porous materials with gas molecules. Nitrogen adsorption and desorption isotherms of the materials were tested on Quantachrome NOVAtouch LX4 instrument with BET method at 77K. It gave a general estimation of specific surface area and pore size distribution of catechol-coated nanoparticles.

(g) TENG measurement

Vertical contact separation motion of the fabricated TENG was simulated by ZX-A03 keyboard life tester, and the force exerted was monitored by ZNHB-P-50 KG force gauge with ZN5S digital panel meters (Bengbu city Zhongnuo Sensor Ltd.). Electrical performance of TENG including open circuit voltage (V_{oc}), short circuit current (I_{sc}) and charge (Q) was mainly evaluated by Keithley 6514 electrometer. Load matching analysis was performed with a series of various loads (10, 100, 1k, 10k, 100k, 1M, 10M, 100M, 200M and 300M Ω). The charging performance of TENG was evaluated with different capacitors (0.22, 1, 2.2, 10 and 22 μF).

(h) Dielectric property

The capacitance of the pristine and composite films with the sample size of 1.5 × 1.5 cm^2 was recorded by Agilent 4294A Precision impedance analyzer. Through the conversion of capacitance to relative permittivity, the electron-holding tendency of sample films can be examined.

The relative permittivity of materials can be assessed by the measurement of capacitance using LCR meter and the following equation:

$$C = \varepsilon_0 \cdot S\frac{\varepsilon_r}{d}$$

, where C, ε_0, ε_r, S and d represent capacitance, vacuum permittivity (8.854×10^{-12}), relative permittivity, electrode surface and thickness of film specimen, respectively.

4 Catechol-Based Pigmentation

4.1 Introduction

With the increasing public awareness of eco initiatives, technologies aimed for sustainable development are eagerly pursued in different fields. Green chemistry has been contributing to the future of sustainability, and it emphasizes on the characteristics like elimination of hazardous materials and organic solvents, enhancement of reaction efficiency, minimization of toxic waste production, and mild reaction conditions with lower temperature and pressure [12, 13]. To achieve these goals, biomimetics is an attractive approach since nature demonstrates numerous fascinating biological phenomena with perfectly optimized characteristics [16-18]. These phenomena are highly eco-benignant after long evolution process, which can be utilized for the development of green technologies.

Recently, marine mussel adhesion has been extensively studied due to their versatile adhesiveness on almost every kind of substrates including adhesion-resistant Teflon surfaces [123, 124]. Intensive research on this adhesion revealed that the rich presence of catechol moiety in 3,4-dihydroxy-L-phenylalanine (DOPA) is believed to be responsible for the versatile adhesion via multiple physicochemical interactions such as oxidation-induced crosslinking, hydrogen bonding, π-π stacking and other bond formation [125, 126]. With an akin chemical structure and physicochemical properties of catechol moiety as DOPA, dopamine has been widely used as a mussel-inspired material in many applications including textile coloration [127-129], functional polymer coating [130-133], water treatment [134, 135], drug delivery [136-138] and cosmetics [139]. These studies have succeeded in reproducing the

main features of mussel adhesion and verified the high application feasibility. Catechols with an ortho-dihydroxyphenyl structure can readily form oxidation-induced pigmentation under mild conditions [140-142]. To mimic the natural formation of colour, catechols can be oxidized into catecholic radicals and quinone forms, which may further couple with themselves or exogenous molecules to form heteromolecular compounds via radical rearrangement and nucleophilic reactions [143, 144]. These would alter the related chemistry of catechols, thus showing different physicochemical functionalities of the generated chromophores [145]. In addition, naturally originated catechols like plant-derived phenolic acids are safe to be used even in the production of food colorants [146-148] and antioxidants [149]. Therefrom, catechols attract great interest in various adhesive applications, which can simultaneously fulfill the requirement of green chemistry and functionalities.

Textile coloration is known as one of the major contributors to water and air pollution in textile wet processing [150]. The conventional textile coloration process usually produces huge amount of wastewater containing high concentration of residue colorants and dyeing auxiliaries; involves high energy consumption in the relatively high temperature dyeing processes. Severe pollution arising from dyeing process has posed risks to environment, wildlife, and humans. The consequences of textile processing activities have driven the sustainable development in textile production. The integration of catechol chemistry into textile coloration technology has already been proposed. For instance, the employment of plant-derived catechols can efficiently eliminate the use of synthetic colorants and metal-containing mordanting agents for fixation, and also require no complicated extraction process of natural colorants and high energy-consuming dyeing conditions.

Continuing our research interests [127-129, 151, 152], we herein report the development of mussel-related adhesive pigmentation under room temperature using a naturally occurring catechol. Caffeic acid (CA) widely exists in a variety of plants, such as illicium verum, sunflower seed, and salvia officinalis [153, 154]. This phenolic acid possesses similar catechol and carboxylic structures as DOPA and dopamine, and thus it can show similar physicochemical properties. In contrast, CA has comparatively lighter inherent colour, allowing the formation of a more diverse colour range for catechol coating. Furthermore, studies suggested that amino acids could involve in the formation of natural pigments with quinones [155, 156]. Common amino acids have different chemical moieties in their side chains, which implies that they may have various reactivities towards quinones. Therefore, we aimed to study the pigmentation of catechol with different types of amino acids. The biomimicking pigmentation of CA was first characterized in aqueous solution and the heteromolecular pigmentations with a variety of amino acids were also carefully explored under different experimental parameters. Then, the application feasibility of these pigmentations on wool fabrics was fully studied, and the performance of the pigments adhered on fabrics was further evaluated.

4.2 Results and Discussions

CA as a kind of catechol can be induced by periodate to undergo complicated reactions. These reaction processes are susceptible to the influence of various parameters including solution pH, reactant concentration, reaction time and presence of nucleophiles. To enhance the controllability of the catechol-based pigmentation under different influences, the catechol reaction process was first investigated and optimized using few typical amino acids selected

according to their side chain characteristics, of which have electrically charged, hydrophobic, cyclic, aromatic, indolic, thiol or no side chains [157].

4.2.1 Colour formation

4.2.1.1 pH influence

The influence of pH on the colour formation of catechol was first investigated since the formation of quinones are usually affected by the solution pH. This may affect the electrophilicity of catecholic ortho-quinones, and therefore their reactions with nucleophilic agents such as amino, imino and thiol groups on amino acids, resulting in different coloured products. The solution of CA had a prominent absorption at ca. 400 nm showing a yellow colour (Figure 4.1(a)). Its absorption spectra and colour had no obvious changes across different pH values. Similar to the CA solution, the addition of Lys insignificantly changed the pH dependence of the colour formation in the catechol solution (Figure 4.1(b)). Nevertheless, the addition of other amino acids like Gly and Pro could increase the pH dependence of the colour formation. Specifically, the absorbance of CA solution with Gly had no obvious changes between pH 5 to 7, and the solution colour started to show obvious changes beyond pH 8 (Figure 4.1(c)). The maximum absorbance has shifted to ca. 600 nm when the pH reached 9. Concomitantly, the solution colour changed from yellow to reddish brown and to blue with increasing pH. As for the solution with Pro, its absorbance increased slightly between pH 5 to 8 (Figure 4.1(d)). In contrast, the absorbance showed a slight bathochromic shift and a significant increase in absorbance level at pH 9, from about 0.4 to 1.0. Meanwhile, the solution colour altered from reddish brown to purple with increasing pH. The differences found in Lys, Gly and Pro could be possibly explained by the differences in their side chains. Lys has an

amino side chain group having pKa 10.67, which is much higher than most of the other amino acids [158]. Thus, it remained to be protonated form at the reaction pH 5 to 9, and carried positive charges during the reactions with catechol. In theory, the greater the positive charge the moiety had, the less likely an atom would give up its pair of electrons to form a bond. Therefore, less reaction phenomenon could be observed in the case with Lys. To conclude, the higher degree of variations in solution at pH 9.0 were expected because catecholic ortho-quinones formed could react with amino acids more easily under higher pH conditions, and thus showed different colour formation than those under lower pH conditions.

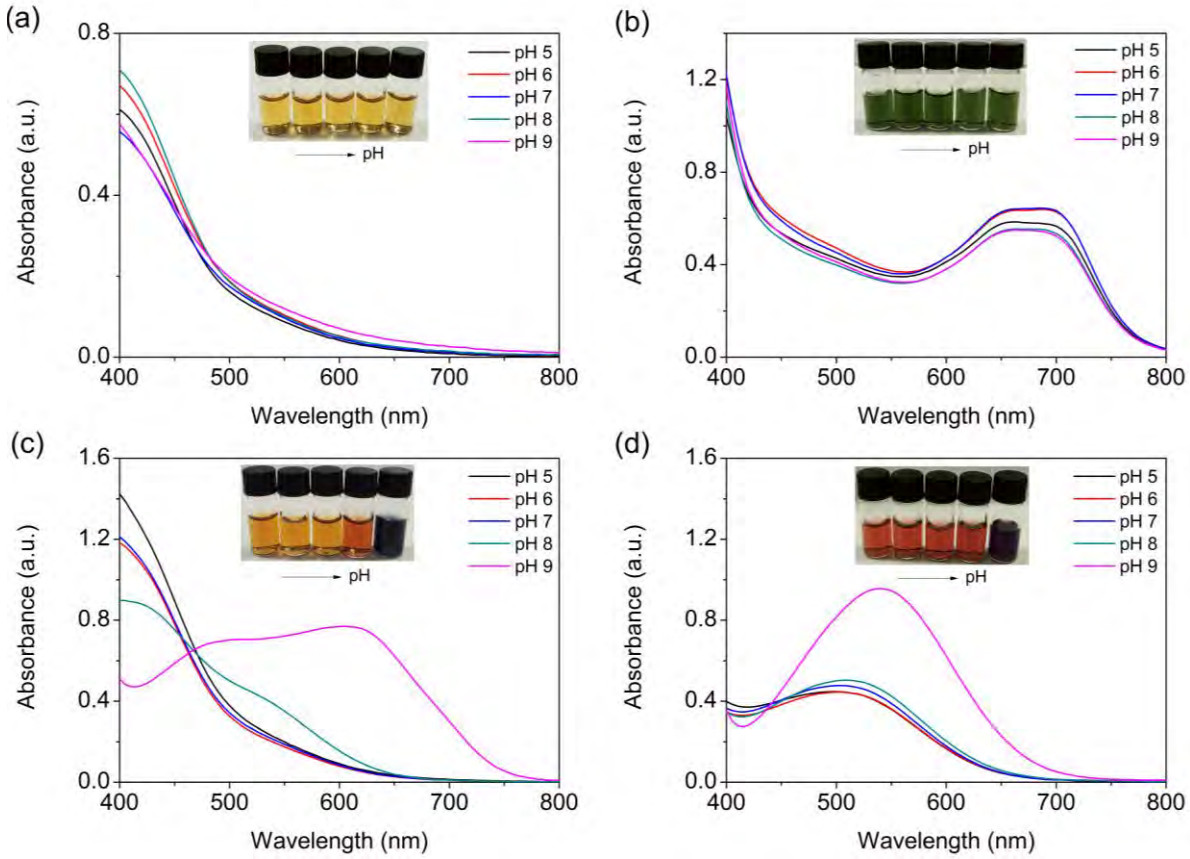

Figure 4.1 pH influence on UV-Vis absorption spectra of (a) CA, (b) CA with Lys, (c) CA with Gly, and (d) CA with Pro after 1 hour

4.2.1.2 Molar concentration influence

The concentration ratio of reactants is a crucial factor affecting the reaction rate and colour strength. The solution absorbance of CA with Lys showed a growing trend when the molar concentration increased from 6:25 to 6:150 (Figure 4.2(a)). The solution colour became darker progressively with a maximum absorption peak at ca. 690 nm remaining unchanged. However, the solution absorbance gave a lower absorbance intensity and hypsochromically shifted to ca. 665 nm when the molar ratio was further increased to 6:200. One of the possible reasons was that the excessive amount of amino acid prohibited the reaction rate of catechol, leading to a decrease in the formation of catechol-amino acid pigment. In another case, the solution absorbance of CA with Gly generally showed a similar growing trend until the molar concentration reached 6:200 (Figure 4.2(b)). The solution with the molar ratio of 6:25 had a maximum absorbance peak at ca. 500 nm with a reddish brown colour. It is interesting to note that the solution had a new shoulder absorption band at around ca. 600 nm with a blue colour when the molar ratio reached 6:50. The absorbance attained maximum with the molar ratio of 6:150. The results implied that the molar concentration of CA and amino acids could affect the molecular interaction between catechol and amino acids, serving as a parameter to adjust the colour depth.

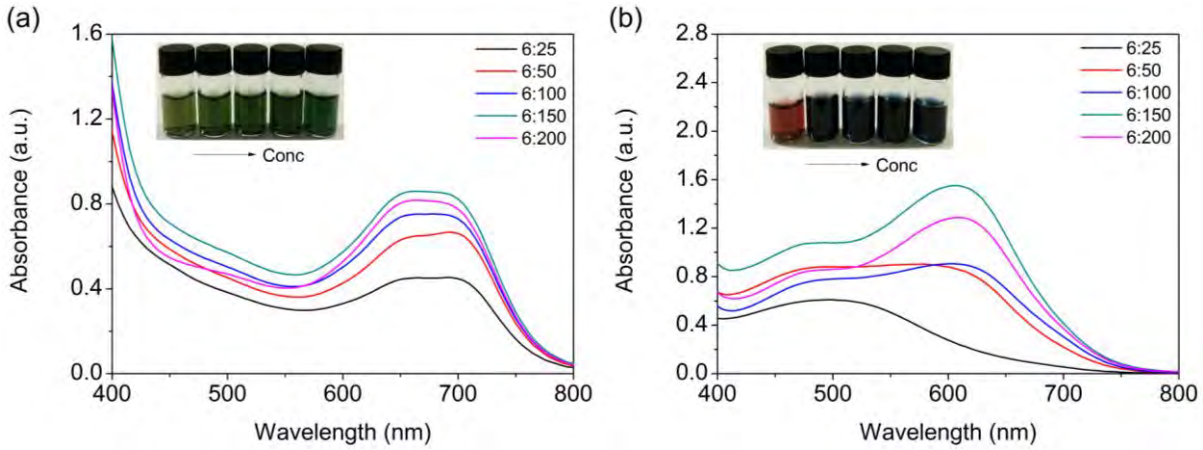

Figure 4.2 Molar concentration influence on UV-Vis absorption spectra of (a) CA with Lys and (b) CA with Gly after 1 hour

4.2.1.3 Time dependence

Reaction time is an important indicator for the reaction rate and efficiency. The changes in visible absorbance of CA with Lys and Gly were continuously recorded, as shown in Figure 4.3. For CA with Lys solution, it could be seen that the absorbance at ca. 660 nm generally increased, and the solution colour became deeper progressively with the extension of reaction time (Figure 4.3(a)). The solution of CA with Lys showed an unobvious shift in spectral band position along the reaction period, implying that the process was reaching an equilibrium at an earlier stage. For CA with Gly solution, the absorbance revealed a bathochromic shift with time extension (Figure 4.3(b)). The solution colour progressively changed from red, purple and to blue. The reaction process attained an equilibrium after 1 day. The results demonstrated that reactions of catechol with different amino acids could have different time dependency.

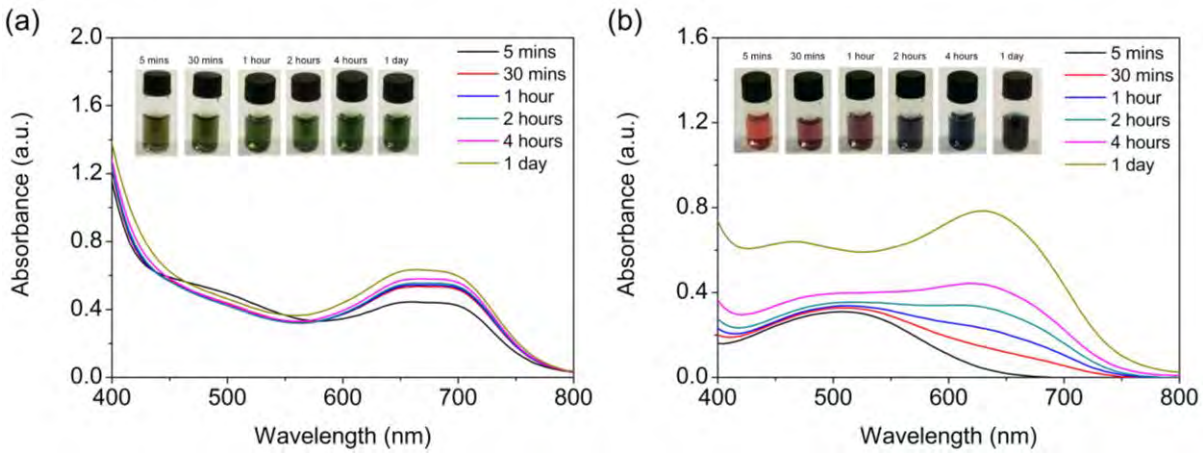

Figure 4.3 Time influence on UV-Vis absorption spectra of (a) CA with Lys and (b) CA with Gly

4.2.1.4 Amino acids influence

We have previously noted that nucleophilicity of amino acids could contribute to the colour changes of the catechol solution. Therefore, it is worth investigating the tunability of amino acids in the colour formation. Seven amino acids including Arg, His, Lys, Gly, Leu, Phe and Met could tune the colours of CA solution into various green or blue hues (Figure 4.4(a)). Their solutions had obvious absorption bands beyond 600 nm and the maximum absorption peaks located at ca.700, 645, 665, 615, 630, 625 and 630 nm, respectively. In contrast, the presence of other amino acids like Asp, Glu, Pro and Trp could induce various yellow or brown colours in CA solution (Figure 4.4(b)). Besides, majority of the remaining solutions had no obvious maximum absorption peaks. These results suggested that the colour formation could be efficiently modified through reacting catechol with various amino acids of different reactivities.

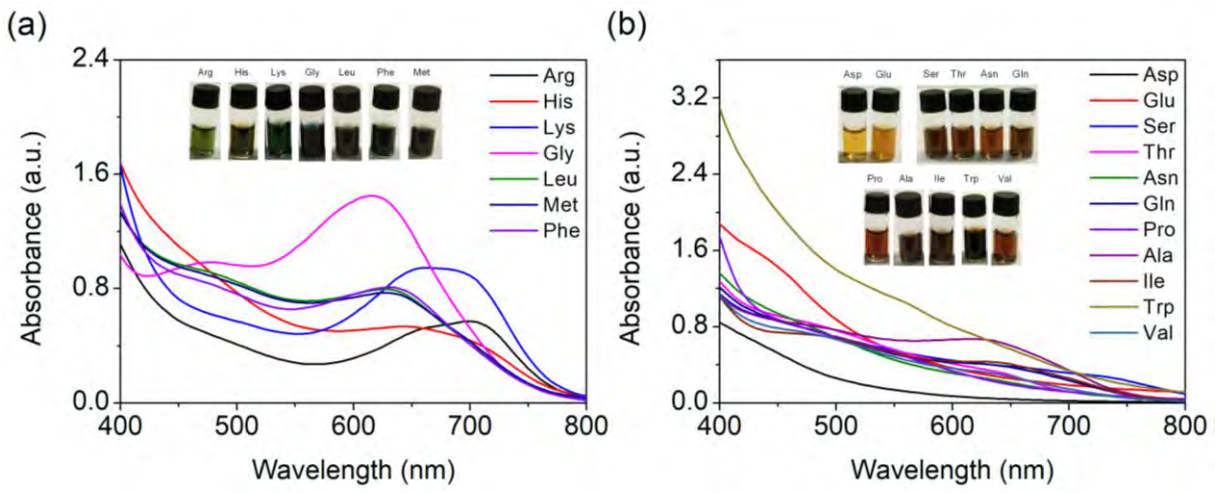

Figure 4.4 UV-Vis absorption spectra of CA with amino acids showing (a) green and blue colours; (b) yellow and brown colours after 24 hours

4.2.2 Catechol-amino acid pigmentation on textile material

Encouraged by the high tunability of catechol-amino acid pigmentation, we then explored the application of this natural-inspired colorants on textile coloration with the optimized conditions. It has been found that this heteromolecular pigments successfully adhered on the textile materials. To further enhance the adsorption of catechol-amino acid pigment on textiles, other parameters like buffer concentration and fibre pretreatment were probed.

Tris influence on textile coloration

Tris buffer concentration could be a capable tuning factor for the catechol-amino acid pigmentation. Some studies have suggested that Tris as a conventional buffer involved in the catechol reactions, in which it together with nucleophilic reactants target the reactive quinone forms [159, 160]. Therefore, it was predicted that the interaction between Tris and catechols could interfere the reactions between amino acids and catechols, leading to different colour

formation. When Tris buffer concentration of CA with Gly solution increased from 1 mM to 10 and 100 mM, a bathochromic shift to 620 and 645 nm was induced with colour changing from brownish green to blue (Figure 4.5(a)). It was also found that the absorbance level of 10 mM Tris buffer was relatively higher than that of 1 and 100 mM. For CA with Phe solution, a similar absorption trend and absorption intensity could be observed. The solution had a yellow colour in 1 mM Tris buffer, but blue and brown colours in 10 and 100 mM Tris buffers with the absorption bands bathochromically shifting to ca. 640 and 685 nm (Figure 4.5(b)). These findings possibly reflected that low concentration of Tris might inefficiently induce the quinone formation from catechol due to fairly low buffer capacity, which delayed the chromophore formation process. On the contrary, excessively high concentration of nucleophilic Tris possibly competed with amino acids to participate in the reaction with catechol, leading to an adverse effect on the chromophore formation. It was concluded that buffer concentration could be an alternative tunable factor for catechol-based pigmentation.

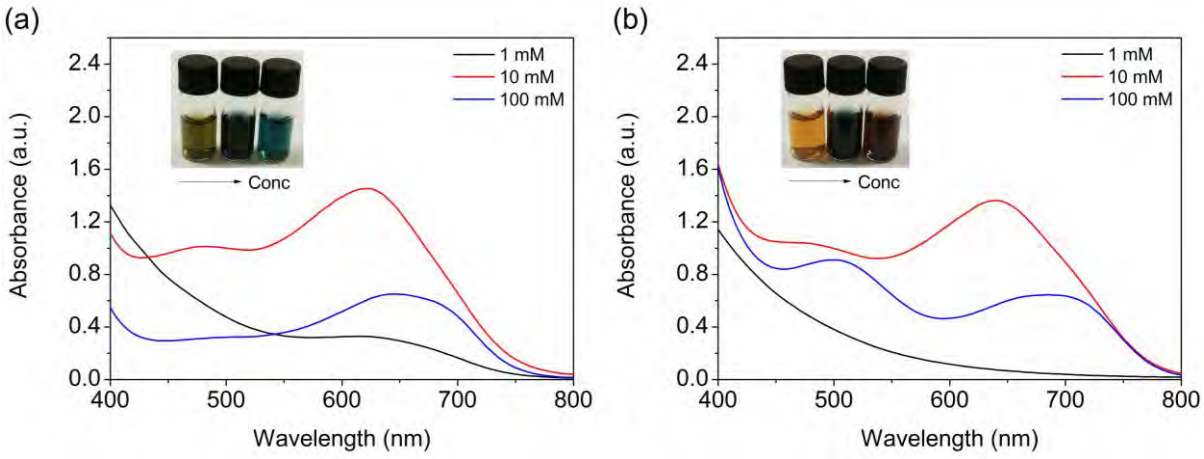

Figure 4.5 Buffer concentration influence on UV-Vis absorption spectra of (a) CA with Gly and (b) CA with Phe after 24 hours

With the support of the aforementioned results (*Section 4.1 - 4.5*), catechol-amino acid pigmentation was proved to be a simple and tunable process for colorant formation. The

adhesive pigments manifested the feasibility of coating textile materials with attractive appearance. Hence, the application of catechol-based pigments on textile materials under optimum coloration conditions was studied. Fabrics dyed in 10 mM Tris buffer displayed a comparatively higher depth of shade than that dyed in 1 and 100 mM Tris buffer. This was in line with the greater amount of pigments formed in 10 mM buffer concentration. Nevertheless, different buffer concentrations could still present the ability to alter the colour formation on substrates. CA with Gly could tune the fabric to pale green, cyan and pale green colours with increasing buffer concentration (Figure 4.6(a)). Besides, CA with Phe could endow fabric with light orange, olive green and dark orange colours (Figure 4.6(b)). Furthermore, EDC pretreatment could enhance the colour strength of the dyed wool fabrics. As verified by the control experiment, the EDC-treated wool fabric could be dyed with a deeper shade when compared with the untreated one (Figure 4.6(c)). This result could possibly be attributed to the activation of carboxylic groups on wool, which promoted the coupling of wool fibers with the oxidized catechols [113].

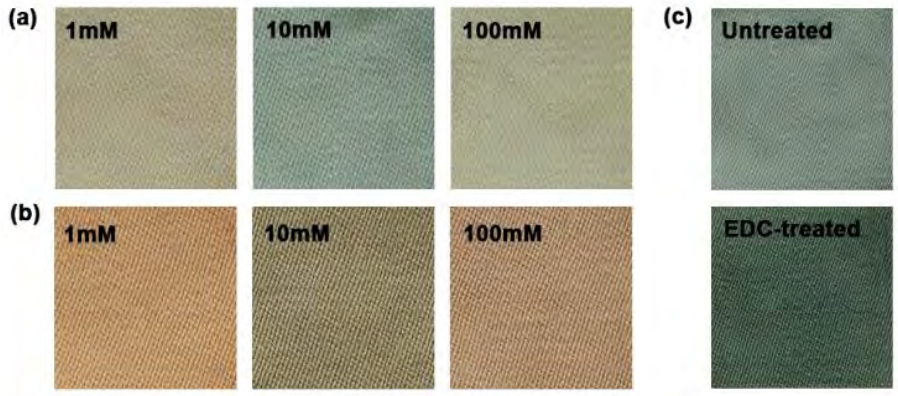

Figure 4.6 Photographic images of dyed wool fabrics: (a) CA with Gly in 1, 10, 100 mM tris, respectively; (b) CA with Phe in 1, 10, 100 mM tris, respectively; (c) treated and untreated wool fabrics dyed with CA and Gly

Based on the discoveries of recent research studies [22, 161, 162], it is difficult to clearly explain our experimental phenomena with a simple mechanism due to the complexity of the catechol reactions involved. However, several widely accepted chemosorption and physisorption mechanisms have already been proposed. Catechol can exhibit versatile adhesion mechanisms, including both non-covalent and covalent interactions such as hydrogen bonding, π-π stacking, cation-π interaction, crosslinking polymerization and covalent bonding through Michael addition or Schiff base [126, 163, 164]. In our study, the oxidation of catechol CA could generate metastable radicals and reactive quinone forms, which might be prone to free radical aryl-aryl coupling and nucleophilic reactions [165, 166], as presented in Scheme 1(a). Highly reactive o-quinones possibly reacted with nucleophilic amino groups of amino acids to form adducts, and continued to have intermolecular self-crosslinking to form a mixture of reaction products [22, 125, 162]. Concurrently, CA polymers or CA-amino acid adducts had chances to adhere to the protein substrate with their catechol or quinone moieties through π-π interaction, hydrogen bonding or covalent bonding [167], as illustrated in Scheme 1(b). Minor adhesions like hydrophobic interaction and cation-π interaction between catechol ring and NH_3^+ on protein fibres might also occur [168]. Multiple physicochemical interactions allowed catechol-amino acid pigments to firmly deposit on the fibre substrate.

(a)

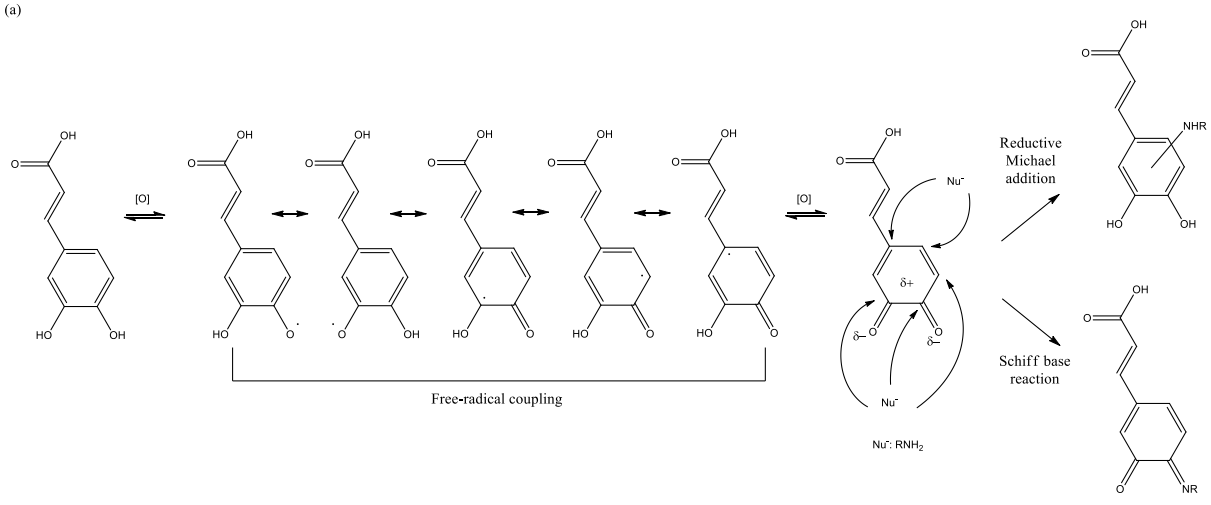

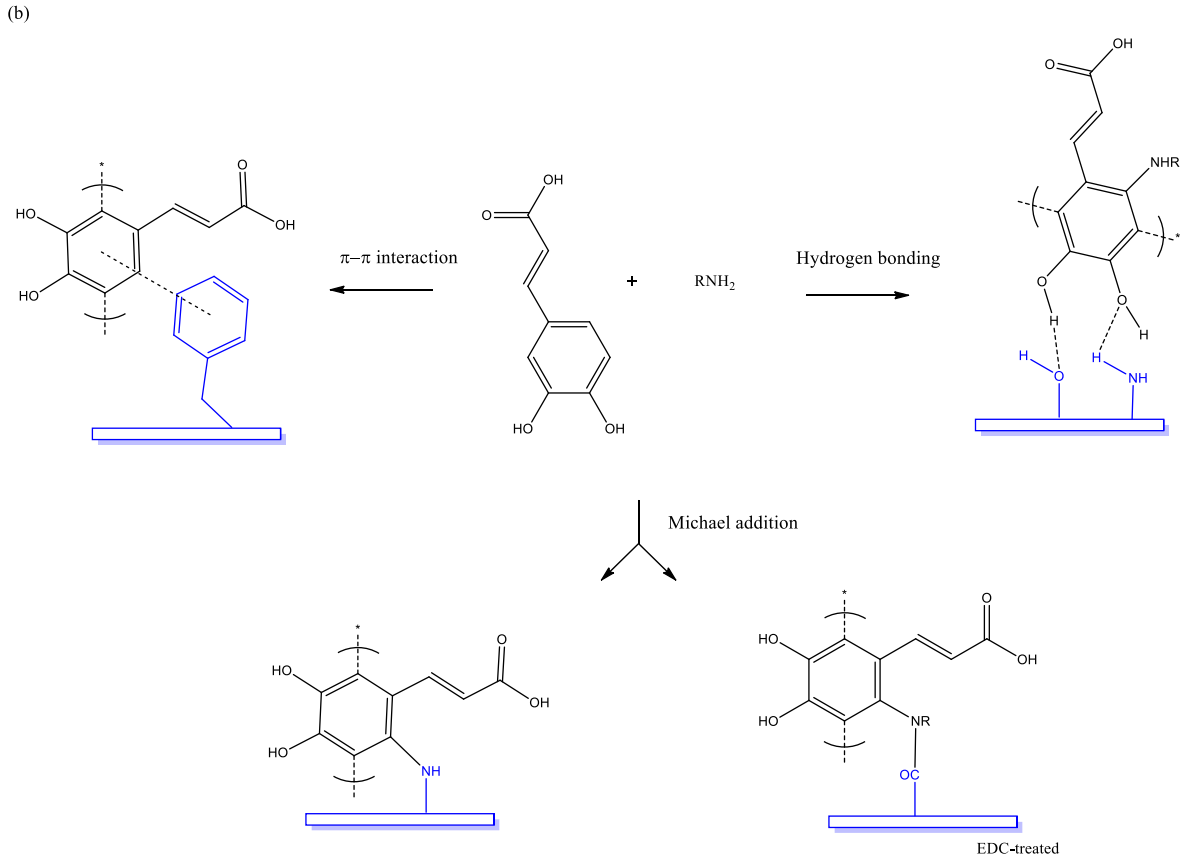

Scheme 1 (a) Possible reactions of oxidized CA, (b) Proposed scheme of chemosorption and physisorption of CA with amino acid on wool substrate [22, 126, 164, 165, 169-171]

To further illustrate the coloration mechanism, Raman spectra of untreated, catechol-treated and catechol-amino acid treated wool were invested. As shown in Figure 4.7(a), untreated wool fibre showed strong amide bands at 1685, 1605 and 1230-1260 cm^{-1}, which could be assigned to the typical structures of wool material [172]. After the introduction of CA, new bands emerged particularly at 1491, 1468, 1416, 1312 and 1251 cm^{-1} likely corresponding to the catechol ring vibrations [173]. For the pigmentation between CA and Met on wool, bands induced at 1071, 702 and 690 cm^{-1} could be attributed to the C-N and C-S stretching of Met [174-176]. In addition, increasing intensity at c.a. 1604 cm^{-1} corresponding to aromatic C=C might indicate the Michael addition of nucleophiles to the catechol ring, suggesting the possible formation of CA-Met adducts [177]. The small band appeared at 1630 cm^{-1} could be assigned

to C=N stretching, originating from the lower occurrence of Schiff base reactions [169, 178]. The colour depth of CA treated material was comparable to that treated with CA and Met, yet the intensity of most bonding regions found in CA was less significant than that of CA with Met. This might imply that some physisorption also participated in the adhesion.

The catechol-amino acid pigments were revealed to be better immobilized on the EDC-treated materials. This was because water-soluble carbodiimides could activate the carboxylic groups of the fibres through the formation of active o-acylisourea intermediates [179], which could further promote the stable amide linkage formation between the material and nucleophilic pigments [112, 180]. The appearance of o-acylisourea groups in the wool structure could be confirmed by the FTIR spectra (Figure 4.7(b)). The characteristic peaks observed at 1633, 1518, 1230 and 1164 cm^{-1} assigning to the C=O, C=N, C-N and C-O stretching vibrations were enhanced [181, 182]. The changes indicated the reaction between EDC and wool fibres.

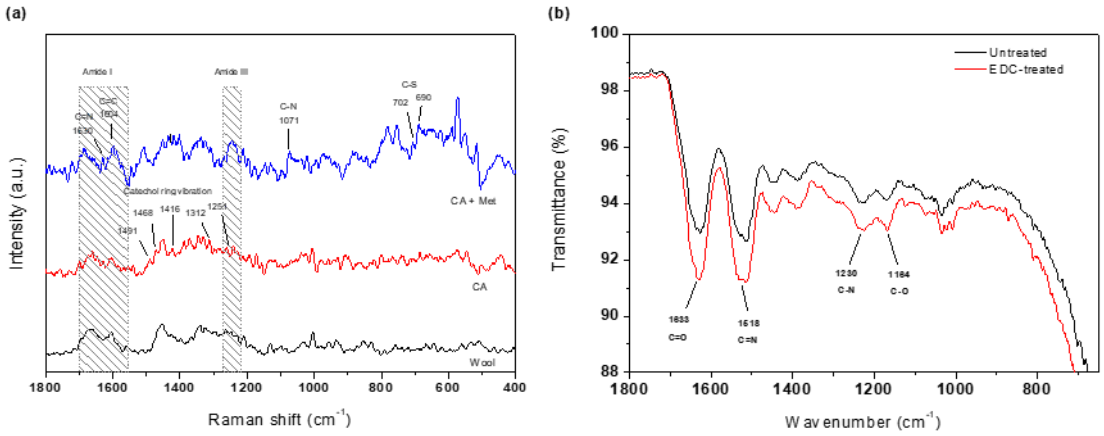

Figure 4.7 (a) Raman spectra of untreated and dyed material, (b) FTIR spectra of untreated and EDC-treated material

4.2.3 Properties of dyed materials and performances of pigmentation process

4.2.3.1 Colour analysis

Wool fabric coloration was successfully attempted via the developed catechol-based pigmentation method. It is worth noting that the introduction of 11 amino acids could efficiently tune the colours of the wool fabrics. Despite the remaining amino acids being less favourable to coloration, the results undoubtedly proved the potential application of catechol-amino acid pigments on textile substrates. As shown in Figure 4.8, the catechol pigment solely could dye wool fabric with beige colour. Through the incorporation of several amino acids including Pro, His, Asp, Glu and Trp, the catechol-amino acid solution could endow wool fabrics various brown shades. In contrast, the incorporation of other 6 amino acids including Asn, Ile, Phe, Met, Leu and Gly could respectively tune the wool fabric into different grey, green and blue shades. The samples dyed with pigments could exhibit a different pattern of visible light absorption, originating from pigment's chemical structures, especially the conjugated pi systems [183]. With the presence of Phe, Met, Leu and Gly, the samples showed clear peaks in the absorption band range from ca. 643 to 665 nm, corresponding to the blue-green region of perceived colour [184]. With the presence of other amino acids, the materials generally had bands across the visible light spectrum with no obvious peaks, contributing to brown and dull colours observed [185]. In addition, the significant increase in UV absorption bands might be ascribed to the unsaturated and aromatic moieties of catechol-amino acid pigments adhered on the fabric surface.

Figure 4.8 The photographic images of the dyed wool fabrics: (a) Blank; (b) CA only; (c) CA with Pro; (d) CA with His; (e) CA with Asp; (f) CA with Glu; (g) CA with Trp; (h) CA with Asn; (i) CA with Ile; (j) CA with Phe; (k) CA with Met; (l) CA with Leu; (m) CA with Gly

This intriguing tunability of amino acids on colour appearance of wool fabrics was illustrated with the colorimetric findings, as listed in Table 4.1. Upon the incorporation of amino acids to catechol, the colorimetric scales L*, a*, b*, C* and h* of dyed fabrics were obviously changed. It could be seen that wool fabrics dyed with both catechol and amino acids had lower L* values than that dyed with catechol only, implying that amino acids could enhance colour formation on fabrics. In addition, catechol-amino acid pigments could improve the shade depth of dyed fabrics, which was basically consistent with their K/S (at the wavelength of maximum absorbance) values. It was found that the incorporation of Asp and Glu could tune the fabrics with redder hues (higher a* value), while that of Gly, Leu, Met and Phe afforded greener hues (lower a* value). Furthermore, introducing Asp, Glu, Trp, Pro and His tuned the fabric with yellower hues (higher b* value). On the contrary, introducing other amino acids such as Gly, Asn, Ile, Leu, Met and Phe gave the fabric colours much bluer hues (lower b* value). The C* values revealed that the brown shades of catechol-amino acid colorants could endow fabrics with a relatively vivid appearance. In contrast, the grey, blue and green shades of catechol-amino acid pigments endowed fabrics with a duller appearance. All these colorimetric results

of the obtained colours were consistent with the photographic images of dyed wool fabrics in Figure 4.8. The results have therefore demonstrated the perceived colours of catechol-based pigmentation formed on textile materials.

Table 4.1 Colorimetric measurement of dyed wool fabrics

Components	L*	a*	b*	C*	h*(°)	ΔL*	Δa*	Δb*	K/S
CA only	71.5	6.2	10.2	11.9	58.7	-	-	-	2.3
With His	60.0	3.6	11.6	12.1	72.8	-11.5	-2.6	1.4	3.3
With Asp	52.6	10.3	22.3	24.6	65.2	-18.9	4.1	12.1	6.8
With Glu	50.0	11.3	24.5	27.0	65.2	-21.5	5.1	14.3	8.8
With Asn	57.2	1.0	3.0	3.2	71.6	-14.3	-5.2	-7.2	3.2
With Gly	63.3	-2.8	-3.3	4.3	229.7	-8.2	-9.0	-13.5	2.0
With Pro	58.9	3.8	12.4	13.0	73.0	-12.6	-2.4	2.2	3.5
With Ile	57.7	1.4	2.6	3.0	61.7	-13.8	-4.8	-7.6	3.0
With Leu	56.2	-1.6	-1.6	2.3	225	-15.3	-7.8	-11.8	2.9
With Met	57.3	-2.6	1.2	2.9	155.2	-14.2	-8.8	-9.0	3.0
With Phe	62.8	-0.8	3.1	3.2	104.5	-8.7	-7.0	-7.1	2.7
With Trp	51.5	3.6	18.9	19.2	79.2	-20	-2.6	8.7	7.7

4.2.3.2 Microscopic analysis

To further investigate the dyeing properties of catechol-amino acid pigments on wool fabrics, the dyed yarns were studied via microscopic analysis. According to Figure 4.9, it could be clearly seen that interior fibres of the dyed yarns showed reddish brown, beige or blue colours, which exhibited a noticeable difference from the original pale grey colour of the blank yarns. In addition, the surface morphology of fibres was studied using scanning microscopy. It could be found that the blank fibres generally had a smooth surface with sharp scales (Figure 4.10(a)). The EDC-treated fibre surface resembled the untreated one, indicating that the pretreatment

caused insignificant effect on fibre surface morphology (Figure 4.10(b)). However, the fibre surface morphology was distinctly changed after the fabrics were dyed with catechol and amino acids. The sharpness of scales on the treated fibres became less prominent and the roughness on the fibre surface was clearly increased (Figure 4.10(c-d)). Furthermore, this was more significant in the case of CA with Trp. The rough coating formed on the fibre surface also led to higher surface area exposure, causing the treated material more susceptible to abrasion. Besides, the decrease in lightness and increase in colour depth could be ascribed to the rough coating formed on the fibre surfaces, which had higher absorption and scattering of light. The evident contrasts in their cross-sections and surface morphology fully confirmed the successful dyeing of fabrics with catechol-based pigments. The deposition of catechol and catechol-amino acid pigments could also affect their appearance and performance.

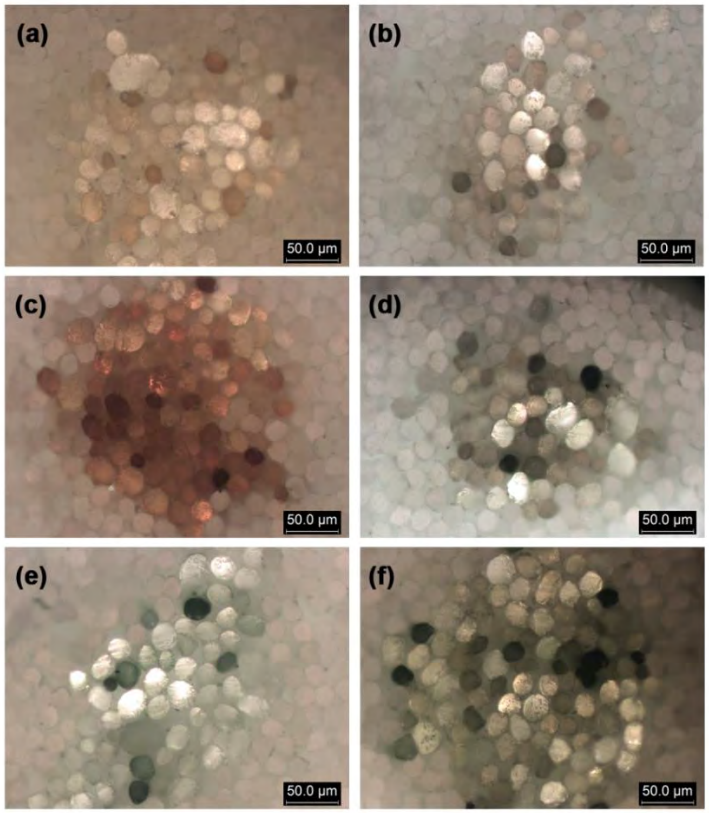

Figure 4.9 Micrographs of wool yarn cross-sections: (a) CA only; (b) CA with His; (c) CA with Glu; (d) CA with Asn; (e) CA with Gly; (f) CA with Met

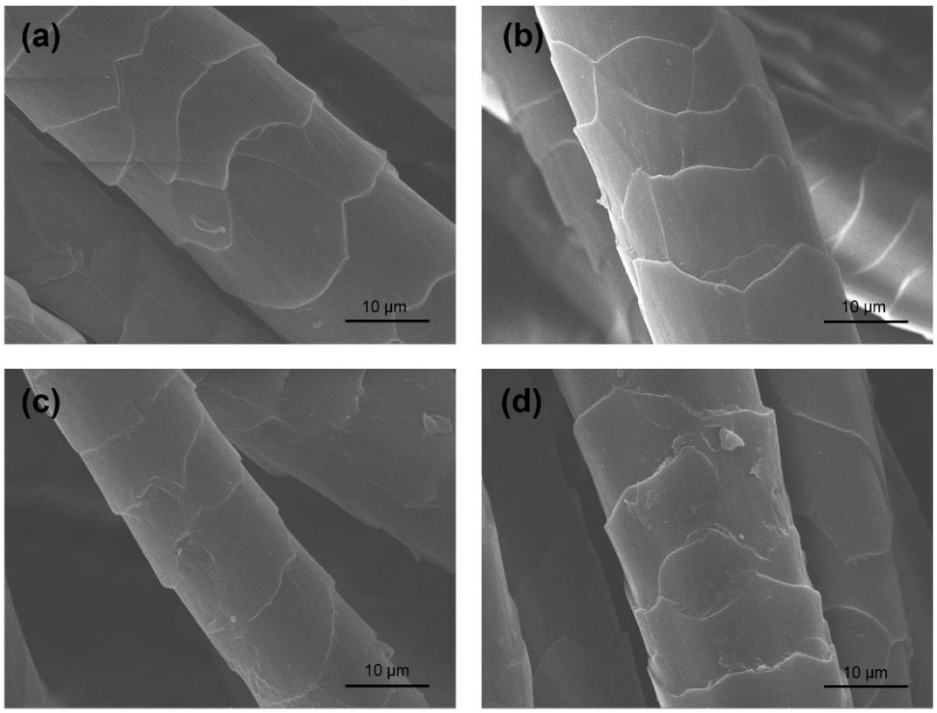

Figure 4.10 SEM images of wool fibres: (a) Untreated blank; (b) EDC-treated blank; (c) CA; (d) CA with Trp

4.2.3.3 Colour fastness

The colour fastness of fabrics dyed with catechol-amino acid pigments was evaluated according to the AATCC standardized procedures, as listed in Table 4.2. The ratings of colour change after laundering were in the range of 4-4/5 for most dyed samples, and 3-3/4 for the dyed samples in the presence of His, Gly, Met, Phe and Trp. This meant that only small or moderate amount of pigments was lost during the laundering process, indicating good or acceptable immobilization of catechol-amino acid pigments on fibres. For colour staining evaluations, almost all the dyed samples attained the highest rating of 5, except for the sample dyed with CA with Trp having moderate ratings of 3/4-4 on nylon, cotton and acetate. This was in line with the rougher fibre surface found on this treated sample (*Section 4.2.3.2*). For

crocking fastness, all the samples dyed with catechol-amino acid pigments achieved 4-5 ratings for dry crocking fastness. Most dyed samples scored 4/5 for wet crocking fastness, except for CA with Asp, Glu and Trp. These combinations were previously revealed to have higher colour depth (*Section 3.2.3.1*). The catechol-amino acid pigments could be well retained after the vigorous laundering and crocking conditions, which demonstrated the strong adhesiveness of the pigments towards the substrate. Unlike most of the other natural dyeing process, good colour fastness could be achieved without the use of mordanting agents.

Table 4.2 Fastness evaluation of the dyed wool fabrics based on AATCC 61-2010 2A and AATCC 8-2016

Components	Laundering fastness							Crocking fastness	
	Colour change	Staining						Dry	Wet
		Wool	Acrylic	Polyester	Nylon	Cotton	Acetate		
CA only	4/5	5	5	5	5	5	5	4/5	4/5
With His	3/4	5	5	5	5	5	5	5	4/5
With Asp	4	5	5	5	5	5	5	4/5	2/3
With Glu	4/5	5	5	5	5	5	5	4	2/3
With Asn	4	5	5	5	5	5	5	4/5	4/5
With Gly	3	5	5	5	5	5	5	5	4/5
With Pro	4	5	5	5	5	5	4/5	5	4/5
With Ile	4	5	5	5	5	5	5	5	4/5
With Leu	4	5	5	5	5	5	5	5	4/5
With Met	3/4	5	5	5	5	5	5	5	4/5
With Phe	3	5	5	5	5	5	5	4/5	4/5
With Trp	3/4	5	5	5	3/4	3/4	4	4	3

For practical applications, it is essential to consider the safety, ease of production and integrability of the catechol-amino acid pigmentation on textile materials. Therefore, the

cytotoxicity of the treated textiles, the reproducibility of the pigmentation, the integration between exhaust dyeing and cold-pad batch were probed.

4.2.3.4 Cytotoxicity assay

To assess the potential of catechol-amino acid pigments as textile colorants, the cytotoxicity of the pigments on wool fabrics was therefore evaluated with mouse fibroblast cells. Catechol and its combinations with different amino acids of various side chains were selected for the pigmentation on textile materials, and these samples were then undergone cytotoxicity assay. As shown in Figure 4.11, nearly all samples treated with different catechol-amino acid combinations exhibited good cell viability of more than 85%, which indicated that the pigmentation produced insignificant alternation to the cell viability. Since the result has showed negligible harmful effect on the cell lines, the safety in the use of catechol-amino acid pigments on textiles was preliminarily confirmed.

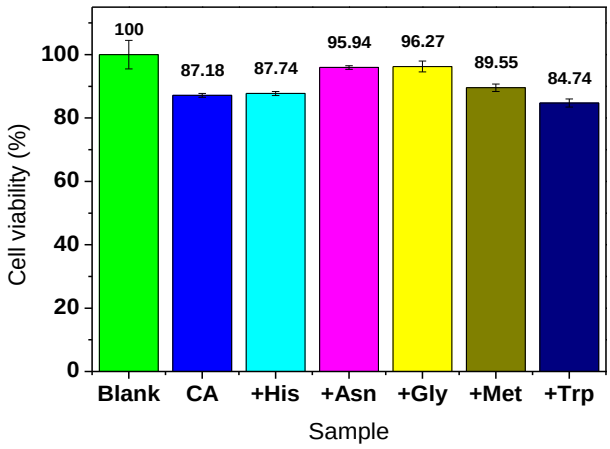

Figure 4.11 Effect of catechol-amino acid pigmentation on the viability of mouse fibroblast cells

4.2.3.5 Batch-to-batch reproducibility

The reproducibility of catechol-based pigmentation is a crucial criterion for mass production. Since the degree of interactions between catechol-amino acid pigments on textile substrates might be susceptible to the environmental conditions, the colour difference of wool fabrics dyed in different batches should be investigated. As listed in Table 4.3, the delta E difference between dyed fabrics of different batches were below 2, which implied that the colour difference was only obvious and perceptible with very close observation. The result suggested that the colour appearance on wool fabrics dyed with catechol-amino acid pigmentation could be successfully reproduced with acceptable variation. As shown in Figure 4.12, the reflectance curves of the samples resembled each other, also indicating that fabrics dyed in different batches had similar object colours.

Table 4.3 Colorimetric measurement of samples dyed with CA and Gly in different batches

Components	L*	a*	b*	ΔE*
Sample 1	56.37	-1.64	2.82	-
Sample 2	57.00	-1.92	1.85	1.19
Sample 3	56.98	-1.61	1.95	1.07
Sample 4	57.02	-1.72	1.13	1.81
Sample 5	56.08	-2.04	1.31	1.59

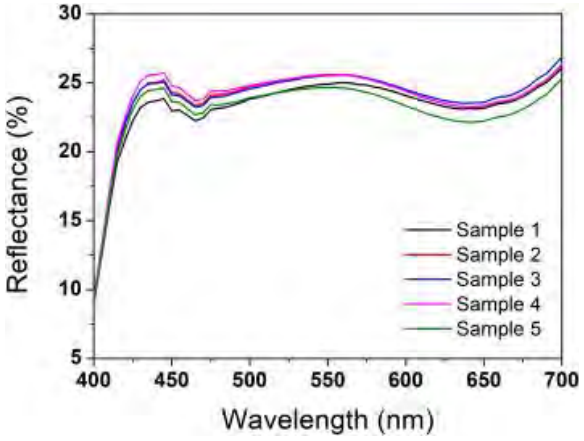

Figure 4.12 Reflectance curves of samples dyed with CA and Gly in different batches

4.2.3.6 Cold pad batch

The integrability of catechol-based pigmentation method with other sustainable technologies is worth investigating since this may offer synergistic advantages. The feasibility of cold pad-

batch dyeing with catechol-amino acid pigments could open a novel sustainable direction for textile coloration through preserving the colorants and water. As shown in Figure 4.13, wool fabrics could be successfully dyed with different colours by padding with different catechol-amino acid combinations. This preliminary result has verified the potential of applying CA with amino acids on textile fabrics via cold pad-batch method. However, colour discrepancy found between exhausted and padded fabrics could be attributed to the limited solubility of the reactants in padding solution. Therefore, further study is needed to deduce concentration proportions for a wider range of colour.

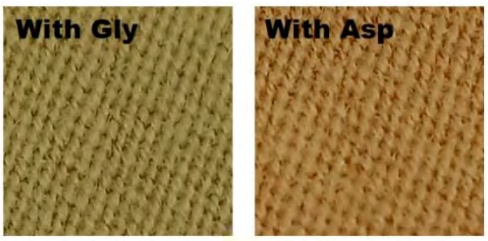

Figure 4.13 The photographic images of the padded wool fabrics: CA with Gly and CA with Asp

In contrast to natural dyeing, this novel coloration method with plant-derived catechols and amino acids offers various advantages. It was found that milligrams of catechol and amino acids were sufficient to dye a gram of textile fabrics with attractive shades. In addition, the pigmentation could be easily tuned to give different shades. Furthermore, the extraction processes of natural organic colorants and the use of mordanting agents could be eliminated.

4.3 Conclusions

We have developed a facile approach for the heteromolecular pigmentations of plant-derived catechols and amino acids on textile materials. The pigmentation could be easily tuned by varying parameters such as pH, molar concentration, types of amino acids and the concentration of Tris buffer to give a wide colour gamut. The pigments could simply be immobilized on wool fabrics at room temperature without dyeing auxiliaries. The colour depth and colour fastness could be further enhanced by EDC pretreatment. This simple coloration method was safe for textile application and also exhibited good batch-to-batch reproducibility. Besides, the catechol-derived colorants could be employed in combination with cold pad-batch method. These results strongly suggest that the developed catechol-based pigmentation can be a sustainable alternative for conventional textile coloration, which promotes the reduction of synthetic raw materials, utilization of renewable resources, and minimization of water and energy consumption in textile industry.

5 Catechol-Induced Tunable Surface Charges

5.1 Introduction

With the fast pace of industrial development, an enormous amount of toxic pollutant-laden wastewater is produced and discharged every day. Textile industry is well-known to be one of the big water polluters. Approximately 1000-3000 m^3 of wastewater is produced for manufacturing 12 to 20 tons of clothing per day [186]. For most dyeing processes, the effluents discharged usually contain a high concentration of unfixed dyes and dyeing auxiliaries. These coloured substances usually contain azo groups and other bulky aromatic structures. They are generally non-biodegradable and some may also produce carcinogens in certain scenarios [187]. Without proper treatment, dyes and pigments in wastewater could lower the water transparency and interfere the photosynthesis of the marine plants and their eco-systems [188]. Furthermore, the chemical pollutants in the dyehouse effluents could seriously affect the environment and cause severe health consequences in humans. Therefore, much attention has been given to the dyehouse wastewater treatment.

Current approaches such as adsorption, precipitation, membrane filtration, photocatalysis and degradation have been being adopted for wastewater treatment [189-193]. Among these methods, adsorption is a relatively high-efficiency method for removing pollutants at a lower cost [194]. In addition, it is comparatively easier to collect and reuse the spent adsorbents. In contrast, other methods have some inevitable limitations. Precipitation, which may involve the conversion of dissolved pollutants to insoluble substances, causes another problem of handling the solid wastes. Membrane filtration is effective for the removal of pollutants, but the

installation and operation costs are comparatively higher. Furthermore, photocatalysts may be susceptible to deactivation issues and the degradation reaction is usually specific to certain types of substances. Besides, both photocatalysis and degradation process may involve the release of harmful by-products. Therefore, adsorption is more preferable in terms of the cost, efficiency and reuse, when compared with the aforementioned methods. Among different types of adsorption, selective adsorption aims to utilize the adsorbates and simplify the subsequent handling process, which are favourable for advanced wastewater treatment. However, the recovery of adsorbents and the separation of adsorbates usually involve large consumption of organic solvents in extraction process, which causes secondary pollution in the treatment process [195-197]. In addition, the collection of the spent adsorbent from a large volume of wastewater is sophisticated to be accomplished with traditional separation technologies like filtration and centrifugation [198, 199]. Hence, adsorption selectivity towards adsorbates, adsorption capacity, efficiency in adsorbate desorption and ease of handling have to be taken into consideration for the development of advanced adsorbents [194].

Biopolymers including polydopamine (PDA), carrageenan and chitosan have been gaining much attention in their potential adsorption capacity for the removal of wastewater pollutants [200-202]. PDA, inspired from the strong adhesion of the marine mussels to the rocks even under severe tidal wave impact, has drawn much attention from multidisciplinary areas including water treatment, colorimetric detection, and bio-medical application [192, 199, 203, 204]. The presence of abundant functional groups like amino, catecholic and imino groups in PDA contributes to its remarkable adhesive properties and multifunctional nature. Numerous research studies have been actively exploring the improvement of PDA material adsorbability to water pollutants, for instance, by altering the morphology of PDA, and incorporating graphene, metals, or metal oxides into PDA [115, 205-212]. It has already been confirmed that

PDA-based composites had fascinating adsorbability for the removal of heavy metals and organic pollutants like methylene blue, methyl orange and Congo red [10, 213]. Some studies have showed that the catechol rings of PDA could adsorb rhodamine B with aromatic structure via π–π interaction [116], and the negatively charged oxygen-containing groups of PDA could adsorb cationic methyl blue via electrostatic interaction [214]. Therefore, different surface functional groups of PDA can offer different attraction mechanisms towards various types of dyes, which facilitate the adsorption of distinct dyes in co-contaminated wastewater [215, 216]. In addition, one of the highlighted features of PDA is its zwitterionic character, which enables it to change the surface charge when induced by the solution pH. This property allows PDA to adsorb different charged dyes in specific conditions and thus enhances the adsorption selectivity and subsequent separation process [116, 217]. To further improve the adsorption capacity of PDA, approaches for developing hollow structures, nanoflower structures, and composites of PDA can be taken [218, 219]. From the aspects of production and application, PDA is biodegradable and has relatively low manufacturing cost. It also demonstrates the ability to recognize the ionic dyestuffs through the molecular interaction under different pH conditions, which is crucial in practical treatment.

Organic-inorganic hybrid system offers a new strategy to exploit different material properties for specific purposes [220]. This gains synergistic effect in enhanced physical properties and chemical functionalities from combining the advantages of both organic and inorganic materials [221]. Some studies suggested that the manufacture of adsorbents in the form of membranes or fibres, while others proposed the production of adsorbent particles with magnetic property originating from Fe_3O_4, $CoFe_2O_4$ or MgO [217, 222-227]. Inorganic materials like metal oxides have the potentials to increase the efficiency of reusing the adsorbent, which could be a key benefit of adsorption method. Fe_3O_4 having a simple structure

is one of the most common substances to be incorporated for providing strong magnetic property [228-230]. It is also known to have high stability and low risk in long-term usage [231, 232]. These magnetic nanoparticles offer convenient separation process of dispersed adsorptive nanocomposites from wastewater with external magnetic field [233]. The ease of collection promotes the adsorbent reusability and reduces energy consumption for handling the spent adsorbent [234]. Furthermore, the biocompatibility and biodegradability of Fe_3O_4 has already been confirmed in recent studies [235, 236]. Even though Fe_3O_4 has a high specific surface area, it can barely possess versatile adhesion capacity as mesoporous PDA layer [237]. The superior adhesion properties of PDA originate from their ability to interact with adsorbate via π-π stacking, hydrogen bonding, electrostatic interaction, complexing and covalent reactions [7, 22, 123]. In addition, PDA is a suitable biodegradable material for the development of sustainable adsorbent for environmental remediation. Hence, the formation of stable organic coating on the iron oxides can further enhance the adsorption capacity and biodegradability without sacrificing the magnetic features.

A considerable number of studies have proven the effectiveness of PDA in dye adsorption wastewater treatment, and some research focused on the application of PDA on dye separation or selection. However, few studies about the use of magnetic PDA composites for both dye adsorption and separation have been reported. Besides, the synthesis process involved in the known studies were relatively complicated [238], the efficiencies were as low as 2 to 3 mg g^{-1} [239] or the universal adsorption properties of the composites were not comprehensively demonstrated [240]. We herein present a bio-inspired magnetic adsorbent for selective adsorption and desorption of universal ionic dyestuffs. Magnetic PDA nanocomposites (Fe_3O_4@PDA) were synthesized for the adsorption and separation of dyes using a facile, low-cost, and scalable method. The effect of dopamine content for synthesis on the adsorption

efficiency of Fe_3O_4@PDA formed was investigated. The zwitterionic characteristic of the nanocomposites were studied for developing charge controllable application. The dye adsorption efficiency and selectivity of Fe_3O_4@PDA were examined with cationic crystal violet (CV) and rhodamine B (RB) dyes, and also with anionic direct blue 71 (DB) and orange G (OG) dyes. The reusability and dye separation ability of these magnetic Fe_3O_4@PDA were further evaluated.

5.2 Results and Discussions

5.2.1 Characterizations of adsorbents

As shown in Figure 5.1(a-c), the morphological features of pristine Fe_3O_4, pristine PDA and Fe_3O_4@PDA were distinct. Small Fe_3O_4 nanoparticles tended to form particle clusters, attributing to their superparamagnetic properties. For the formation of pristine PDA with the presence of TMB/F127 template, 20 nm nanospheres were observed. Upon the DA polymerization on the pristine Fe_3O_4, the adhesiveness of PDA allowed themselves to form greater aggregates with the Fe_3O_4 nanoparticles, leading to the different appearance of Fe_3O_4@PDA. From the TEM image (Figure 5.1(d)), it could be noted that the sizes of individual Fe_3O_4 were below 10 nm and many Fe_3O_4 particles were agglomerated with each other because of the magnetic dipole and Van der Waals' forces [241]. Fe_3O_4 were mostly embedded in the layer structures of PDA, which were indicated using different colour lines. In addition, the PDA structure of Fe_3O_4@PDA was in the form of multilayers, which was different from the conformation of magnetic PDA and its derivatives found in other reports [238, 242,

243]. The multilayer structures could increase the surface area of the nanocomposites for adsorption, which would contribute to the significant enhancement of the adsorption efficiency.

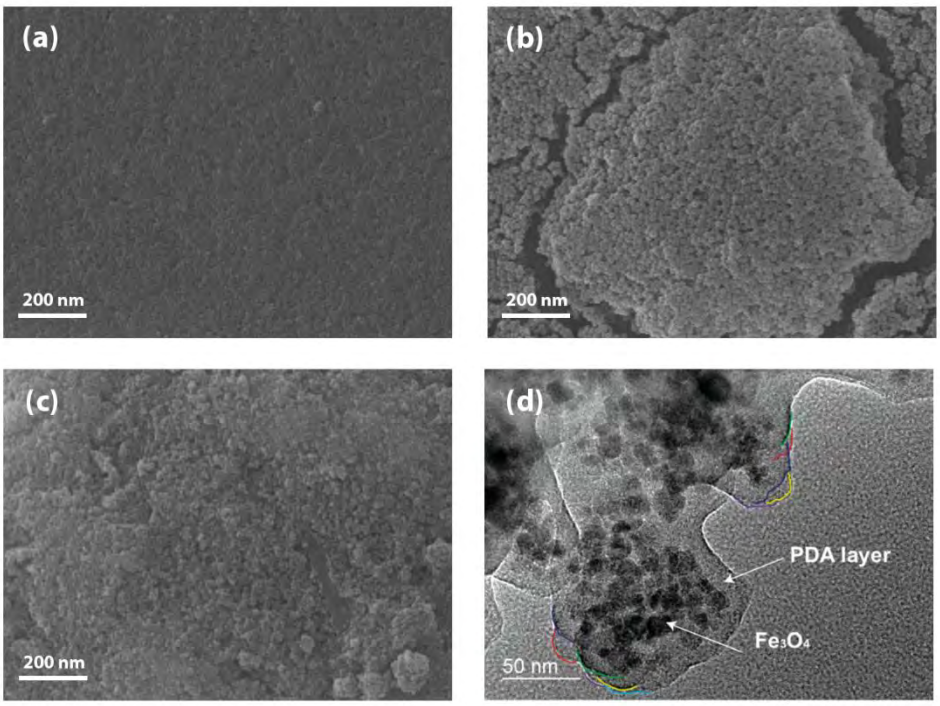

Figure 5.1 FESEM images of (a) Fe_3O_4, (b) PDA and (c) Fe_3O_4@PDA, and (d) TEM image of Fe_3O_4@PDA

The XRD patterns in Figure 5.2(a) were in agreement with the JCPDS file of Fe_3O_4 (JCPDS No. 19-0629). The diffraction peaks at 2θ values of 30.2, 35.5, 43.2, 53.6, 57.1 and 62.7 degree corresponded to (220), (311), (400), (422), (511) and (440) planes of Fe_3O_4. The characteristic peaks of pristine Fe_3O_4 could be clearly found in Fe_3O_4@PDA, indicating that the structure of Fe_3O_4 was well preserved. ATR-FTIR measurement was performed to investigate the surface characteristics of Fe_3O_4@PDA. It could be observed that some characteristic adsorption bands related to PDA emerged after DA polymerization onto Fe_3O_4 (Figure 5.2(b)). Peaks at 3375, 1617, 1486, 1423, and 1265 cm^{-1} could be attributed to the O-H stretching, C=C-C aromatic

ring stretching, C-C stretching, NH_3 in-plane bending, and C-O-H symmetric bending of PDA structure [182, 244]. This confirmed the formation of PDA on the Fe_3O_4 nanoparticles. The results indicated that the DA polymerization on Fe_3O_4 nanoparticles was successful, and insignificantly altered the structure of Fe_3O_4.

With functional groups like amino, catechol and imino groups, the surface charges of PDA can be altered simply by varying the pH conditions. This charge control feature could be confirmed by zeta potential. According to Figure 5.2(c), the surface charges of Fe_3O_4@PDA showed a decreasing trend from 7.8 to -39.9 with pH increasing from 3 to 9. The zeta potential of Fe_3O_4@PDA dropped significantly from pH 3 to pH 7, but it showed leveling off from pH 7 to pH 9. It was found that Fe_3O_4@PDA particles generally carried positive charges or no charge under acidic conditions while they carried negative charges under alkaline conditions. The variation in surface charges of Fe_3O_4@PDA was similar to that of magnetic PDA particles found in other research, of which the particles also carried negative charges in alkaline conditions [245-247]. The phenomenon contributed to the dye adsorption selectivity via the electrostatic attraction or repulsion between Fe_3O_4@PDA particles and dyes of different charges. In addition, the isoelectric point of these nanoadsorbents was approximately at pH 4.3, which revealed that they had a wider effective range for attracting positively charged adsorbates. Hence, the pH-induced changes in the surface charges of adsorbents could directly influence their capacity for textile dyes carrying different charges. Besides, Fe_3O_4@PDA nanoadsorbents could be easily collected from an aqueous suspension of 1‰ Fe_3O_4@PDA by an external magnetic field (Figure 5.2(d)), suggesting the magnetic property of Fe_3O_4 was retained.

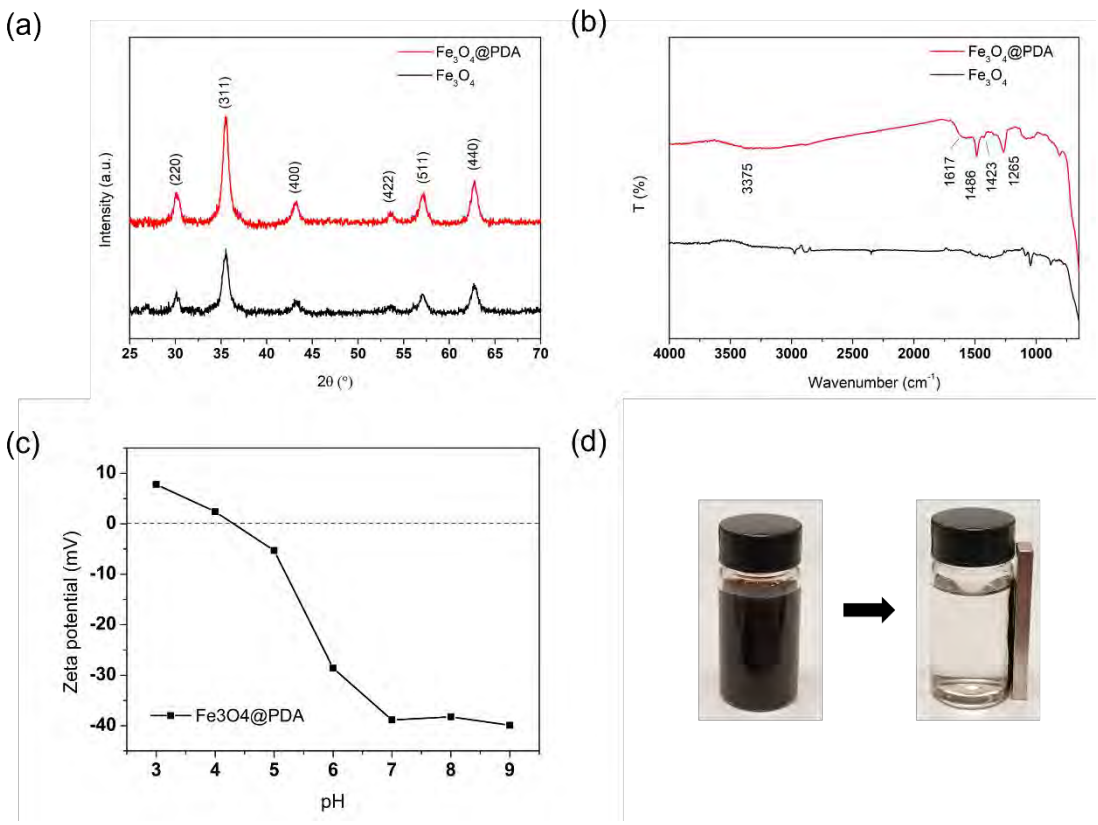

Figure 5.2 (a) XRD patterns and (b) FTIR spectra of Fe_3O_4 and Fe_3O_4@PDA, (c) Zeta potential of Fe_3O_4@PDA between pH 3 to pH 9, and (d) Collection of nanoadsorbents from 1‰ Fe_3O_4@PDA suspension with a magnet

N_2 sorption was conducted to evaluate the surface porosity of the adsorbent. From Figure 5.3(a), the results of Fe_3O_4 and Fe_3O_4@PDA were found to be similar to that reported in the previous studies [116, 248]. Fe_3O_4 showed an isotherm Type IV with a Type H1 hysteresis loop at a relative pressure of 0.5 to 0.9, according to the IUPAC classification. The mesoporosity discovered was likely caused by the interparticle volume of the small Fe_3O_4 nanoparticles [249]. Fe_3O_4@PDA showed an isotherm Type IV with a steep Type H3 loop at 0.9 to 1.0, which implied the possible formation of hollow cavities on the PDA coating. In addition, Fe_3O_4 and Fe_3O_4@PDA gave a BET surface area of 104.4 and 95.6 m^2 g^{-1}, respectively. The decrease in the surface area of Fe_3O_4@PDA suggested that some Fe_3O_4 nanoparticles were embedded inside the PDA, which reduced the exposure of nanoparticles. It could still be noted that the

surface area and porosity of PDA were improved by the TMB/F127 template. From Barrett-Joyner-Halenda (BJH) pore distribution curves (Figure 5.3(b)), the PDA coating could widen the pore size distribution of the nanocomposites, favoring the diverse adsorption purposes.

The chemical composition of Fe_3O_4@PDA was evaluated with TGA. As shown in Figure 5.3(c), the weight loss increased gradually from Fe_3O_4 to Fe_3O_4@100mgDA and the equilibrium of the weight loss achieved at 700 to 850 °C, depending on the DA content used. Comparing the TGA curves between Fe_3O_4 and Fe_3O_4@PDA, the weight loss from about 100 to 700 °C and 100 to 850 °C might indicate the decomposition of organic substances of PDA in the nanocomposites. The percentage of weight loss of Fe_3O_4 from 100 to 1000 °C was only negligible while that of the Fe_3O_4@PDA samples formed with DA (20/40/60/80/100 mg) were 27.5, 36.8, 46.9, 50.1 and 53.6, respectively. Since Fe_3O_4 will only be converted to Fe_2O_3 at much higher temperature under N_2 condition, the amount of magnetic Fe_3O_4 can be estimated from the residual mass percentages in this study. For the same amount of Fe_3O_4@PDA nanocomposites, it was found that the residual Fe_3O_4 content decreased with higher amount of DA added in the synthesis process, which implied that more PDA layers were formed on the particles. Besides, Fe_3O_4@20mgDA and Fe_3O_4@40mgDA reached equilibrium at a slightly higher temperature at around 850 °C. This might possibly be explained by the small PDA molecules trapped in the Fe_3O_4@PDA synthesized with low DA content, which was relatively hard to be decomposed. Insignificant weight loss between 850 to 1000 °C was observed. These variations in residue weight of samples found were similar to other reports [238]. With higher DA content for synthesis, more PDA layers generally could be formed on the nanocomposites.

Since PDA is a major contributor to dye adsorption, the DA content of Fe_3O_4@PDA was expected to be a tuning factor for dye adsorption efficiency. The specific surface chemistry of

PDA could render the substrates versatile adhesion properties. More PDA layers implied higher amount of adsorption sites available, therefore the adsorbent capacity could be increased. The dye adsorption trends of Fe_3O_4@PDA synthesized with different amount of DA (20/40/60/80/100 mg) were demonstrated using four different types of dyes (Figure 5.3(d)). With increasing DA content for the Fe_3O_4@PDA synthesis process, a growing trend for both cationic and anionic dye adsorption could be observed. The result verified that increasing DA content could enhance the formation of PDA layers on the Fe_3O_4@PDA nanoparticles, resulting in more adsorption sites available for dyes.

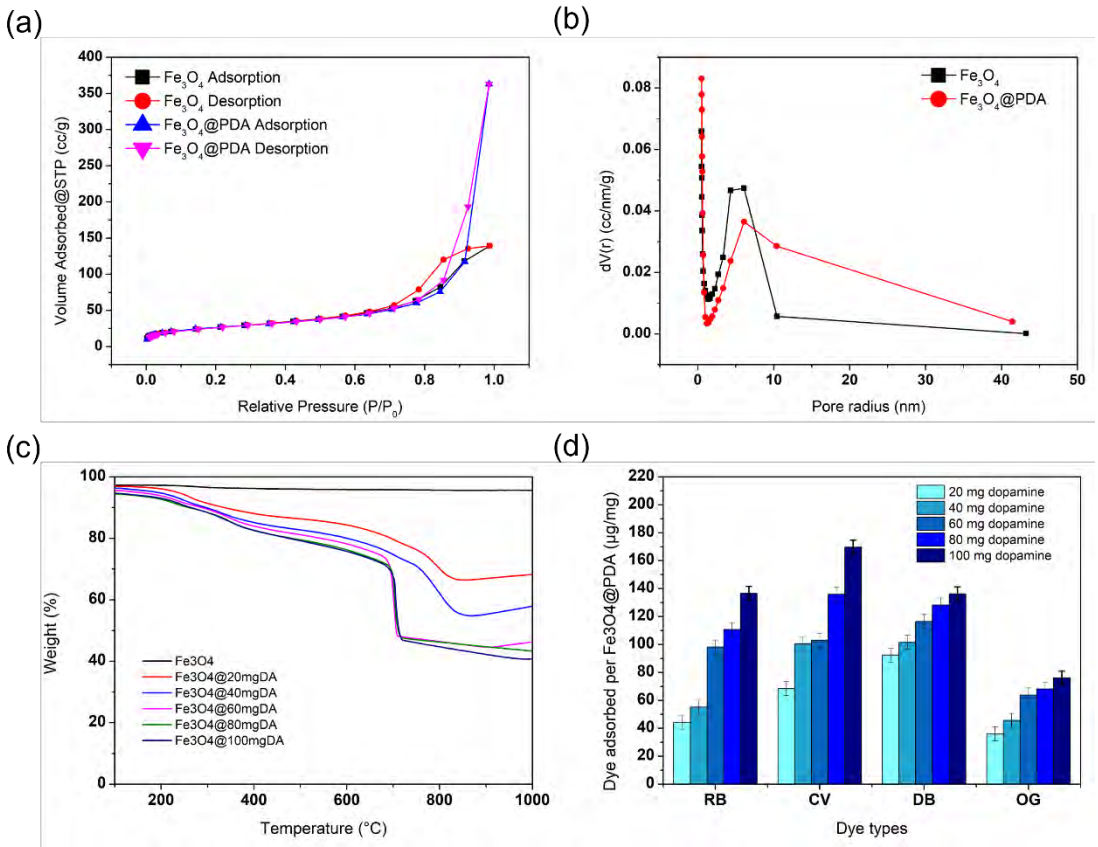

Figure 5.3 (a) N_2 sorption isotherms at 77K, (b) BJH pore distribution of Fe_3O_4 and Fe_3O_4@PDA, (c) TGA curves of Fe_3O_4 and Fe_3O_4@PDA synthesized with different DA amount, (d) Effect of DA amount in the synthesis of Fe_3O_4@PDA on the dye adsorption (cationic dyes RB and CV at pH 7; anionic dyes DB and OG at pH 4)

All these results have demonstrated the physical and chemical features of the Fe_3O_4@PDA nanocomposites, and also confirmed their potential in wastewater treatment.

5.2.2 Dye adsorption

The universal adsorption of cationic and anionic dyestuffs was successfully demonstrated with the use of Fe_3O_4@PDA. The adsorption properties of as-prepared Fe_3O_4@PDA toward different dyes in aqueous solution were then investigated in detail. The reaction time required to attain the equilibrium adsorption for four different dyes was first studied (Figure 5.4(a)). It could be seen that the adsorption proceeded rapidly from 0 to 50 min. Afterwards, the rate exhibited slight changes, and the adsorption process started reaching equilibrium ranged from 100 to 400 min. The equilibrium adsorption capacity for RB, DB, CV and OG were around 90, 105, 87 and 62 μg mg^{-1}, respectively. The reason for fast adsorption rate at the first 50 min could be explained by the large number of sites available for dye adsorption. The adsorption between dyes and Fe_3O_4@PDA could be attributed to the π–π attraction between the aromatic rings, and electrostatic interactions between the charged functional groups of the dye molecules and PDA layers [116]. When the reaction reached 100 min, most of the available sites on Fe_3O_4@PDA composites were occupied and the adsorption process was approaching equilibrium. Besides, the accumulation of adsorbed dyestuffs on nanocomposites might increase the charge repulsion between the adsorbed and free dye molecules found in the solution, leading to the gradual decrease in rate.

The effect of initial dye concentration on dye adsorption of Fe_3O_4@PDA was studied (Figure 5.4(b)). For all four types of dyes, the dye adsorption rate increased rapidly at an initial dye

concentration from ca. 42 to 80 μg mL^{-1}. When the initial dye concentration reached round 100 μg mL^{-1}, the dye adsorption of Fe_3O_4@PDA attained its equilibrium. The adsorption efficiency of Fe_3O_4@PDA showed an uptrend with the rise of initial dye concentration as there were enough vacant adsorption sites for the dye adsorption when the initial dye concentration was below 80 μg mL^{-1}. With further increase of initial dye concentration, the adsorption rate kept constant indicating saturation of Fe_3O_4@PDA. The dye adsorption capacity of different ionic dyes ranged from 60 to 120 μg mg^{-1}. The finding showed that the equilibrium adsorption for RB, DB, CV and OG could generally be enhanced with higher initial dye concentration. This might suggest that higher initial concentration could lessen the effect of repulsion between adsorbed dyes and free dyes at the early stage, and this could promote the initial adsorption amount, contributing to the overall growth of uptake.

To investigate pH effect on dye adsorption efficiency for different dyes, the buffer solution was adjusted in the range of pH 4 to 9, and the dye concentration in different buffer solutions were kept at 80 μg mL^{-1}. As shown in Figure 5.4(c), it discovered that the Fe_3O_4@PDA composites had relatively more uniform and relatively high adsorbability for cationic dyes (RB and CV) in both acidic and alkaline conditions. For the anionic dyes (DB and OG), the Fe_3O_4@PDA reached the highest adsorption efficiency at pH 4. In contrast, the adsorption efficiency was comparatively low in neutral condition, and significantly dropped to nearly zero in more alkaline conditions (pH 8-9). The maximum dye adsorption was ca. 100 μg mg^{-1} for RB at pH 8, ca. 103 μg mg^{-1} for CV at pH 7, ca. 116 μg mg^{-1} for DB at pH 4, and ca. 64 μg mg^{-1} for OG at pH 4. The adsorption discrepancy could be explained by the adjustment of surface charges on Fe_3O_4@PDA with response to pH change. The presence of catechol and amine groups in the outer PDA layers endowed the nanocomposites specific pH sensitivity, which allowed the interaction of Fe_3O_4@PDA with different dyes under various pH conditions [219, 249]. For

cationic RB and CV dyes at pH 7, the quaternary ammonium cations (N^+) of the dye molecules could be attracted by the oxygen-containing groups (O^-) present on Fe_3O_4@PDA, enhancing the dye adsorption. For anionic DB and OG dye adsorption at pH 4, the electrostatic attraction between negatively charged sulfonate groups (SO_3^-) of the dye molecules and protonated amino groups (NH_3^+) of Fe_3O_4@PDA preceded in the dye adsorption process. The pH-induced changes in the surface charges of Fe_3O_4@PDA contributed to their selective adsorption-desorption ability.

It is worth noting that Fe_3O_4@PDA had the highest adsorption capacity for DB and the lowest for OG, whereas they had comparable performance for RB and CV. In terms of molecular size, DB is much larger than OG, while RB resembles CV. Smaller adsorbate molecules often have less steric hindrance and faster kinetics in the adsorption process [250, 251], but the adsorption capacity for OG was found to be lower than that for DB. This result was likely attributed to the differences of ionizable constituents on dye molecules. In contrast to OG, DB possessed a greater number of more evenly distributed ionizable constituents and a more extensive conjugated system for generating surface charges and stabilizing the ionized form. Hence, better electrostatic interaction between DB and nanoadsorbents could possibly lead to the differences in adsorption capacity for OG and DB. Besides, the similar adsorption capacity for RB and CV could be explained by their akin molecular size and number of ionizable groups present.

According to the aforementioned observation, it could be proposed that the main adsorption process involved was charge-dependent mechanism. pH conditions had influence on the degree of ionization of the adsorbates as well as the active sites of the adsorbents, thus the electrostatic interactions between different ionic dyestuffs and Fe_3O_4@PDA could be tuned with different

pH conditions. This study emphasized on the potential of Fe_3O_4@PDA as a universal nanoadsorbents for dye adsorption based on the highlighted pH-induced charge control properties.

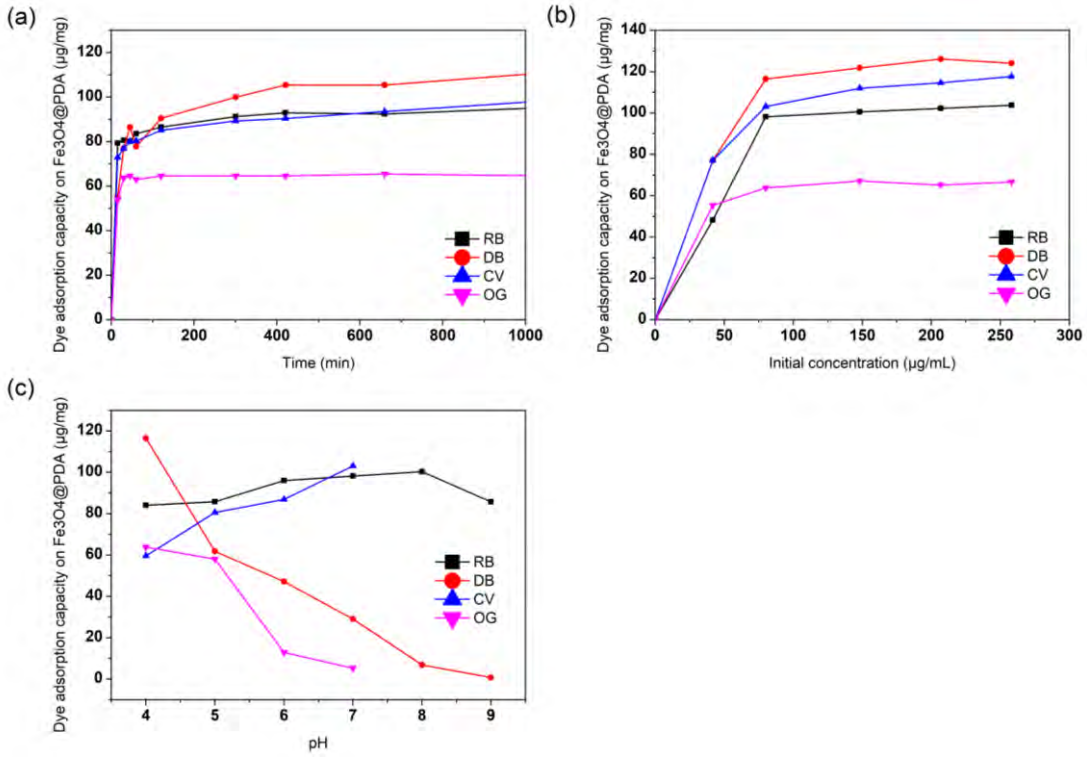

Figure 5.4 Effect of (a) reaction time and (b) dye concentration on the dye adsorption of Fe_3O_4@PDA (RB and CV at pH 7; DB and OG at pH 4), and (c) pH effect on the dye adsorption

The reusability of Fe_3O_4@PDA is a practical consideration for application. Therefore, this was investigated using common anionic DB as the example. Since the adsorption of anionic dyes were low under neutral and alkaline conditions, DB adsorbed on the nanoadsorbents could be desorbed in the solution mixed with pH 7 Tris buffer and a small amount of DMF. The recovered Fe_3O_4@PDA particles were reused for the subsequent adsorption processes. As shown in Figure S2, the dye adsorption efficiency of the Fe_3O_4@PDA particles decreased gradually after five cycles. This might be caused by the loss of adsorbent mass and the

incomplete desorption of previously adsorbed dye molecules. Further investigation is needed to improve the recovery efficiency of the nanoadsorbents. Nevertheless, reversible adsorption and desorption assisted by the electrostatic interactions could still be observed in this study.

Based on the isotherm and kinetic plots (Figure S3, Figure S4, Figure S5 and Figure S6) and the calculated parameters (Table 1), we could deduce the best-fit model for adsorption isotherm and kinetics. The linear regression coefficient values of the Langmuir model were higher than that of Freundlich model, and this indicated that the adsorption of different dyestuffs generally followed a Langmuir isotherm. In addition, Langmuir model could be used to describe the monolayer adsorption of dyestuffs onto the finite number of adsorption sites of the nanocomposites. Furthermore, the R_L values for different dyestuffs were found to be less than 1, implying that the adsorption process was favourable. From kinetic parameters shown in Table 5.1, the linear regression coefficient values in pseudo-second order model were better than that of pseudo-first order model. The adsorption capacity calculated with the pseudo-second order model was in good agreement with the experimental value. These indicated that pseudo-second order kinetics was more suitable to describe the observed adsorption behaviors. The results suggested that both adsorbate and adsorbent took part in the rate-determining step.

Table 5.1 Isotherm and kinetic parameters for the adsorption process

Isotherm parameters:

Dye	Langmuir				Freundlich		
	q_{max} (mg g^{-1})	K_L (L mg^{-1})	R_L	R^2	K_f (mg g^{-1} · (L $mg^{-1})^{1/n}$)	1/n	R^2
RB	109.7695	0.1959	0.5428	0.9973	82.3474	0.1222	0.9679
DB	126.4223	5.4931	0.0615	0.9985	90.5899	0.1434	0.9750
CV	112.4859	4.8054	0.0375	0.9945	87.6193	0.1385	0.9890
OG	71.3267	2.5445	0.0383	0.9972	54.2338	0.1160	0.9654

Kinetic parameters:

Dye	Pseudo-first order			Pseudo-second order		
	$q_{e,cal}$ (mg g^{-1})	k_1 (min^{-1})	R^2	$q_{e,cal}$ (mg g^{-1})	k_2 (g mg^{-1} min^{-1})	R^2
RB	19.1113	-7.6429×10^{-6}	0.9757	98.6193	0.0007	0.9992
DB	40.1684	-7.3095×10^{-6}	0.9448	115.4734	0.0003	0.9976
CV	26.0647	-4.2143×10^{-6}	0.9081	105.8201	0.0004	0.9968
OG	48.1264	-1.9367×10^{-4}	0.8248	64.6831	-0.0103	0.9998

5.2.3 Dye separation

From what we have found in Section 3.2, Fe_3O_4@PDA has shown relatively distinct adsorption behaviors to anionic OG and cationic CV under different pH conditions. Therefore, this pair of dyestuffs was chosen to demonstrate the dye separation property using the magnetic nanocomposites. Mixtures of anionic OG and cationic CV were prepared respectively at pH 4 and pH 7. With the presence of functional groups like amino, catechol and imino groups, the surface charges of PDA would alter with respect to the change of pH. Therefore, charge differences between dye molecules and PDA layers resulted in electrostatic attraction or repulsion between each other [116, 249, 252]. For dye solution mixed at pH 4, the solution colour faded from dark purple (Figure 5.5(a)) to purple (Figure 5.5(b)) after adsorption. The electrostatic attraction between Fe_3O_4@PDA particles and anionic dyes facilitated the adsorption of OG dye, and the dye solution generally contained the remaining cationic CV dyes. When Fe_3O_4@PDA adsorbed with OG dye was placed in the solution at pH 7, the surface charges of the particles changed from slightly positive to negative, causing the OG dye to desorb. The desorption yielded an orange colour (Figure 5.5(c)). On the contrary, the solution mixed at pH 7 changed from dark purple (Figure 5.5(d)) to dark orange (Figure 5.5(e)) after

the adsorption process, which was attributed to the preferential adsorption of cationic CV dye by negatively charged Fe_3O_4@PDA at pH 7. The colour change was significant as there was negligible OG dye adsorption at pH 7. Therefore, CV dye could be separated out, and OG remained in the solution. When the Fe_3O_4@PDA particles adsorbed with CV dye underwent desorption process at pH 4, the solution colour became light purple due to the desorption of the CV dyes (Figure 5.5(f)). The results confirmed that Fe_3O_4@PDA can be utilized in separating different ionic dyes in a mixture.

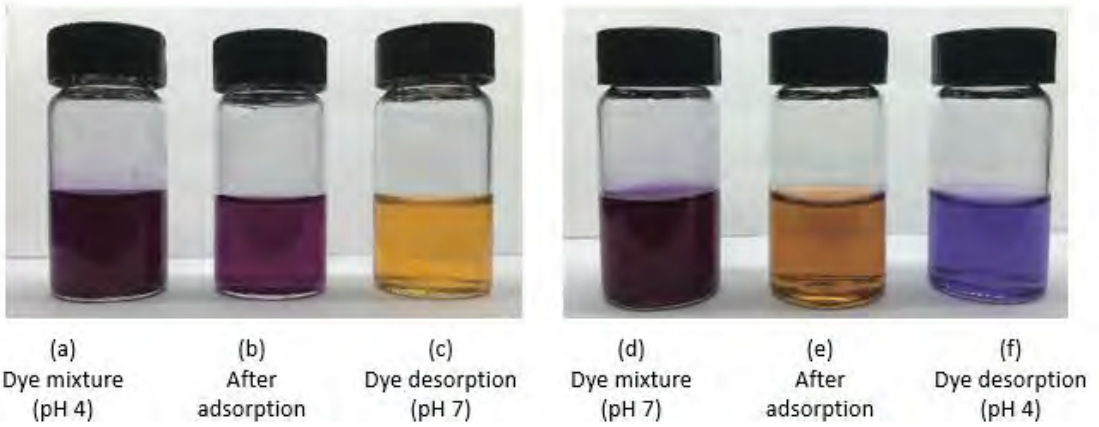

Figure 5.5 Photographs of dye solutions. (a) and (d) were the solutions that contained OG and CV at pH 4 and 7 buffer respectively, (b) and (c) were the solutions left after adsorption process, and (e) and (f) were the solutions after desorption process of Fe_3O_4@PDA adsorbed with dye at pH 7 and 4 buffer respectively

5.2.4 Interactions involved in the adsorption process

The catechol-enhanced adsorbents have demonstrated the ability to recognize the ionic dyestuffs through the molecular interaction under different pH conditions. The adsorption behaviors of PDA layer are originated from their interaction with adsorbate via hydrogen bonding, electrostatic interaction, π-π stacking and covalent reactions (Figure 5.6). It is worth

mentioning that the reversible adsorption and desorption of ionic dyestuffs on the charged PDA layer is mainly facilitated by the electrostatic interactions. However, it should be noted that the formation of some adsorbent-dye interactions is irreversible, this is one of the reasons for the loss of adsorption sites after repeated usage. Therefore, further investigation is needed to improve the adsorption capacity and recovery efficiency of the nanoadsorbents.

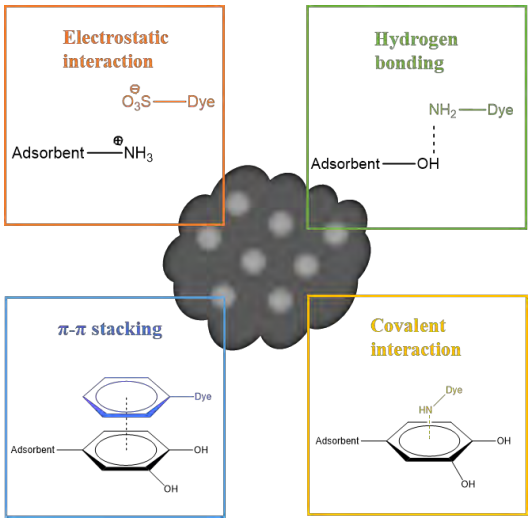

Figure 5.6 Potential interactions between nanoadsorbent and dyestuff

5.3 Conclusions

The magnetic PDA nanocomposites (Fe_3O_4@PDA) were successfully synthesized for the application of selective dye adsorption and separation. Our facile and sustainable synthesis method of Fe_3O_4@PDA could promote the adsorption efficiency of the nanocomposites for universal types of common ionic dyes. The PDA content of the nanoadsorbents could also be tuned with the amount of DA in the synthesis process. It was found that the adsorption efficiency of cationic dyes (RB and CV) could be generally improved with increasing pH, and that of anionic dyes (DB and OG) adsorption could be enhanced with decreasing pH. Fe_3O_4 contributed to the magnet-assisted collection of the spent adsorbents, which offered the ease of

reusability. The synthesized hybrid nanocomposites showed pH-inducible surface charge changes, which enabled smart adsorption and separation selectivity in ionic dye mixtures under different pH conditions. These results have successfully demonstrated that Fe_3O_4@PDA had potential to be an efficient and reusable nanoadsorbents for wastewater treatment. To tackle the existing limitations, further study is needed to broaden the adsorption selectivity, increase the adsorption capacity of nanocomposites, and boost the efficiency of desorption for the recovery of adsorption sites. In addition, PDA can be a critical research direction in the future, owing to its substantial possibilities in structural modification for functionality enhancement.

6 Catechol-Enhanced Functional Material

6.1 Introduction

In the era of energy crisis, the ground-breaking discovery of triboelectric nanogenerators (TENG) has attracted substantial attention in multidisciplinary areas for novel energy supply. TENG has incontrovertibly become one of the most studied mechanical energy harvesters in the past decade. Despite that the energy conversion efficiency is still way behind the conventional fuels, triboelectric nanogenerator offers a more flexible way to generate electrical energy in our daily lives. This is also a favourable decentralized energy production method, minimizing the loss of energy caused by transmission [15, 95]. The generation of triboelectric energy is assisted by the coupling effect of contact electrification of dielectric materials and electrostatic induction of electrodes. Therefore, the material properties of dielectric layers are a critical factor determining the triboelectric performance. It is worth noting that there are a broad variety of materials, designs and production methods available for the fabrication of TENGs. In addition, it is feasible to select more elastic and softer materials for TENG. These types of materials impose less restrictions on bending, folding and rolling of energy harvesting device, contributing to the subsequent production of highly flexible devices. These open a less complicated and more sustainable way to develop mechanical energy harvesters for potential wearable applications.

With the demand of more multifunctional and higher-performance dielectric materials for energy applications, doping polymers with fillers of distinct properties is commonly adopted

to achieve the purposes. Nevertheless, the performance of this composites is often limited by the incompatible interfaces, especially between inorganic and organic materials. The interfacial incompatibility between fillers and host substrates likely causes some negative influences on the intrinsic properties of host substrates and lowers the synergistic benefits between host and fillers. To lessen the effect of this interfacial incompatibility, the addition of coupling agents aim at enhancing the interfacial bonding between host and fillers to create better linkages between two materials with distinct properties [253]. However, most of coupling agents are only limited to certain doping conditions. These imminent needs of solution to address the current incompatibility problems can be alleviated by introducing the catechol derivatives as an interfacial buffer for more versatile surface interactions between dissimilar materials. The enhanced interfacial interactions between the fillers and the host matrices facilitate the uniform dispersion of fillers and avoid the formation of interfacial defects. Besides, the properties of doped composites can possibly be tuned or altered with the addition of catechol material. Since catechol derivatives often possess some intrinsic properties and reactivities that can be imparted to or react with the substrate [9, 23]. In recent year, multifunctional polydopamine (PDA) layer has been highlighted as a promising surface modification agent for fabricating organic-inorganic composite materials [106]. This bio-inspired PDA interlayer can efficiently wrap the entire surface and also preserve the morphology and structures of the fillers. Besides, it has been proposed that PDAs demonstrate a certain degree of hybrid electronic-ionic conductivity, which allows themselves to support electrical-related applications [254].

Metal-organic framework (MOF) is a potential nanofiller candidate for imparting diverse functions to the substrate material. They show tailorable architectures and functionalities through bridging different metal nodes with various organic linkers for the advancement of diverse material properties [255]. It should be noted that MOF is regarded as a hybrid organic-

inorganic material, and thus it still displays some characteristic features of inorganic crystal. MOF as a crystal structure generally possesses higher structural rigidity. Therefore, it is foreseeable that defects form between the interfaces of MOF fillers and organic polymer matrix. To produce a functional polymer material with more homogeneously distributed of inorganic content, surface modification of these fillers with catechol coating was proposed with the intention of increasing the compatibility between the fillers and polymer matrix [256].

The influence of catechol coating on MOF fillers on their performances as composite dielectric material is yet to be studied comprehensively. Herein, we report a bio-inspired approach to modulate the incompatibility between the inorganic filler and organic matrix. Zeolitic imidazolate framework-8 (ZIF-8) is well known as a type of MOF structure with high surface area, chemical stability and thermal stability, and it has already demonstrated to be a potential tribopositive material [109, 257]. In addition, polylactic acid (PLA) polymer is renewably sourced, highly transparent material and biodegradable for sustainable development of functional materials. Hence, PLA substrate and ZIF-8 filler were chosen to explore the effect of catechol-based interfacial layer on the properties of PLA composite film. The characterization of catechol-coated fillers, and the differences in electrical, tensile, and antibacterial performances of PLA doped with pristine ZIF-8 and ZIF-8@PDA were evaluated.

6.2 Results and Discussions

6.2.1 Characterization of catechol-coated ZIF-8

Surface modification of ZIF-8 was first performed with PDA coating under alkaline conditions. From the XRD diffractograms (Figure 6.1(a)), it could be confirmed that PDA was successfully

coated on the ZIF-8 nanocrystals without much interference to the ZIF-8 structure. Both diffractograms showed strong peaks at 2θ = 7.32, 10.35, 12.72, 14.74, 16.48 and 18.0°, which corresponded to (110), (200), (211), (022), (013) and (222) planes, respectively [119]. The FTIR spectra of the pristine ZIF-8, ZIF-8@PDA and PDA powders were presented in Figure 6.1(b). The spectrum of ZIF-8@PDA generally resembled that of ZIF-8, except for slightly enhanced absorption peaks at 3361, 1610, 1500 and 1417 cm^{-1} being ascribed to O–H stretching, C=C stretching vibration of aromatic structure, –NH bending vibration and in-plane deformation of phenolic O–H, respectively [258-260]. This also implied that PDA layers were successfully deposited on the surface of ZIF-8 structures.

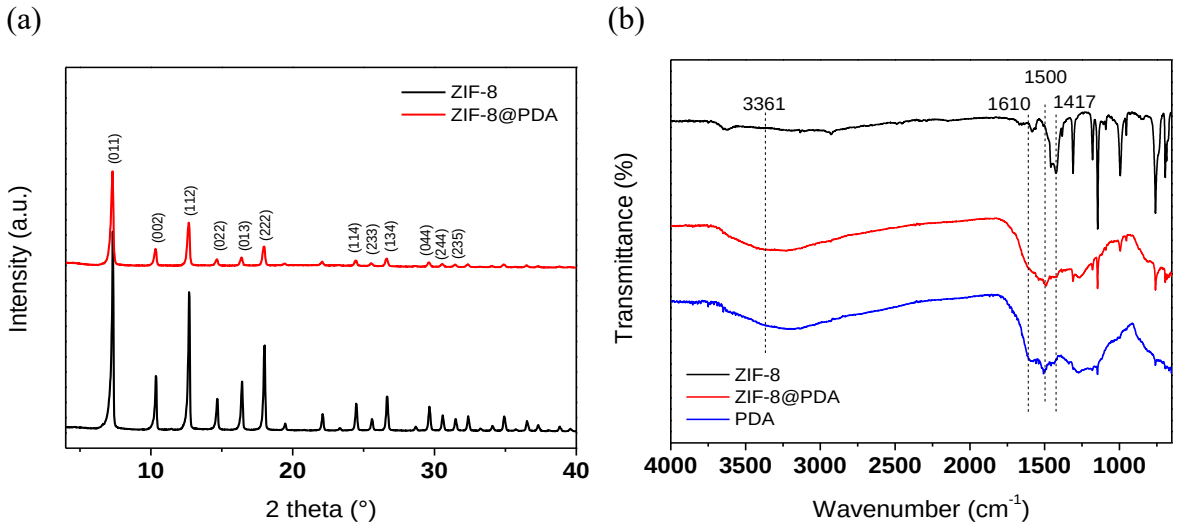

Figure 6.1 (a) XRD diffractograms of pristine ZIF-8 and ZIF-8@PDA, (b) FTIR spectra of pristine ZIF-8, ZIF-8@PDA and PDA

From the SEM micrographs (Figure 6.2(a-b)), ZIF-8 nanocrystals with the size of ca. 200 nm were synthesized. After coating with PDA, the surface of ZIF-8 appeared to be rougher, and some layer structures were deposited on top of ZIF-8 nanocrystals. Under the same condition as the PDA coating process of ZIF-8 (Figure 6.2(c)), PDA nanoparticles with the size of ca. 40

nm were obtained and the particles tended to aggregate. The formation of PDA layer on ZIF-8 nanocrystals was further confirmed by TEM. As shown in TEM micrographs (Figure 6.2(d-e)), it could be clearly observed that a ca. 20 nm thick catechol layer was formed on the ZIF-8 crystal structure. This layer was responsible for coupling the ZIF-8 nanocrystals with the PLA polymer substrate.

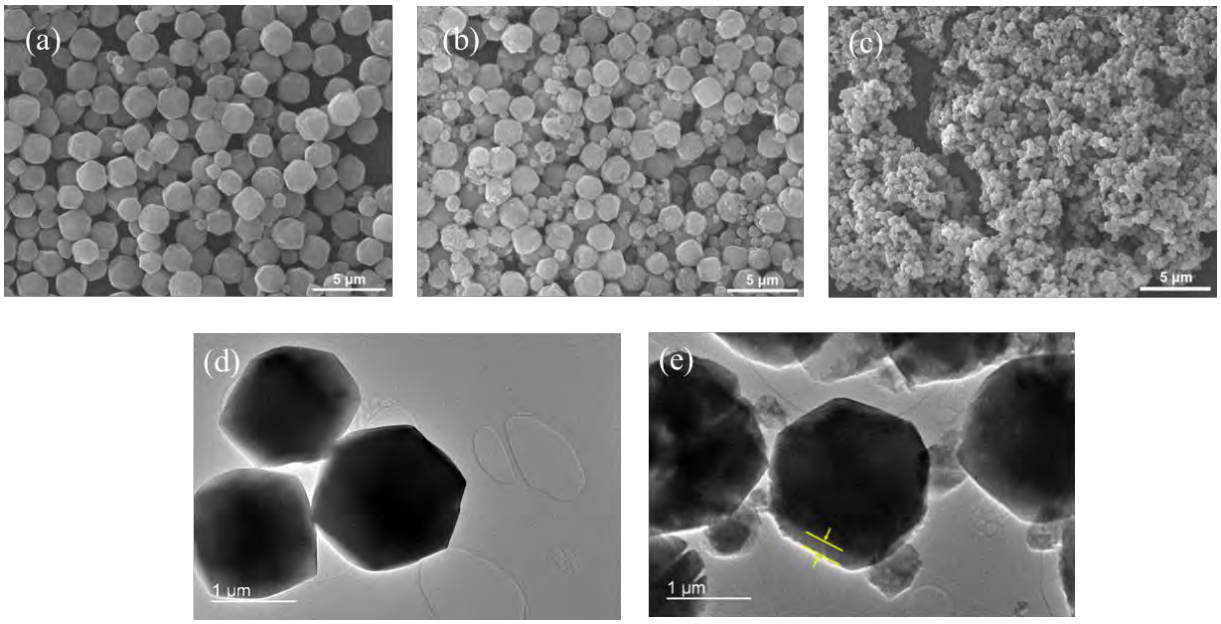

Figure 6.2 SEM micrographs of (a) pristine ZIF-8, (b) ZIF-8@PDA and (c) PDA. TEM micrographs of (d) pristine ZIF-8 and (e) ZIF-8@PDA

6.2.2 Properties of catechol-enhanced PLA composite films

The differences in surface morphologies of PLA thin films with or without dopants were visually evaluated in nanoscale (Figure 6.3). It could be observed that PLA films containing ZIF-8@PDA or PDA had more uniform appearance with less aggregates and less obvious interfacial defects found on the film surface, when compared with that containing pristine ZIF-8. This implied that ZIF-8@PDA fillers could be more homogeneously distributed than pristine

ZIF-8 in the PLA matrix, indicating that PDA interfacial layer could promote the compatibility between ZIF-8 nanofillers and PLA matrix. The formation of catechol coating on ZIF-8 served as an additional buffer layer between the MOF nanofillers and organic polymer matrix. The chemical structure of this PDA buffer minimized the inorganic crystal features of ZIF-8 nanocrystals and facilitated them to better incorporate into the PLA matrix. Hence, catechol-coated MOF fillers could be more uniformly dispersed in the polymer matrix, contributing to the formation of a more homogenous doped material.

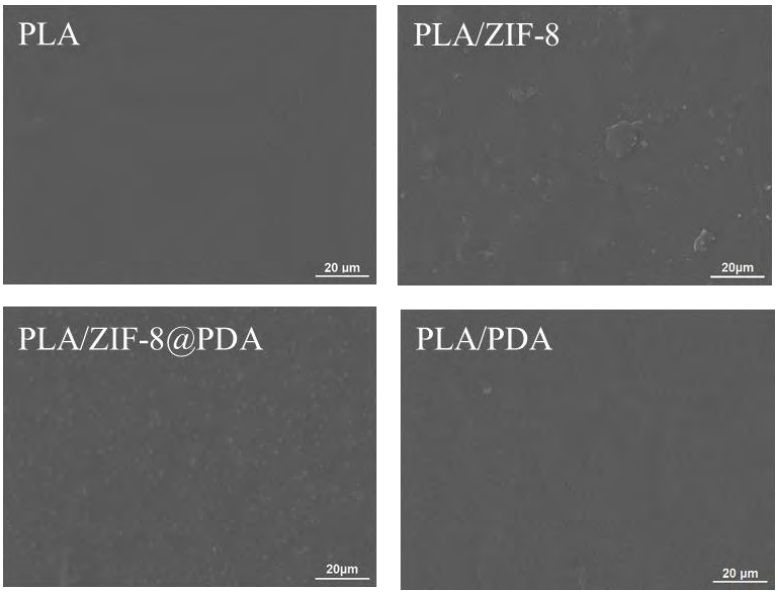

Figure 6.3 SEM micrographs of PLA thin films with different dopants

The distribution of dopants could be further evaluated with the EDX elemental mapping of PLA/ZIF-8 and PLA/ZIF-8@PDA films. The Zn element was only originated from ZIF-8, and the N element was from both ZIF-8 and PDA particles. C and O element gave the strongest signals as they are the fundamental content of PLA substrate and PDA. As shown in Figure 6.4, it clearly revealed that the signals of the Zn and N element of the PLA/ZIF-8@PDA were more uniformly distributed with smaller voids than that of PLA/ZIF-8. The slight differences found were attributed to the low concentration of filler content doped in PLA films. Nevertheless, the

results still verified the ability of PDA interfacial layer to modulate the interfacial compatibility between fillers and polymeric substrate, promoting a more uniform distribution of nanofillers.

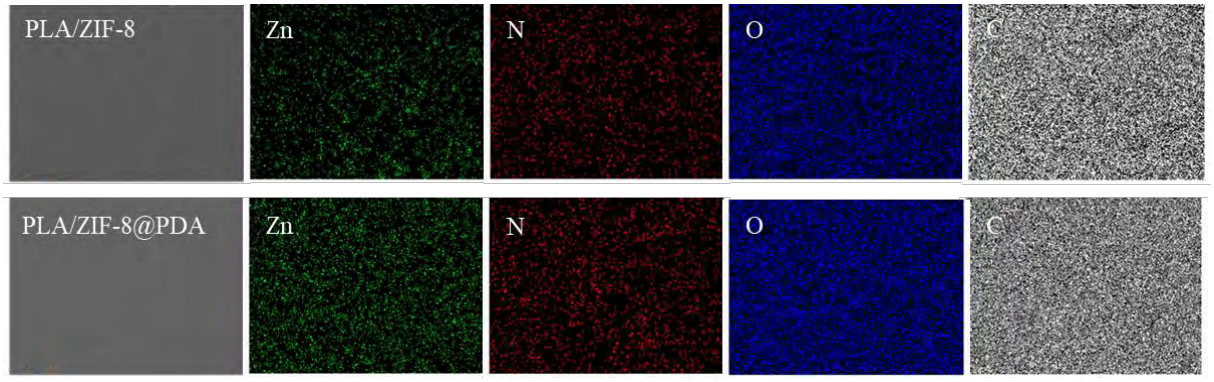

Figure 6.4 EDX elemental mapping of PLA/ZIF-8 and PLA/ZIF-8@PDA films

The effect of catechols on the physical properties of the doped PLA materials were investigated with thermal analytical techniques. From the TGA plots of the percentage of weight loss as a function of increasing temperature (Figure 6.5(a)), it was found that the temperature of major weight loss in pristine PLA and PLA/PDA film was ca. in the range from 340 to 420°C. With the presence of ZIF-8 nanofillers, the major weight loss occurred at a much lower temperature, from 180 to 300°C. The significant change of thermal decomposition pattern indicated that the dopants possibly impeded heat transfer [261], imposing negative impact on the thermal stability of PLA material. It could be emphasized that the major weight loss of PLA/ZIF-8@PDA occurred at a higher temperature than PLA/ZIF-8, from 240 to 330°C. This implied that PDA coating on ZIF-8 acted as a buffer between two distinct interfaces and better interacted with PLA, alleviating the negative impact caused by the interfacial incompatibility. All the doped PLA films levelled off at a higher percentage of weight and left a small amount of black residues. These might be attributed to the incomplete decomposition of dopants. The findings showed that catechol layer on the MOF nanofillers could successfully serve to modulate the interaction between the nanofillers and polymer, better preserving the properties of PLA.

From the DSC thermograms in Figure 6.5(b), it could be observed that the presence of ZIF-8 fillers induced obvious changes in T_g, T_{cc} and T_m to the pristine PLA film. The T_g of pristine PLA resembled that of PLA/ZIF-8@PDA. On the contrary, the T_g of PLA/ZIF-8 decreased from ca. 67.5°C to 55.5°C, while that of PLA/PDA decreased to ca. 55.7°C. It has been proposed that the glass phase transition of composites can be influenced by the distribution of fillers and also the interfacial interaction between host and fillers [262]. Filler aggregating and networking are often related to the loading amount of nanofillers [263].The formation of ZIF-8 nanofiller aggregates contributed to the formation of free volume of the PLA molecular chains, lowering the T_g of PLA/ZIF-8. In contrast, PDA fillers could better interact with the PLA, leading to the decrease in T_g of PLA/PDA. More importantly, the PDA layer on the surface of ZIF-8@PDA could couple with the PLA polymer matrix more efficiently. This interfacial dynamic alleviated the T_g depression, and therefore normal T_g of PLA was recovered [264].

It is worth mentioning that PDA coating on ZIF-8 could lessen the effect of ZIF-8 on pristine PLA and restored some of the thermal properties of pristine PLA in PLA/ZIF-8@PDA. T_{cc} shifted significantly towards lower temperature with the addition of ZIF-8. The T_{cc} peak is associated with the molecular chain order of PLA polymers, and the presence of nanofillers likely exerted impacts on polymer crystallization. Due to the differences between polymer matrix and fillers, ZIF-8 fillers acted as heterogenous nuclei for crystallization, promoting T_c depression [265]. With the introduction of PDA layer on ZIF-8, PLA/ZIF-8@PDA film displayed a similar T_{cc} and exothermic peak as pristine PLA. This confirmed that catechol layer minimized the effect of dopants and allowed comparable rearrangement of a less ordered phase into a more ordered crystalline phase as in the pristine polymer matrix.

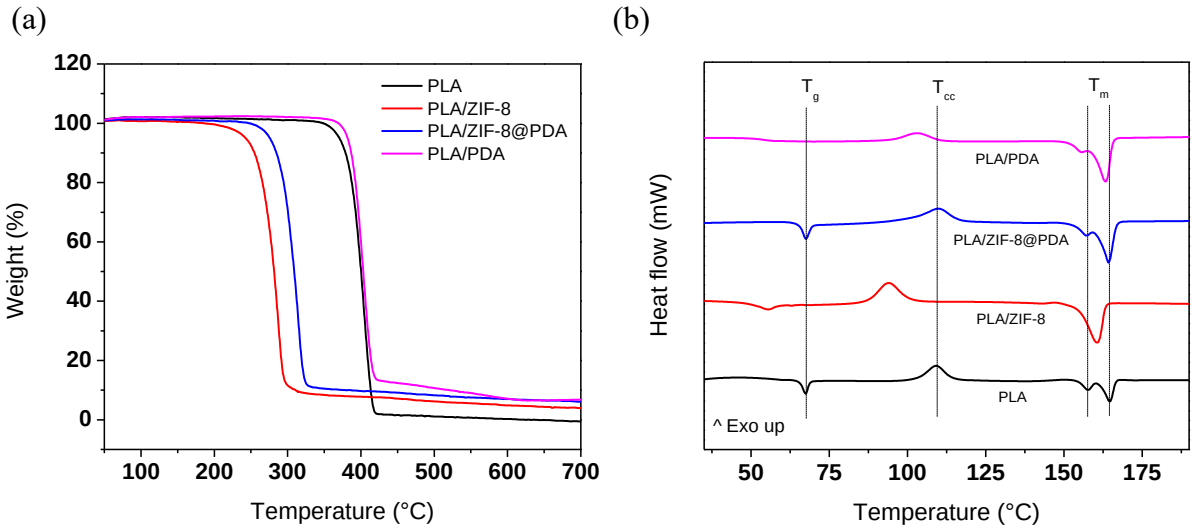

Figure 6.5 (a) TGA plots and (b) DSC thermograms of pristine PLA, PLA/ZIF-8, PLA/ZIF-8@PDA and PLA/PDA composite films

The presence of ZIF-8 content altered the melting behaviors, resulting in lower melting temperature and single peak of melting. The enhanced T_m exothermic peak was linked to the enhanced T_{cc} peak. In contrast, the T_m and double peak of melting of PLA with PDA-coated fillers were akin to that of pristine PLA. The phenomena of double melting peak can be explained by the phenomena of crystals occurred upon heating. Less perfect crystals first undergo cold crystallization, and then melt recrystallization at a temperature right before melting point, followed by subsequent melting at higher temperature [266]. The higher-temperature endotherm of PLA/ZIF-8@PDA and PLA/PDA was more prominent than that of pristine PLA. This possibly implied that the PDA content promoted the melt recrystallization.

For the fillers having poor interaction with polymer host, they likely influence the mobility of polymeric chain molecules and the formation of interfaces [267]. Hence, significant changes in physical properties were resulted in doping PLA with ZIF-8. It is worth noting that the presence of PDA coating could improve the tensile property of the PLA/ZIF-8 composite film

via increasing the interfacial compatibility. As shown in Figure 6.6(a), the tensile properties of PLA films generally decreased with the presence of foreign nanofillers, owing to the non-uniform distribution of fillers and the formation of interfacial defects due to inhomogeneity. PLA/ZIF-8 exhibited the weakest tensile strength since pristine ZIF-8 nanocrystals having inorganic feature was less compatible with PLA substrate. It has been pointed out that the rigidification of surrounding polymer caused by the addition of heterogenous dopants has negative impact on the mechanical properties of host polymer [106]. The introduction of PDA coating on ZIF-8 showed that the load was increased by ca. 19.97 % and the extension was increased by ca. 22.21%. This is because PDA interfacial layer allowed ZIF-8 to better dispersed in the polymer matrix. The catechol buffer minimized the formation of defects, and thus strengthened the tensile property of the PDA/ZIF-8@PDA films.

From the aforementioned results, the coating of PDA on ZIF-8 demonstrated different physical properties than pristine ZIF-8. The differences may be caused by the changes in interfacial interactions. The possible interactions between PLA and ZIF-8@PDA for improving interfacial compatibility is illustrated in Figure 6.6(b). The hydroxyl, amino and protonated amino groups of catechol layer on fillers could interact with the hydroxyl and carboxylate groups of PLA polymer via hydrogen bonding and ionic interactions [258]. These contributed to the homogeneity of PLA/ZIF-8@PDA composite. It can be concluded that catechol coating can be employed as a potential candidate to improve the interfacial interaction between the polymer matrix and fillers. The loss of intrinsic properties and synergistic effect caused by dispersed phase of heterogenous fillers can therefore be modulated by catechol layer on fillers.

(a) (b)

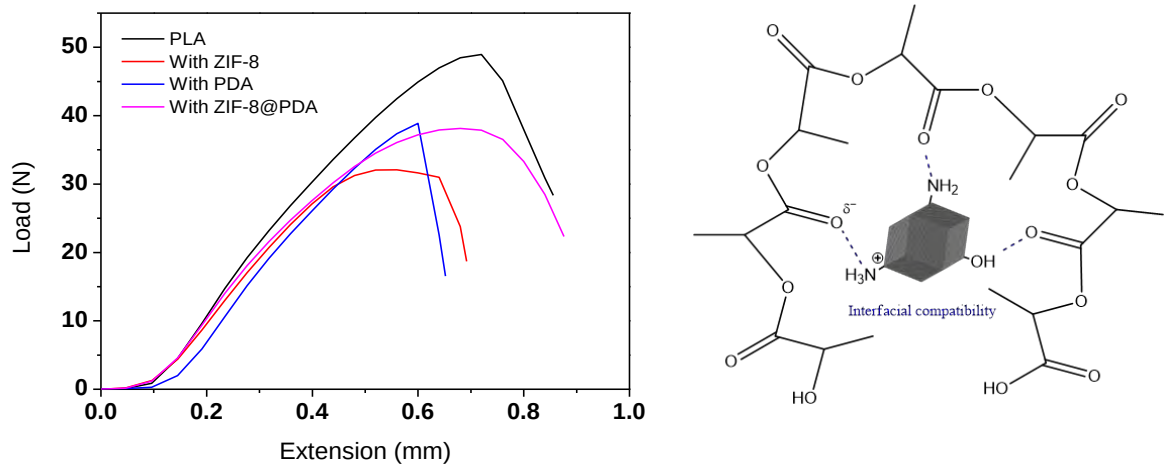

Figure 6.6 (a) Load-extension curves of pure PLA film and films with pristine ZIF-8, ZIF-8@PDA or PDA. (b) Interactions between PLA and ZIF-8@PDA

To investigate the potential of catechol-based PLA composite film, the electrical performance of TENG fabricated with the dielectric films of pristine PLA and PLA with different nanofillers were evaluated. It is worth noting that the electrical performance of PLA films could be enhanced with catechol-coated ZIF-8 (Figure 6.7). The presence of pristine ZIF-8 generally caused a decrease in V_{oc}, I_{sc}, and Q of the PLA film, and this could be owing to the interfacial incompatibility between ZIF-8 and PLA. In contrast, the introduction of PDA coating on ZIF-8 nanocrystals could increase the V_{oc}, I_{sc}, and Q of the PLA composite film by ca. 23.95%, 27.10% and 25.70%, respectively. The power density of this PLA/ZIF-8@PDA could reach up to ca. 312 mW/m^2. The electrical performance of PLA/ZIF-8@PDA film outperformed that of pure PLA film. To explore the effect of the incorporation of nanofillers on the relative permittivity of PLA film, the capacitance of materials versus different frequency from 40 Hz to 30 MHz was probed. Since the capacitance is directly proportional to the relative permittivity of material, the capacitance value can be used to assess the electrical polarizability of material. PLA film with presence of ZIF-8@PDA had an obvious enhancement in the capacitance, and therefore the relative permittivity (Figure S7). The intermediate permittivity of PDA could

partly overcome the permittivity mismatch between fillers and matrix. The findings were in line with the enhanced electrical performance of PLA/ZIF-8@PDA film. The synergistic effect shown by the ZIF-8@PDA could be attributed to the catechol-coated porous structures and the formation of more hydrogen bonding with the organic polymer substrate [104].

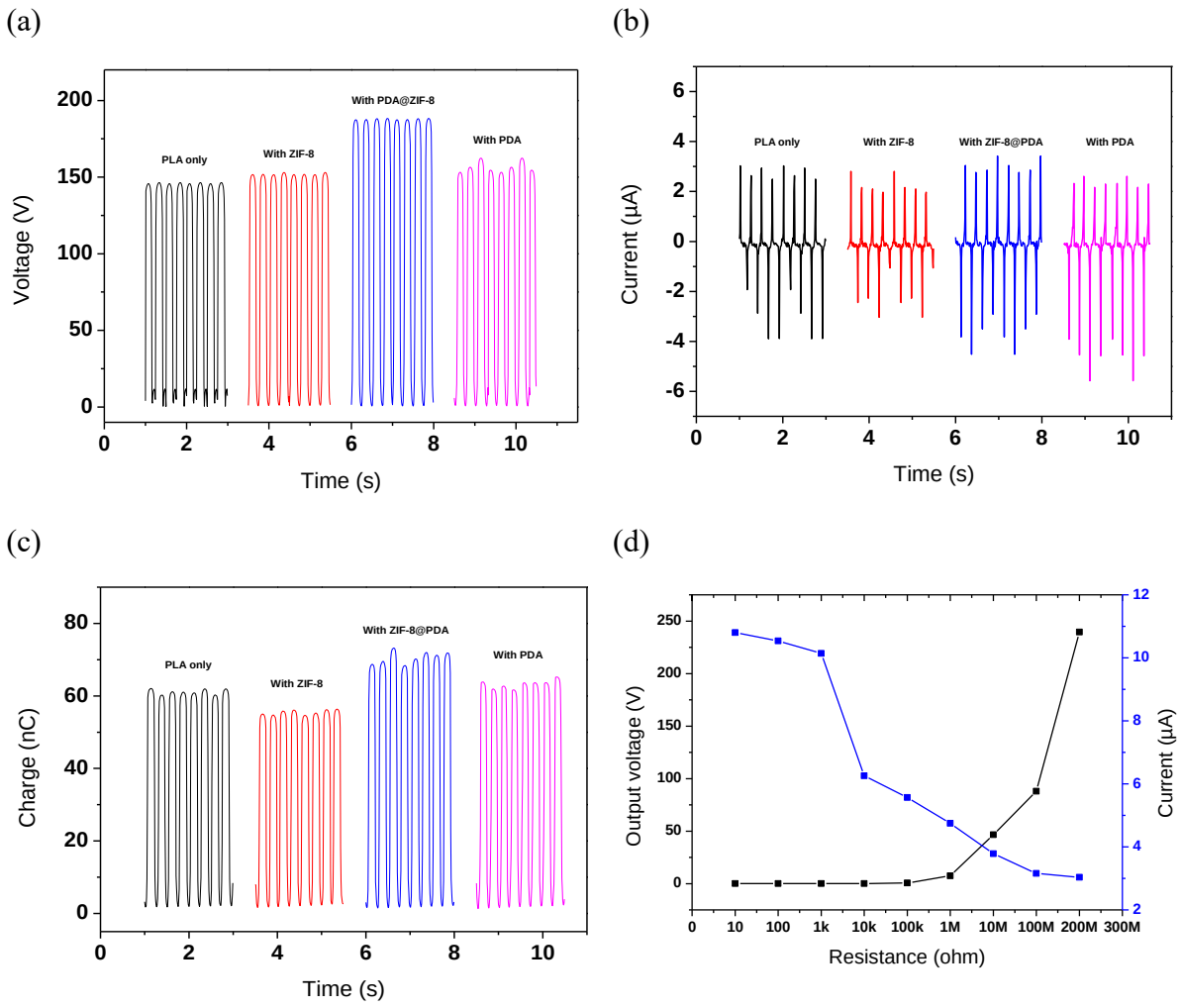

Figure 6.7 Electrical performance of TENG fabricated with different dielectric specimens (a) V_{oc}, (b) I_{sc} and (c) Q of pure PLA film and PLA films with pristine ZIF-8, ZIF-8@PDA or PDA; (d) Output voltage and current of PLA/ZIF-8@PDA at a series of external loads

Both ZIF-8 and ZIF-8@PDA exerted antibacterial effect on PLA film even at low concentration. As shown in Figure 6.8, it can be noted that the PLA/ZIF-8@PDA composite

film exhibited stronger antimicrobial activity against S. aureus (97.58 %) than E. coli (46.79 %). The PLA composite film with 1% ZIF-8@PDA achieved ca. 1.75-log reduction for S. aureus. The composites were found to be more effective on gram-positive bacteria, and this might be explained by the ability of Zn ions released that better disorganized the cell wall of bacteria [268]. Another aspect of this result, the synergistic effect between ZIF-8 and PDA enabled their composites to gain better antibacterial effect on gram-negative bacteria E. coli. This might possibly be attributed to the enhanced destruction of bacterial cell membrane through the electrostatic interactions with PDA. Besides, PDA coating on ZIF-8 promoted the adhesion between ZIF-8@PDA fillers and the surface of bacteria, accelerating the cell distortion process [269].

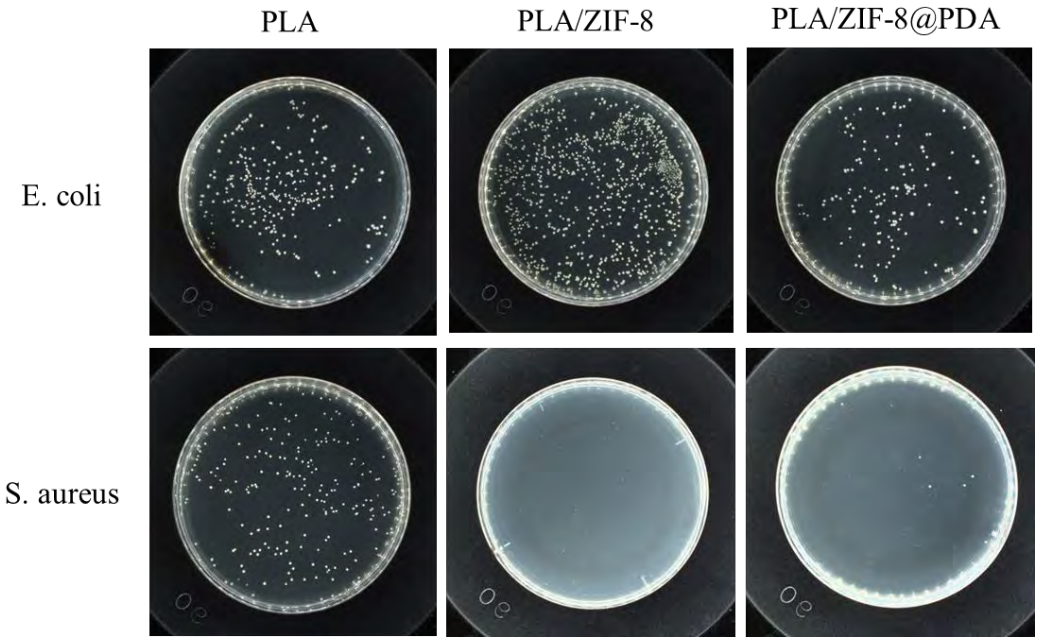

Figure 6.8 Antibacterial assay of PLA and composite films in plate agars after 18-hour incubation with E. coli and S. aureus

6.2.3 Working principle of TENG fabricated with PLA composite film

When the mechanical movement was applied on a triboelectric system, the generation of energy was based on the mechanism shown in Figure 6.9. TENG in vertical contact-separation mode were fabricated with a single layer of tribopositive PLA composite film and a single layer of tribonegative PDMS film. The generation of triboelectric energy was based on the coupling effect of contact electrification of dielectric materials and electrostatic induction of electrodes. At the initial state, there was no electric potential difference in TENG. When an external force was exerted on the triboelectric pair, two layers generate equal number of opposite charges. PLA composite film had the positive charges while PDMS had the negative charges. When the force started releasing and the layers began returning to their original position, electric potential difference was produced. This caused the electron transfer from the electrode of PDMS to the electrode of PLA composite, giving the half output cycle. When the force was fully released, the electric potential difference attained the maximum. When an external force was being exerted on the triboelectric pair again, the decrease of electric potential difference caused the reverse transfer of electrons, giving another half output cycle. When the two layers came into contact again, the charges were neutralized. The cycles could be repeated continuously for the generation of triboelectric energy.

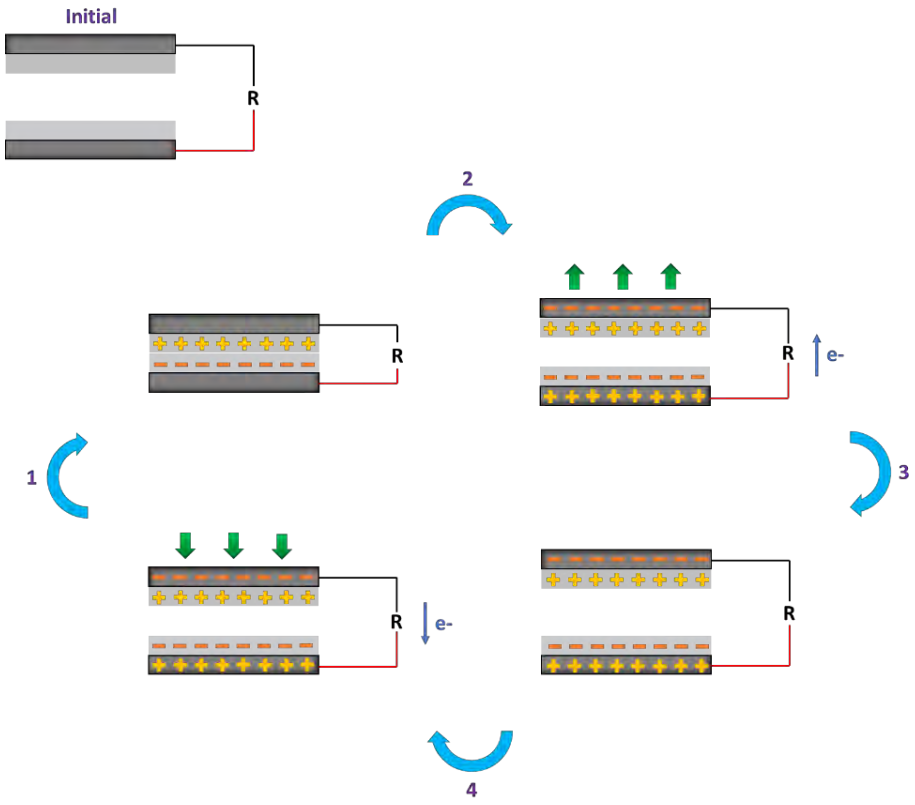

Figure 6.9 Mechanism of TENG fabricated with PLA composite film under the stages of (1) force exerted, (2) releasing, (3) released and (4) exerting

6.2.4 Potential application as a power source

To demonstrate the potential application of the PLA/ZIF-8@PDA TENG, its charging property was first evaluated with a series of commercial capacitors (0.22, 1, 2.2, 10 and 22 μF). As shown in Figure 6.10(a), 0.22 μF capacitor could be charged to 8 V within 8 s, giving a charging rate of 1 V s^{-1}. In Figure 6.10(b), the equivalent circuit diagram for charging/discharging of electronic devices using the proposed TENG, rectifier and capacitor was illustrated. In Figure 6.10(c-e), PLA/ZIF-8@PDA TENG system could successfully light up 120 LED light bulbs, and it could also power up both commercial electrical watch and calculator. The results indicated that TENG fabricated with PLA/ZIF-8@PDA had potential to provide a source of electrical energy for small electronic devices.

(a)

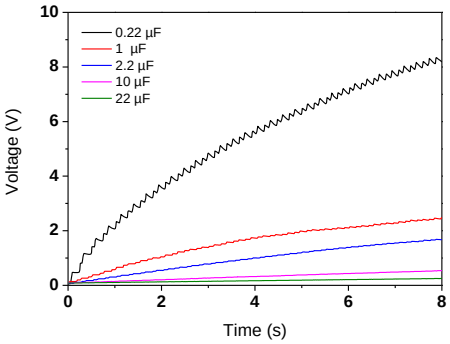

(b)

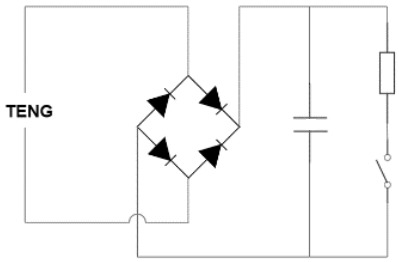

(c)

(d)

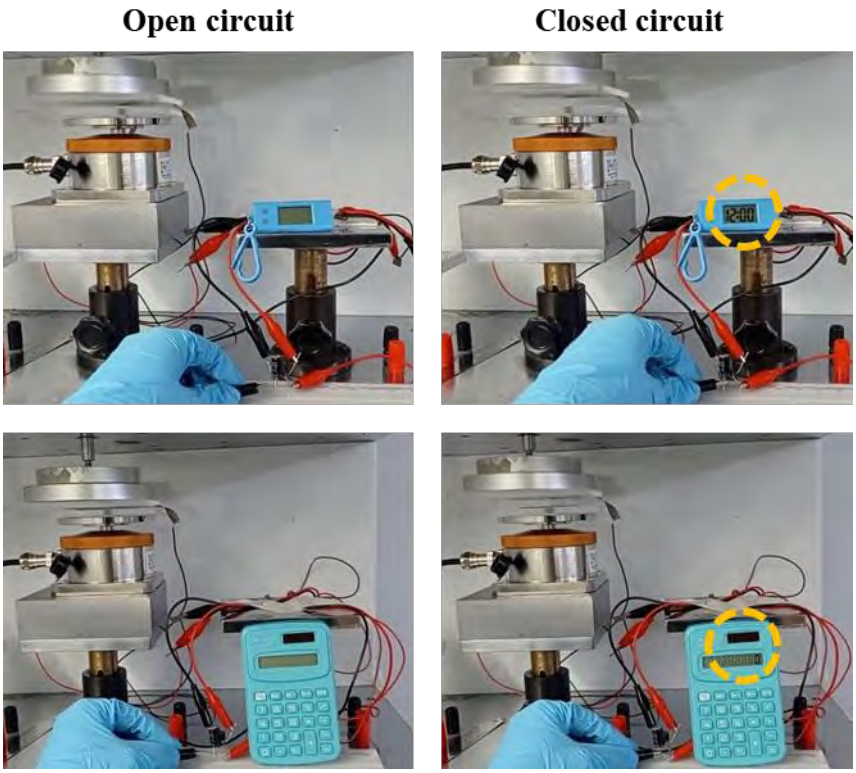

Figure 6.10 Potential application: (a) Charging graphs of different capacitors charged by PLA/ZIF-8@PDA TENG; (b) Circuit diagram for charging/discharging of electronic devices using the proposed TENG; Photographs of (c) green LED bulbs lightened up and (d) a commercial electronic digital clock and a calculator powered by PLA/ZIF-8@PDA TENG

6.3 Conclusions

The effect of catechol layer on the interfacial compatibility between MOF and polymer, and their application as composite dielectric material for TENG were explored. The presence of PDA layer between ZIF-8 fillers and PLA polymeric matrix promoted the uniform distribution of dopants, retained the physical properties of pristine PLA, and enhanced certain degree of antibacterial activity. The catechol-enhanced composite dielectric materials also improved the electrical performance of PLA thin films in TENG. These results have preliminarily proved that catechol-enhanced surface modification of MOF could be an approach to modulate the interfacial interaction between distinct materials. The catechol buffer between filler and matrix can also boost the triboelectric energy-generating ability of sustainable triboelectric materials. Therefore, the devisable MOF with catechol coating demonstrate high prospect in the future fabrication of energy functional materials. However, more comprehensive studies for optimization of catechol effect and further development of practical TENG applications are highly demanded.

7 CONCLUSIONS AND SUGGESTIONS FOR FUTURE RESEARCH

7.1 Conclusions

This thesis has highlighted the diverse features of catechols including adhesiveness, light absorption, pH sensitivity, compatibility, and sustainability. Catechols have shown their prospects to play a main or auxiliary role in sustainable material functionalization. Their compatibility with a wide range of materials allows catechol chemistry applications to merge the multidisciplinary and interdisciplinary research trend. Specifically, the findings have shown that catechol derivatives have potential in the improvement of applications in the aspects of textile coloration, wastewater treatment, and energy generation.

For the first study, heteromolecular pigmentations of plant-derived catechol caffeic acid with amino acids as a novel sustainable alternative to conventional process was reported. The catechol-based pigments can be formed with trace amount of naturally occurring reactants at room temperature via the oxidation-induced reactions. The colour formation of catechol-based pigments can be easily tuned with various parameters for a wider colour range. Textile fabrics dyed with blue, green and grey colours are rarely achieved using polycatechols. This simple in-situ coloration also exhibits good batch-to-batch reproducibility, and the dyed materials show excellent colour fastness even without the presence of mordanting agent. The catechol-based pigmentation manifests potential in integrating with other sustainable methods like cold pad-batch coloration for further waste reduction. The proposed technology offers the

advantages of utilization of renewable resources, elimination of extraction processes of natural organic colorants, and energy conservation.

For the second study, the magnetic polydopamine nanocomposites (Fe_3O_4@PDA) with smart dye adsorption-desorption behavior for dye wastewater treatment was reported. Bio-inspired PDA endowed the polymer-based hybrid adsorbent with unique surface chemistry for universal application, and Fe_3O_4 mainly contributed to the magnetic character for easy separation from bulk wastewater. This composite could expand the variety of dye adsorption and simplify the collection process of the adsorbent. It has been found that Fe_3O_4@PDA tends to adsorb anionic dyes but desorb cationic dyes with decreasing pH, and vice versa with increasing pH. The hybrid adsorbent could efficiently adsorb four different types of anionic and cationic dyes. Separation of dyestuffs with opposite ionic properties could be successfully attained through tuning pH-induced surface charges of PDA layers. This controllable behavior allowed simple separation of waste dyestuffs without large consumption of energy and organic solvent. In addition, these adsorption-desorption behaviors of this bio-inspired adsorbent exhibited reversibility, and therefore recyclability was possible. The results have indicated that adsorbent with enhanced efficiency and universality in ionic dye adsorption and separation could be achieved with our proposed strategy. This study can offer fundamental results for high-quality wastewater treatment with the aim of utilizing recovered dyes.

For the third study, the catechol-enhanced functional material was fabricated for triboelectric energy-generating purposes. The interfacial modulation feature of PDA between zeolitic imidazolate framework-8 (ZIF-8) and polylactic acid (PLA) better preserves the PLA property and gains synergistic effect from distinct materials in the PLA composites. It was found that the presence of PDA buffer layer on nanofillers could facilitate a more uniform distribution of

ZIF-8 in PLA matrix, retain the physical properties of polymer and enhance the antibacterial activity of the composites. It has demonstrated that the PLA thin film doped with catechol-coated porous nanoparticles could improve the electrical performance of the TENG system. The results have preliminarily proved that catechol interfacial modification can be an approach to modulate the interfacial compatibility between MOF fillers and polymer matrix, as well as to boost the development of sustainable energy materials with multifunctionalities.

7.2 Suggestions for Future Research

Even though the versatility of catechol chemistry for material functionalization in different disciplines has been illustrated in this thesis, comprehensive future studies are required to optimize the performance and explore the mechanisms behind the phenomena. Future multidisciplinary and interdisciplinary research based on catechol chemistry is eminently expected. Some of the highlighted limitations and recommendations are listed below:

1. The colour range of catechol-based pigments is still relatively narrow, limiting their commercialization success. In order to expand the diversity of colour range, the reaction mechanism of catechol moiety with various amino acids should be further investigated for facilitating the design of catechol-based pigments in the subsequent work.

2. Since some of the interactions between catechol adsorbent and dyestuffs is irreversible, the adsorption capacity gradually decreases with increasing number of reuse cycles. To enhance the adsorption capacity and reusability, surface modification of catechol layer

on the adsorbents may be required to induce favourable adsorption and restrict undesirable reactions.

3. The effect of thickness and chemical compositions of catechol interfacial layer on MOFs is worth investigating to deduce the favourable conditions for obtaining optimized performance. To satisfy the demand for self-powered sensing applications for monitoring human activities, the sensitivity and specificity of TENG for multi-modal strains found in human motions are yet to be enhanced with novel materials and structural designs. Machine-learning analysis may also be employed to solve the potential confusion problems.

4. The uniform formation of catechol coating on substrates is still a challenging topic since the polymerization process of catechols is often susceptible to the minor changes in reaction conditions. Therefore, the study of controlling uniform coating of catechol on substrate is crucial for the development of stable, reproducible and high-quality composites.

5. Numerous catechol-related applications often focus on a particular type of functionality that catechols exhibit. The high chemical tailorability of catechol derivatives essentially enables themselves to be customized into materials with multifunctionalities. More efforts can be dedicated to the integration of distinct features of catechols into one single material for multiple applications.

6. Most of the current studies are based on the phenomena found, and there is lack of well-developed mechanisms to comprehensively explain the catechol-related interactions.

Thus, in-depth investigation of mechanisms involved in the catechol phenomena is highly demanded for better control of catechol reactions and therefore their development of functional applications.

APPENDICES

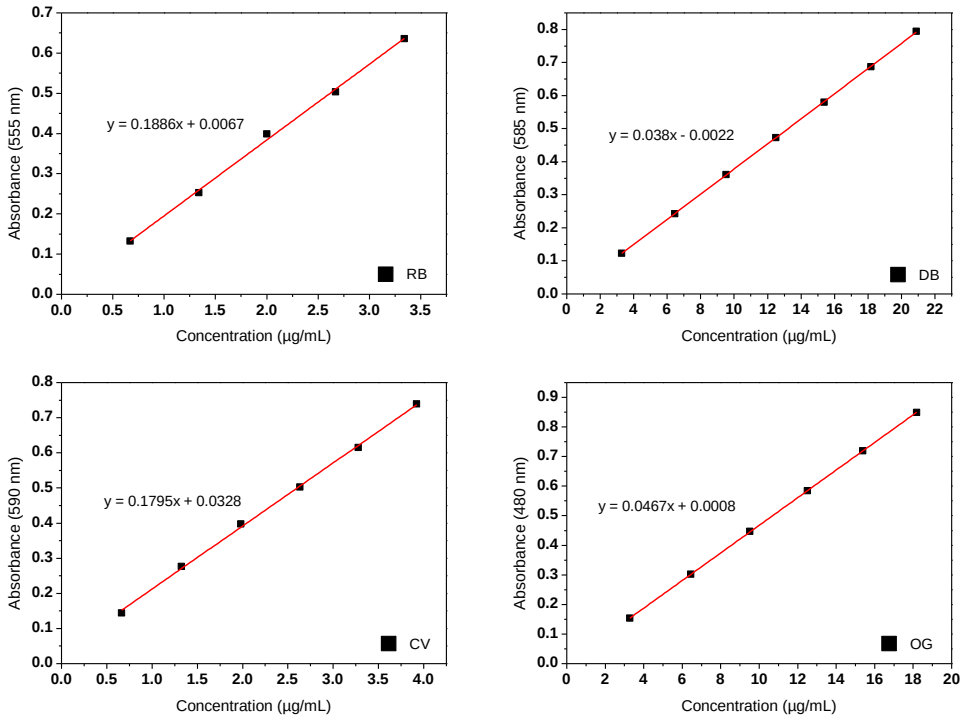

Figure S1 Calibration curves of Rhodamine B (RB), Direct Blue 71 (DB), Crystal Violet (CV) and Orange G (OG)

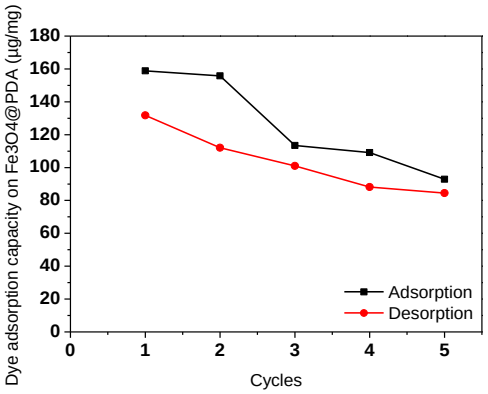

Figure S2 The graph of reusability of Fe_3O_4@PDA in anionic DB dye adsorption for five cycles

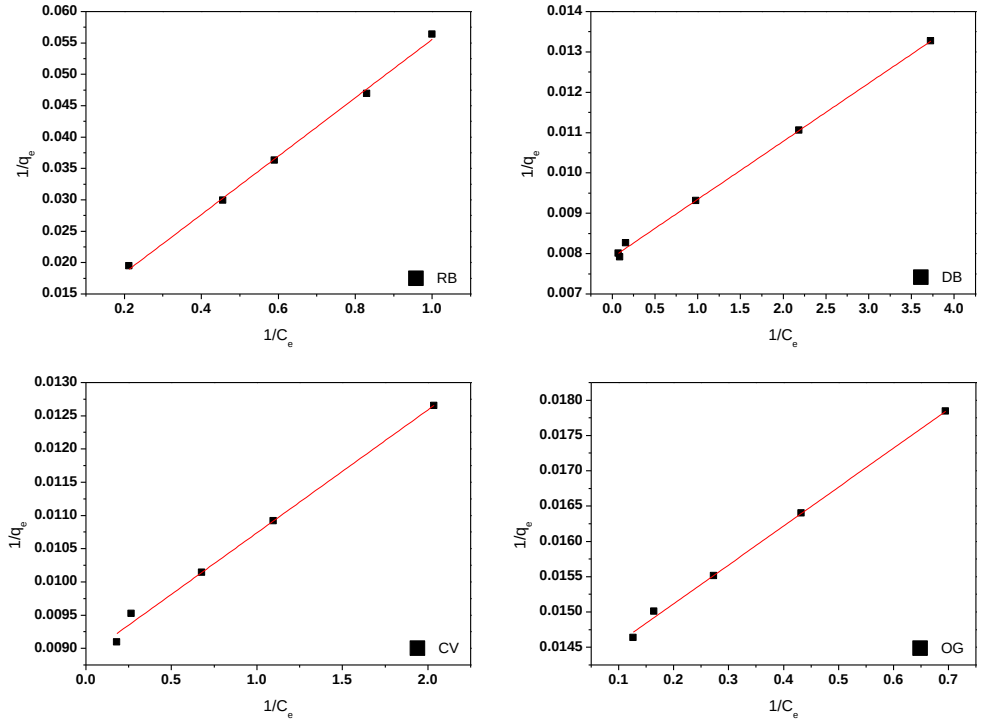

Figure S3 Langmuir isotherm plots for the adsorption of RB, DB, CV and OG onto Fe_3O_4@PDA

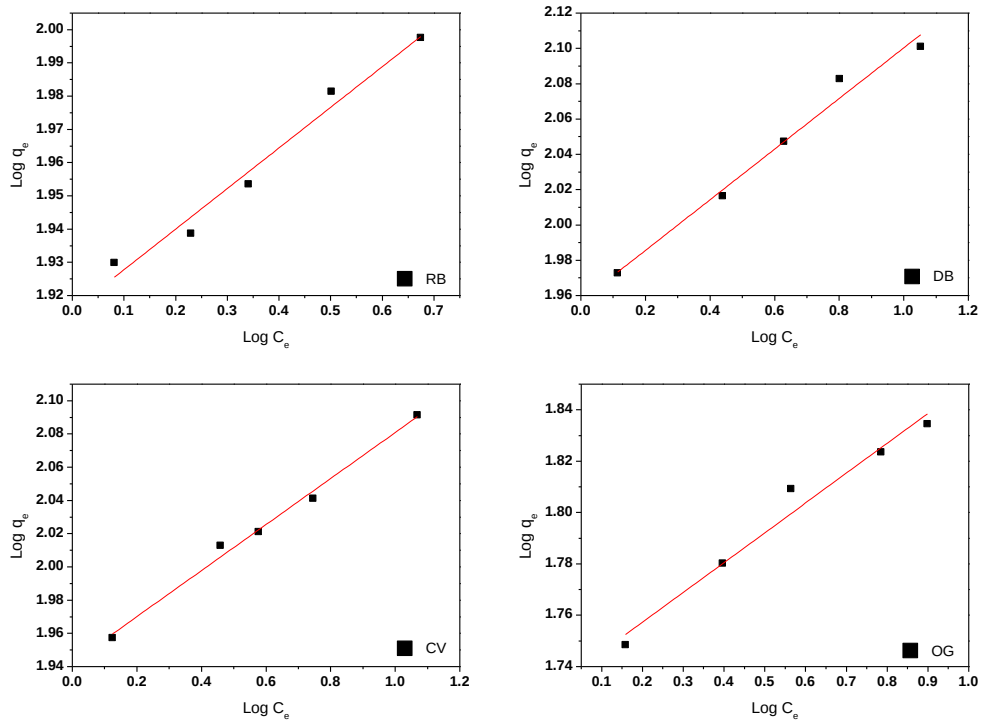

Figure S4 Freundlich isotherm plots for the adsorption of RB, DB, CV and OG onto Fe_3O_4@PDA

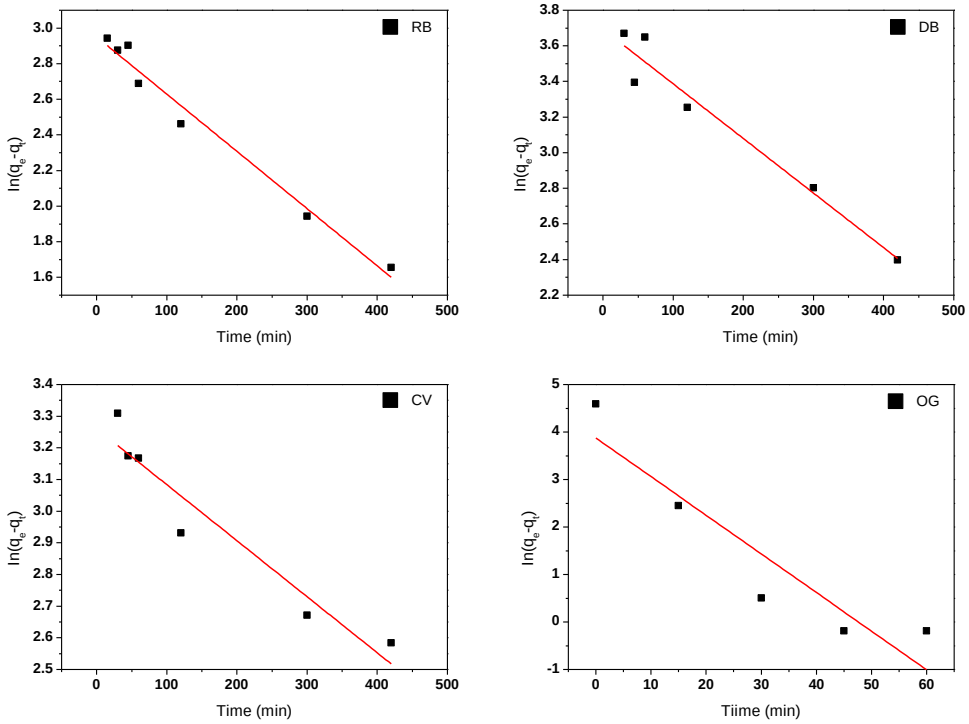

Figure S5 Pseudo-first-order kinetic plots for the adsorption of RB, DB, CV and OG onto Fe_3O_4@PDA

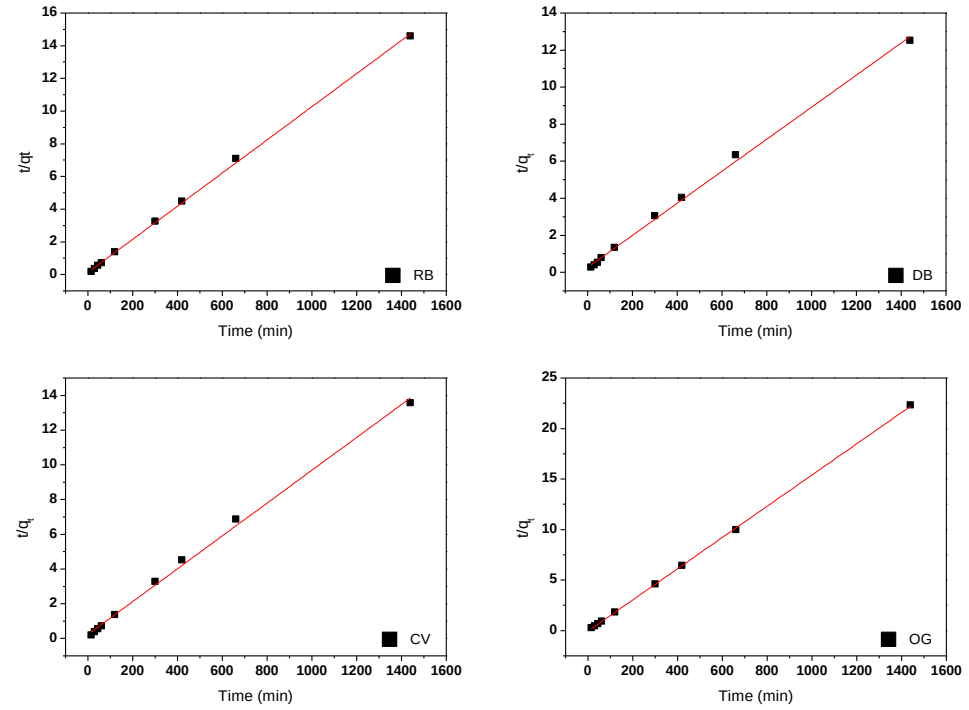

Figure S6 Pseudo-second-order kinetic plots for the adsorption of RB, DB, CV and OG onto Fe_3O_4@PDA

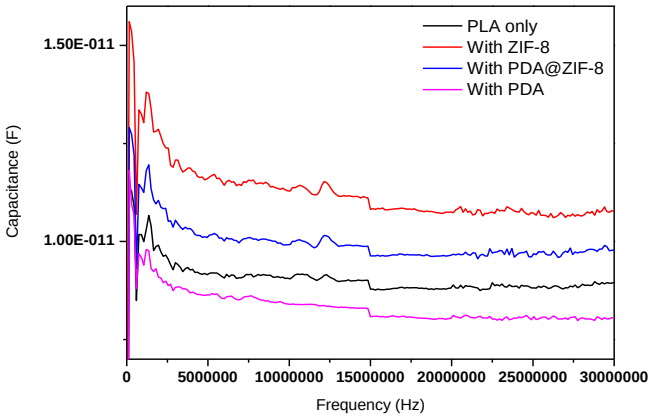

Figure S7 Capacitance of PLA specimens versus different frequency from 40 Hz to 30 MHz

REFERENCES

[1] J. H. Waite and M. L. Tanzer, "Polyphenolic substance of Mytilus edulis: novel adhesive containing L-dopa and hydroxyproline," *Science,* vol. 212, no. 4498, pp. 1038-1040, 1981, doi: https://doi.org/10.1126/science.212.4498.1038.

[2] Q. Lin *et al.*, "Adhesion mechanisms of the mussel foot proteins mfp-1 and mfp-3," *Biophysics and Computational Biology,* vol. 104, no. 10, pp. 3782-3786, 2007, doi: https://doi.org/10.1073/pnas.0607852104.

[3] H. G. Silverman and F. F. Roberto, "Understanding marine mussel adhesion," *Marine Biotechnology,* vol. 9, no. 6, pp. 661-681, 2007, doi: https://doi.org/10.1007/s10126-007-9053-x.

[4] H. Lee, N. F. Scherer, and P. B. Messersmith, "Single-molecule mechanics of mussel adhesion," *Proceedings of the National Academy of Sciences of the United States of America,* vol. 103, no. 35, pp. 12999-13003, 2006, doi: https://doi.org/10.1073/pnas.0605552103.

[5] M. J. Sever, J. T. Weisser, J. Monahan, S. Srinivasan, and J. J. Wilker, "Metal-mediated cross-linking in the generation of a marine-mussel adhesive," *Angewandte Chemie International Edition,* vol. 43, no. 4, pp. 448-450, 2004, doi: https://doi.org/10.1002/anie.200352759.

[6] J. H. Waite, N. H. Andersen, S. Jewhurst, and C. Sun, "Mussel adhesion: finding the tricks worth mimicking," *The Journal of Adhesion,* vol. 81, no. 3-4, pp. 297-317, 2005, doi: https://doi.org/10.1080/00218460590944602.

[7] J. Saiz-Poseu, J. Mancebo-Aracil, F. Nador, F. Busqué, and D. Ruiz-Molina, "The Chemistry behind Catechol-Based Adhesion," *Angewandte Chemie International Edition,* vol. 58, no. 3, pp. 696-714, 2019, doi: https://doi.org/10.1002/anie.201801063.

[8] H. Lee, S. M. Dellatore, W. M. Miller, and P. B. Messersmith, "Mussel-inspired surface chemistry for multifunctional coatings," *Science,* vol. 318, no. 5849, pp. 426-430, 2007, doi: https://doi.org/10.1126/science.1147241.

[9] T. G. Barclay, H. M. Hegab, S. R. Clarke, and M. Ginic-Markovic, "Versatile Surface Modification Using Polydopamine and Related Polycatecholamines: Chemistry, Structure, and Applications," *Advanced Materials Interfaces,* vol. 4, no. 19, p. 1601192, 2017, doi: https://doi.org/10.1002/admi.201601192.

[10] Q. Huang, J. Chen, M. Liu, H. Huang, X. Zhang, and Y. Wei, "Polydopamine-based functional materials and their applications in energy, environmental, and catalytic fields: State-of-the-art review," *Chemical Engineering Journal,* vol. 387, p. 124019, 2020, doi: https://doi.org/10.1016/j.cej.2020.124019.

[11] M. Liu *et al.*, "Recent developments in polydopamine: an emerging soft matter for surface modification and biomedical applications," *Nanoscale,* vol. 8, no. 38, pp. 16819-16840, 2016, doi: https://doi.org/10.1039/c5nr09078d.

[12] R. A. Sheldon, "The E factor 25 years on: the rise of green chemistry and sustainability," *Green Chemistry,* vol. 19, no. 1, pp. 18-43, 2017, doi: https://doi.org/10.1039/c6gc02157c.

[13] H. C. Erythropel *et al.*, "The Green ChemisTREE: 20 years after taking root with the 12 principles," *Green Chemistry,* vol. 20, no. 9, pp. 1929-1961, 2018, doi: https://doi.org/10.1039/c8gc00482j.

[14] S. ul-Islam and B. S. Butola, *The Impact and Prospects of Green Chemistry for Textile Technology*. San Diego: San Diego: Elsevier Science & Technology, 2018.

[15] W.-G. Kim, D.-W. Kim, I.-W. Tcho, J.-K. Kim, M.-S. Kim, and Y.-K. Choi, "Triboelectric Nanogenerator: Structure, Mechanism, and Applications," *ACS Nano,* vol. 15, no. 1, pp. 258-287, 2021, doi: https://doi.org/10.1021/acsnano.0c09803.

[16] P. E. Fayemi, K. Wanieck, C. Zollfrank, N. Maranzana, and A. Aoussat, "Biomimetics: process, tools and practice," *Bioinspiration & Biomimetics,* vol. 12, no. 1, pp. 011002-011002, 2017, doi: https://doi.org/10.1088/1748-3190/12/1/011002.

[17] J. Hwang, Y. Jeong, J. M. Park, K. H. Lee, J. W. Hong, and J. Choi, "Biomimetics: Forecasting the future of science, engineering, and medicine," *International Journal of Nanomedicine,* vol. 10, pp. 5701-5713, 2015, doi: https://doi.org/10.2147/IJN.S83642.

[18] J. Wood, "Bioinspiration in Fashion—A Review," *Biomimetics (Basel),* vol. 4, no. 1, p. 16, 2019, doi: https://doi.org/10.3390/biomimetics4010016.

[19] Y. H. Cohen and Y. Reich, *Biomimetic design method for innovation and sustainability*. Springer, 2016.

[20] Y. Brechet *et al.*, *Materials design inspired by nature: function through inner architecture*. Royal Society of Chemistry, 2015.

[21] S. Quideau, D. Deffieux, C. Douat-Casassus, and L. Pouysegu, "Plant polyphenols: chemical properties, biological activities, and synthesis," *Angewandte Chemie International Edition,* vol. 50, no. 3, pp. 586-621, 2011, doi: https://doi.org/10.1002/anie.201000044.

[22] J. Yang, M. A. Cohen Stuart, and M. Kamperman, "Jack of all trades: versatile catechol crosslinking mechanisms," *Chemical Society Reviews,* vol. 43, no. 24, pp. 8271-8298, 2014, doi: https://doi.org/10.1039/C4CS00185K.

[23] M. A. Rahim, S. L. Kristufek, S. Pan, J. J. Richardson, and F. Caruso, "Phenolic building blocks for the assembly of functional materials," *Angewandte Chemie*

International Edition, vol. 58, no. 7, pp. 1904-1927, 2019, doi: https://doi.org/10.1002/anie.201807804.

[24] A. Soto-Vaca, A. Gutierrez, J. N. Losso, Z. Xu, and J. W. Finley, "Evolution of phenolic compounds from color and flavor problems to health benefits," *Journal of Agricultural Food Chemistry,* vol. 60, no. 27, pp. 6658-6677, 2012, doi: https://doi.org/10.1021/jf300861c.

[25] J.-L. Jonker, L. Morrison, E. P. Lynch, I. Grunwald, J. von Byern, and A. M. Power, "The Chemistry of stalked barnacle adhesive (Lepas anatifera)," *Interface Focus,* vol. 5, no. 1, p. 20140062, 2015, doi: https://doi.org/10.1098/rsfs.2014.0062.

[26] L. Petrone *et al.*, "Mussel adhesion is dictated by time-regulated secretion and molecular conformation of mussel adhesive proteins," *Nature communications,* vol. 6, no. 1, pp. 1-12, 2015, doi: https://doi.org/10.1038/ncomms9737.

[27] N. Bandara, H. Zeng, and J. Wu, "Marine mussel adhesion: biochemistry, mechanisms, and biomimetics," *Journal of Adhesion Science Technology,* vol. 27, no. 18-19, pp. 2139-2162, 2013, doi: https://doi.org/10.1080/01694243.2012.697703.

[28] S. Kim, L. K. Jang, H. S. Park, and J. Y. Lee, "Electrochemical deposition of conductive and adhesive polypyrrole-dopamine films," *Scientific Reports,* vol. 6, no. 1, pp. 1-8, 2016, doi: https://doi.org/10.1038/srep30475.

[29] S. K. Madhurakkat Perikamana *et al.*, "Materials from mussel-inspired chemistry for cell and tissue engineering applications," *Biomacromolecules,* vol. 16, no. 9, pp. 2541-2555, 2015, doi: https://doi.org/10.1021/acs.biomac.5b00852.

[30] M. E. Lynge, P. Schattling, and B. Städler, "Recent developments in poly (dopamine)-based coatings for biomedical applications," *Nanomedicine,* vol. 10, no. 17, pp. 2725-2742, 2015, doi: https://doi.org/10.2217/nnm.15.89.

[31] X. Chen *et al.*, "Polydopamine integrated nanomaterials and their biomedical applications," *Current pharmaceutical design,* vol. 21, no. 29, pp. 4262-4275, 2015, doi: https://doi.org/10.2174/1381612821666150901103418.

[32] M. E. Lynge, R. van der Westen, A. Postma, and B. Städler, "Polydopamine—a nature-inspired polymer coating for biomedical science," *Nanoscale,* vol. 3, no. 12, pp. 4916-4928, 2011, doi: https://doi.org/10.1039/C1NR10969C.

[33] F. Cicoira and C. Santato, *Organic electronics: emerging concepts and technologies*. John Wiley & Sons, 2013.

[34] H.-C. Yang, J. Luo, Y. Lv, P. Shen, and Z.-K. Xu, "Surface engineering of polymer membranes via mussel-inspired chemistry," *Journal of Membrane Science,* vol. 483, pp. 42-59, 2015, doi: https://doi.org/10.1016/j.memsci.2015.02.027.

[35] M. Guardingo Melian, *Interfacial chemistry of catechol-based nanostructures*. Universitat Autònoma de Barcelona, 2015.

[36] F. Daayf and V. Lattanzio, *Recent advances in polyphenol research*. John Wiley & Sons, 2009.

[37] K. Gould, K. M. Davies, and C. Winefield, *Anthocyanins: biosynthesis, functions, and applications*. Springer Science & Business Media, 2008.

[38] J. Hu, L. Yang, P. Yang, S. Jiang, X. Liu, and Y. Li, "Polydopamine free radical scavengers," *Biomaterials Science,* vol. 8, no. 18, pp. 4940-4950, 2020, doi: https://doi.org/10.1039/D0BM01070G

[39] A. A. Watt, J. P. Bothma, and P. Meredith, "The supramolecular structure of melanin," *Soft Matter,* vol. 5, no. 19, pp. 3754-3760, 2009, doi: https://doi.org/10.1039/B902507C.

[40] J. Wu *et al.*, "Nanomaterials with enzyme-like characteristics (nanozymes): next-generation artificial enzymes (II)," *Chemical Society Reviews,* vol. 48, no. 4, pp. 1004-1076, 2019, doi: https://doi.org/10.1039/C8CS00457A.

[41] V. Ball, "Polydopamine films and particles with catalytic activity," *Catalysis Today,* vol. 301, pp. 196-203, 2018, doi: https://doi.org/10.1016/j.cattod.2017.01.031.

[42] J. Liebscher, "Chemistry of Polydopamine–Scope, Variation, and Limitation," *European Journal of Organic Chemistry,* vol. 2019, no. 31-32, pp. 4976-4994, 2019, doi: https://doi.org/10.1002/ejoc.201900445.

[43] D. R. Dreyer, D. J. Miller, B. D. Freeman, D. R. Paul, and C. W. Bielawski, "Elucidating the structure of poly (dopamine)," *Langmuir,* vol. 28, no. 15, pp. 6428-6435, 2012, doi: https://doi.org/10.1021/la204831b.

[44] W. Zhang, Z. Pan, F. K. Yang, and B. Zhao, "A facile in situ approach to polypyrrole functionalization through bioinspired catechols," *Advanced Functional Materials,* vol. 25, no. 10, pp. 1588-1597, 2015, doi: https://doi.org/10.1002/adfm.201403115.

[45] Z. Deng, B. Shang, and B. Peng, "Polydopamine Based Colloidal Materials: Synthesis and Applications," *The Chemical Record,* vol. 18, no. 4, pp. 410-432, 2018, doi: https://doi.org/10.1002/tcr.201700051.

[46] A. Lucero, C. Rebolledo, and G. Buono-Core, "Effect of some natural UV-absorbers on the photostabilization of active ingredients in German chamomille floral extracts: part I," *Journal of the Chilean Chemical Society,* vol. 57, no. 3, pp. 1309-1212, 2012, doi: http://dx.doi.org/10.4067/S0717-97072012000300024

[47] S. Lautenschlager, H. C. Wulf, and M. R. Pittelkow, "Photoprotection," *The Lancet,* vol. 370, no. 9586, pp. 528-537, 2007, doi: https://doi.org/10.1016/S0140-6736(07)60638-2.

[48] C. Wang *et al.*, "Skin Pigmentation-Inspired Polydopamine Sunscreens," *Advanced Functional Materials,* vol. 28, no. 33, p. 1802127, 2018, doi: https://doi.org/10.1002/adfm.201802127.

[49] Y. Fu *et al.*, "Polydopamine antibacterial materials," *Materials Horizons,* 10.1039/D0MH01985B vol. 8, no. 6, pp. 1618-1633, 2021, doi: https://doi.org/10.1039/D0MH01985B.

[50] H. Liu *et al.*, "Role of polydopamine's redox-activity on its pro-oxidant, radical-scavenging, and antimicrobial activities," *Acta Biomaterialia,* vol. 88, pp. 181-196, 2019, doi: https://doi.org/10.1016/j.actbio.2019.02.032.

[51] H. Karkhanechi, R. Takagi, and H. Matsuyama, "Biofouling resistance of reverse osmosis membrane modified with polydopamine," *Desalination,* vol. 336, pp. 87-96, 2014, doi: https://doi.org/10.1016/j.desal.2013.12.033.

[52] J.-W. Xu, K. Yao, and Z.-K. Xu, "Nanomaterials with a photothermal effect for antibacterial activities: an overview," *Nanoscale,* 10.1039/C9NR01833F vol. 11, no. 18, pp. 8680-8691, 2019, doi: https://doi.org/10.1039/C9NR01833F.

[53] L. Li, W. Smitthipong, and H. Zeng, "Mussel-inspired hydrogels for biomedical and environmental applications," *Polymer Chemistry,* vol. 6, no. 3, pp. 353-358, 2015, doi: https://doi.org/10.1039/C4PY01415D.

[54] L. Yu and J. Ding, "Injectable hydrogels as unique biomedical materials," *Chemical Society Reviews,* vol. 37, no. 8, pp. 1473-1481, 2008, doi: https://doi.org/10.1039/B713009K.

[55] P. Yang *et al.*, "Tailoring Synthetic Melanin Nanoparticles for Enhanced Photothermal Therapy," *ACS Applied Materials & Interfaces,* vol. 11, no. 45, pp. 42671-42679, 2019, doi: https://doi.org/10.1021/acsami.9b16861.

[56] N. Patil, C. Jerome, and C. Detrembleur, "Recent advances in the synthesis of catechol-derived (bio) polymers for applications in energy storage and environment," *Progress in Polymer Science,* vol. 82, pp. 34-91, 2018, doi: https://doi.org/10.1016/j.progpolymsci.2018.04.002.

[57] L. Yang *et al.*, "Synthetic biopigment supercapacitors," *ACS Applied Materials & Interfaces,* vol. 11, no. 33, pp. 30360-30367, 2019, doi: https://doi.org/10.1021/acsami.9b10956.

[58] W. Zhu *et al.*, "Versatile Surface Functionalization of Metal–Organic Frameworks through Direct Metal Coordination with a Phenolic Lipid Enables Diverse Applications," *Advanced Functional Materials,* vol. 28, no. 16, p. 1705274, 2018, doi: https://doi.org/10.1002/adfm.201705274.

[59] L. Peng *et al.*, "Preserving Porosity of Mesoporous Metal–Organic Frameworks through the Introduction of Polymer Guests," *Journal of the American Chemical Society,* vol. 141, no. 31, pp. 12397-12405, 2019, doi: https://doi.org/10.1021/jacs.9b05967.

[60] D. T. Sun *et al.*, "Rapid, selective heavy metal removal from water by a metal–organic framework/polydopamine composite," *ACS Central Science,* vol. 4, no. 3, pp. 349-356, 2018, doi: https://doi.org/10.1021/acscentsci.7b00605.

[61] S. Ahmed and C. M. Hussain, *Green and Sustainable Advanced Materials: Applications*. Newark: Newark: John Wiley & Sons, Incorporated, 2018.

[62] P. Glavič and R. Lukman, "Review of sustainability terms and their definitions," *Journal of cleaner production,* vol. 15, no. 18, pp. 1875-1885, 2007, doi: https://doi.org/10.1016/j.jclepro.2006.12.006.

[63] R. A. Sheldon, "Metrics of Green Chemistry and Sustainability: Past, Present, and Future," *ACS Sustainable Chemistry & Engineering,* vol. 6, no. 1, pp. 32-48, 2018, doi: https://doi.org/10.1021/acssuschemeng.7b03505.

[64] P. T. Anastas, *Green chemistry : theory and practice*. Oxford, England: Oxford University Press, 1998.

[65] R. A. Sheldon, "Fundamentals of green chemistry: efficiency in reaction design," *Chemical Society Reviews,* vol. 41, no. 4, pp. 1437-1451, 2012, doi: https://doi.org/10.1039/C1CS15219J.

[66] A. Ivanković, A. Dronjić, A. M. Bevanda, and S. Talić, "Review of 12 principles of green chemistry in practice," *International Journal of Sustainable and Green Energy,* vol. 6, no. 3, pp. 39-48, 2017, doi: https://doi.org/10.11648/j.ijrse.20170603.12.

[67] Z. U. Arif, M. Y. Khalid, M. F. Sheikh, A. Zolfagharian, and M. Bodaghi, "Biopolymeric sustainable materials and their emerging applications," *Journal of Environmental Chemical Engineering,* vol. 10, no. 4, p. 108159, 2022, doi: https://doi.org/10.1016/j.jece.2022.108159.

[68] S. S. Muthu, *Environmental Implications of Recycling and Recycled Products*, 1st ed. 2015 ed. Singapore: Singapore: Springer Singapore Pte. Limited, 2015.

[69] S. M. Burkinshaw, *Physico-chemical Aspects of Textile Coloration*. Chicester: Chicester: Wiley, 2015.

[70] S. M. Burkinshaw and G. Salihu, "The role of auxiliaries in the immersion dyeing of textile fibres: Part 1 an overview," *Dyes and pigments,* vol. 161, pp. 519-530, 2019, doi: https://doi.org/10.1016/j.dyepig.2017.08.016.

[71] R. Jain, M. Bhargava, and N. Sharma, "Electrochemical Studies on a Pharmaceutical Azo Dye: Tartrazine," *Industrial & Engineering Chemistry Research,* vol. 42, no. 2, pp. 243-247, 2003, doi: https://doi.org/10.1021/ie020228q.

[72] K. A. Wani and K. Nirmala, *Impact of textile dyes on public health and the environment*. Hershey, Pennsylvania: Hershey, Pennsylvania : IGI Global, 2020.

[73] S. Ul-Islam, *Advanced materials for wastewater treatment*, 1st ed. ed. Newark: Newark: Wiley-Scrivener, 2017.

[74] S. S. Muthu and M. Á. Gardetti, *Sustainability in the Textile and Apparel Industries: Production Process Sustainability*. Cham: Cham: Springer International Publishing AG, 2020.

[75] L. Nambela, L. V. Haule, and Q. Mgani, "A review on source, chemistry, green synthesis and application of textile colorants," *Journal of cleaner production,* vol. 246, p. 119036, 2020, doi: https://doi.org/10.1016/j.jclepro.2019.119036.

[76] J. Adams and D. Pendlebury, *Global Research Report: Materials science and technology*. Leeds, UK: Evidence, a Thomson Reuters business, 2011.

[77] X. Tao, *Handbook of Smart Textiles*, 1st ed. 2015 ed. Singapore: Singapore: Springer Singapore Pte. Limited, 2015.

[78] X. Zhang and X. Tao, "Smart textiles: Passive smart," *Textile Asia,* vol. 32, no. 6, pp. 45-49, 2001.

[79] X. Zhang and X. Tao, "Smart textiles: Active smart," *Textile Asia,* vol. 32, no. 6, pp. 49-52, 2001.

[80] X. Zhang and X. Tao, "Smart textiles: Very smart," *Textile Asia,* vol. 32, no. 8, pp. 35-37, 2001.

[81] V. Koncar, *Smart Textiles and Their Applications*. Cambridge: Cambridge: Elsevier Science & Technology, 2016.

[82] M. Syduzzaman, S. U. Patwary, K. Farhana, and S. Ahmed, "Smart textiles and nano-technology: a general overview," *Journal of Textile Science and Engineering,* vol. 5, p. 1000181, 2015, doi: https://doi.org/10.4172/2165-8064.1000181.

[83] A. Bratek-Skicki, "Towards a new class of stimuli-responsive polymer-based materials – Recent advances and challenges," *Applied Surface Science Advances,* vol. 4, p. 100068, 2021, doi: https://doi.org/10.1016/j.apsadv.2021.100068.

[84] T. Hussain *et al.*, *Textile Engineering: An Introduction*. Berlin/München/Boston: Berlin/München/Boston: Walter de Gruyter GmbH, 2016.

[85] A. Tamayol, M. Akbari, N. Annabi, A. Paul, A. Khademhosseini, and D. Juncker, "Fiber-based tissue engineering: Progress, challenges, and opportunities," *Biotechnology Advances,* vol. 31, no. 5, pp. 669-687, 2013, doi: https://doi.org/10.1016/j.biotechadv.2012.11.007.

[86] J. X. Wu and L. Li, "An Introduction to Wearable Technology and Smart Textiles and Apparel: Terminology, Statistics, Evolution, and Challenges," in *Smart and Functional Soft Materials*: IntechOpen, 2019.

[87] L. Van Langenhove and C. Hertleer, "Smart clothing: a new life," *International journal of clothing science,* vol. 16, no. 1-2, pp. 63-72, 2004, doi: https://doi.org/10.1108/09556220410520360.

[88] S. Zaman, X. Tao, C. Cochrane, and V. Koncar, "Market readiness of smart textile structures—Reliability and washability," in *Proceedings of the IOP Conference Series: Materials Science and Engineering, Nanjing, China*, 2018, pp. 17-19, doi: https://doi.org/10.1088/1757-899X/459/1/012071.

[89] T. Kirstein, *Multidisciplinary know-how for smart-textiles developers*. Elsevier, 2013.

[90] X. Cao, Y. Jie, N. Wang, and Z. L. Wang, "Triboelectric Nanogenerators Driven Self-Powered Electrochemical Processes for Energy and Environmental Science," *Advanced Energy Materials,* vol. 6, no. 23, p. 1600665, 2016, doi: https://doi.org/10.1002/aenm.201600665.

[91] M. Ma *et al.*, "Development, applications, and future directions of triboelectric nanogenerators," *Nano Research,* vol. 11, no. 6, pp. 2951-2969, 2018, doi: https://doi.org/10.1007/s12274-018-1997-9.

[92] C. Xu *et al.*, "On the Electron-Transfer Mechanism in the Contact-Electrification Effect," *Advanced Materials,* vol. 30, no. 15, p. 1706790, 2018, doi: https://doi.org/10.1002/adma.201706790.

[93] J. Chen *et al.*, "Enhancing Performance of Triboelectric Nanogenerator by Filling High Dielectric Nanoparticles into Sponge PDMS Film," *ACS Applied Materials & Interfaces,* vol. 8, no. 1, pp. 736-744, 2016, doi: https://doi.org/10.1021/acsami.5b09907.

[94] H. Zhang, "Structures of Triboelectric Nanogenerators," in *Flexible and Stretchable Triboelectric Nanogenerator Devices*, 2019, pp. 19-40.

[95] Z. L. Wang, "Triboelectric Nanogenerator (TENG)—Sparking an Energy and Sensor Revolution," *Advanced Energy Materials,* vol. 10, no. 17, p. 2000137, 2020, doi: https://doi.org/10.1002/aenm.202000137.

[96] B. Yang, W. Zeng, Z.-H. Peng, S.-R. Liu, K. Chen, and X.-M. Tao, "A Fully Verified Theoretical Analysis of Contact-Mode Triboelectric Nanogenerators as a Wearable Power Source," *Advanced Energy Materials,* vol. 6, no. 16, p. 1600505, 2016, doi: https://doi.org/10.1002/aenm.201600505.

[97] X. Zhang, L. Chen, Y. Jiang, W. Lim, and S. Soh, "Rationalizing the Triboelectric Series of Polymers," *Chemistry of Materials,* vol. 31, no. 5, pp. 1473-1478, 2019, doi: https://doi.org/10.1021/acs.chemmater.8b04526.

[98] R. Zhang and H. Olin, "Material choices for triboelectric nanogenerators: A critical review," *EcoMat,* vol. 2, no. 4, p. e12062, 2020, doi: https://doi.org/10.1002/eom2.12062.

[99] Z. L. Wang, "On the first principle theory of nanogenerators from Maxwell's equations," *Nano Energy,* vol. 68, p. 104272, 2020, doi: https://doi.org/10.1016/j.nanoen.2019.104272.

[100] Z. Liu *et al.*, "Fabrication of triboelectric polymer films via repeated rheological forging for ultrahigh surface charge density," *Nature Communications,* vol. 13, no. 1, p. 4083, 2022, doi: https://doi.org/10.1038/s41467-022-31822-2.

[101] B. Sun *et al.*, "Percolation Model for Renewable-Carbon Doped Functional Composites in Packaging Application: A Brief Review," *Coatings,* vol. 10, no. 2, p. 193, 2020, doi: https://doi.org/10.3390/coatings10020193.

[102] H. Lee *et al.*, "Network-Nanostructured ZIF-8 to Enable Percolation for Enhanced Gas Transport," *Advanced Functional Materials,* vol. 32, no. 47, p. 2207775, 2022, doi: https://doi.org/10.1002/adfm.202207775.

[103] T. T. Moore and W. J. Koros, "Non-ideal effects in organic–inorganic materials for gas separation membranes," *Journal of Molecular Structure,* vol. 739, no. 1, pp. 87-98, 2005, doi: https://doi.org/10.1016/j.molstruc.2004.05.043.

[104] Y. Su *et al.*, "Piezoelectric fiber composites with polydopamine interfacial layer for self-powered wearable biomonitoring," *Nano Energy,* vol. 89, p. 106321, 2021, doi: https://doi.org/10.1016/j.nanoen.2021.106321.

[105] T. Jing, B. Xu, Y. Yang, C. Jiang, and M. Wu, "Interfacial modification boosted permittivity and triboelectric performance of liquid doping composites for high-performance flexible triboelectric nanogenerators," *Nano Energy,* vol. 78, p. 105374, 2020, doi: https://doi.org/10.1016/j.nanoen.2020.105374.

[106] S.-L. Wu, F. Liu, H.-C. Yang, and S. B. Darling, "Recent progress in molecular engineering to tailor organic–inorganic interfaces in composite membranes," *Molecular Systems Design & Engineering,* https://doi.org/10.1039/C9ME00154A vol. 5, no. 2, pp. 433-444, 2020, doi: 10.1039/C9ME00154A.

[107] R. Xu, J. Chen, Q. Huo, W. Pang, and J. Yu, *Chemistry of Zeolites and Related Porous Materials: Synthesis and Structure*, 1. Aufl. ed. Hoboken: Hoboken: Wiley-Interscience, 2009.

[108] R. Haldar, L. Heinke, and C. Wöll, "Advanced Photoresponsive Materials Using the Metal–Organic Framework Approach," *Advanced Materials,* vol. 32, no. 20, pp. 1905227-n/a, 2019, doi: https://doi.org/10.1002/adma.201905227.

[109] G. Khandelwal, A. Chandrasekhar, N. P. Maria Joseph Raj, and S.-J. Kim, "Metal–Organic Framework: A Novel Material for Triboelectric Nanogenerator–Based Self-Powered Sensors and Systems," *Advanced Energy Materials,* vol. 9, no. 14, p. 1803581, 2019, doi: https://doi.org/10.1002/aenm.201803581.

[110] H. Furukawa, K. E. Cordova, M. O'Keeffe, and O. M. Yaghi, "The Chemistry and Applications of Metal-Organic Frameworks," *Science,* vol. 341, no. 6149, p. 1230444, 2013, doi: https://doi.org/10.1126/science.1230444.

[111] S. Wang, L. Lin, and Z. L. Wang, "Triboelectric nanogenerators as self-powered active sensors," *Nano Energy,* vol. 11, pp. 436-462, 2015, doi: https://doi.org/10.1016/j.nanoen.2014.10.034.

[112] T. Zhang *et al.*, "A novel strategy to improve the dyeing properties in laccase-mediated coloration of wool fabric," *Coloration Technology,* vol. 133, no. 1, pp. 65-72, 2017, doi: https://doi.org/10.1111/cote.12252.

[113] S. Slagman, H. Zuilhof, and M. C. R. Franssen, "Laccase-Mediated Grafting on Biopolymers and Synthetic Polymers: A Critical Review," *ChemBioChem,* vol. 19, no. 4, pp. 288-311, 2018, doi: https://doi.org/10.1002/cbic.201700518.

[114] N. S. Hettiarachchy, *Food proteins and peptides chemistry, functionality, interactions, and commercialization*. Boca Raton, Mich.: Boca Raton, Mich. : Taylor & Francis, 2012.

[115] S. Rajput, C. U. Pittman, and D. Mohan, "Magnetic magnetite (Fe3O4) nanoparticle synthesis and applications for lead (Pb2+) and chromium (Cr6+) removal from water," *Journal of Colloid and Interface Science,* vol. 468, pp. 334-346, 2016, doi: https://doi.org/10.1016/j.jcis.2015.12.008.

[116] F. Chen, Y. Xing, Z. Wang, X. Zheng, J. Zhang, and K. Cai, "Nanoscale Polydopamine (PDA) Meets π–π Interactions: An Interface-Directed Coassembly Approach for Mesoporous Nanoparticles," *Langmuir,* vol. 32, no. 46, pp. 12119-12128, 2016, doi: https://doi.org/10.1021/acs.langmuir.6b03294.

[117] A. Ayub, Z. A. Raza, M. I. Majeed, M. R. Tariq, and A. Irfan, "Development of sustainable magnetic chitosan biosorbent beads for kinetic remediation of arsenic contaminated water," *International Journal of Biological Macromolecules,* vol. 163, pp. 603-617, 2020, doi: https://doi.org/10.1016/j.ijbiomac.2020.06.287.

[118] A. Maghsodi and L. Adlnasab, "In-situ chemical deposition as a new method for the preparation of Fe3O4 nanopaeticles embedded on anodic aluminum oxide membrane (Fe3O4@AAO): Characterization and application for arsenic removal using response surface methodology," *Journal of Environmental Chemical Engineering,* vol. 7, no. 5, p. 103288, 2019, doi: https://doi.org/10.1016/j.jece.2019.103288.

[119] J. Ran, L. Xiao, W. Wu, Y. Liu, W. Qiu, and J. Wu, "Zeolitic imidazolate framework-8 (ZIF-8) as a sacrificial template: one-pot synthesis of hollow poly(dopamine) nanocapsules and yolk-structured poly(dopamine) nanocomposites," *Nanotechnology,* vol. 28, no. 5, p. 055604, 2017, doi: https://doi.org/10.1088/1361-6528/28/5/055604.

[120] H. G. Qiangqiang Hu, Hongjing Dou, "Size Control and Biomedical Applications of ZIF-8 Nanoparticles," *Progress in Chemistry,* vol. 32, no. 5, pp. 656-664, 2020, doi: https://doi.org/10.7536/pc190929.

[121] A. Choudhury, *Principles of Colour and Appearance Measurement*, 1 ed. Sawston, Cambridge, UK: Sawston, Cambridge, UK: Woodhead Publishing, 2014.

[122] J. C. Lindon, G. E. Tranter, and D. Koppenaal, *Encyclopedia of spectroscopy and spectrometry*. Academic Press, 2016.

[123] B. K. Ahn, "Perspectives on Mussel-Inspired Wet Adhesion," *Journal of the American Chemical Society,* vol. 139, no. 30, pp. 10166-10171, 2017, doi: https://doi.org/10.1021/jacs.6b13149.

[124] S. Baik, H. J. Lee, D. W. Kim, J. W. Kim, Y. Lee, and C. Pang, "Bioinspired Adhesive Architectures: From Skin Patch to Integrated Bioelectronics," *Advanced Materials,* vol. 31, no. 34, pp. e1803309-n/a, 2019, doi: https://doi.org/10.1002/adma.201803309.

[125] P. Kord Forooshani and B. P. Lee, "Recent approaches in designing bioadhesive materials inspired by mussel adhesive protein," *Journal of Polymer Science Part A: Polymer Chemistry,* vol. 55, no. 1, pp. 9-33, 2017, doi: https://doi.org/10.1002/pola.28368.

[126] J. Saiz-Poseu, J. Mancebo-Aracil, F. Nador, F. Busqué, and D. Ruiz-Molina, "The Chemistry behind Catechol-Based Adhesion," *Angewandte Chemie International Edition,* vol. 58, no. 3, pp. 696-714, 2019, doi: https://doi.org/10.1002/anie.201801063.

[127] L. He, V. L. L. So, and J. H. Xin, "Dopamine polymerization-induced surface colouration of various materials," *RSC Advances,* vol. 4, no. 39, pp. 20317-20322, 2014, doi: https://doi.org/10.1039/C4RA00098F.

[128] L. L. So, L. He, B. Fei, K. Cheuk, and J. H. Xin, "Bio-inspired coloration for wool fabrics at room temperature," in *Key Engineering Materials*, 2016, vol. 671: Trans Tech Publ, pp. 25-31, doi: https://doi.org/10.4028/www.scientific.net/KEM.671.25.

[129] V. L. L. So, L. He, B. Fei, K. K. L. Cheuk, and J. H. Xin, "Correction: Bio-inspired colouration on various textile materials using a novel catechol colorant," *RSC Advances,*

10.1039/C5RA90005K vol. 5, no. 19, pp. 14285-14285, 2015, doi: https://doi.org/10.1039/C5RA90005K.

[130] W.-Z. Qiu, H.-C. Yang, and Z.-K. Xu, "Dopamine-assisted co-deposition: An emerging and promising strategy for surface modification," *Advances in Colloid and Interface Science,* vol. 256, pp. 111-125, 2018, doi: https://doi.org/10.1016/j.cis.2018.04.011.

[131] J. H. Ryu, P. B. Messersmith, and H. Lee, "Polydopamine Surface Chemistry: A Decade of Discovery," *ACS Applied Materials & Interfaces,* vol. 10, no. 9, pp. 7523-7540, 2018, doi: https://doi.org/10.1021/acsami.7b19865.

[132] J. Su *et al.*, "Antimicrobial coating of textiles by laccase in situ polymerization of catechol and p-phenylenediamine," *Reactive and Functional Polymers,* vol. 136, pp. 25-33, 2019, doi: https://doi.org/10.1016/j.reactfunctpolym.2018.11.015.

[133] M. Zahid, G. Mazzon, A. Athanassiou, and I. S. Bayer, "Environmentally benign non-wettable textile treatments: A review of recent state-of-the-art," *Advances in Colloid and Interface Science,* vol. 270, pp. 216-250, 2019, doi: https://doi.org/10.1016/j.cis.2019.06.001.

[134] R. K. Gupta, G. J. Dunderdale, M. W. England, and A. Hozumi, "Oil/water separation techniques: a review of recent progresses and future directions," *Journal of Materials Chemistry A,* vol. 5, no. 31, pp. 1625-1658, 2017, doi: https://doi.org/10.1039/c7ta02070h.

[135] G. Yang, L. Xiao, and L. Lamboni, *Bioinspired Materials Science and Engineering*, 1 ed. Newark: Newark: John Wiley & Sons, Incorporated, 2018.

[136] N. Budisa and T. Schneider, "Expanding the DOPA Universe with Genetically Encoded, Mussel-Inspired Bioadhesives for Material Sciences and Medicine," *ChemBioChem,* vol. 20, no. 17, pp. 2163-2190, 2019, doi: https://doi.org/10.1002/cbic.201900030.

[137] J. H. Ryu, S. Hong, and H. Lee, "Bio-inspired adhesive catechol-conjugated chitosan for biomedical applications: A mini review," *Acta Biomaterialia,* vol. 27, pp. 101-115, 2015, doi: https://doi.org/10.1016/j.actbio.2015.08.043.

[138] W. Zhu, Y. J. Chuah, and D.-A. Wang, "Bioadhesives for internal medical applications: A review," *Acta Biomaterialia,* vol. 74, pp. 1-16, 2018, doi: https://doi.org/10.1016/j.actbio.2018.04.034.

[139] K. M. Im and J.-R. Jeon, "Synthesis of plant phenol-derived polymeric dyes for direct or mordant-based hair dyeing," *Journal of Visualized Experiments,* vol. 2016, no. 118, 2016, doi: https://doi.org/10.3791/54772.

[140] K. M. Im, T.-W. Kim, and J.-R. Jeon, "Metal-Chelation-Assisted Deposition of Polydopamine on Human Hair: A Ready-to-Use Eumelanin-Based Hair Dyeing Methodology," *ACS Biomaterials Science & Engineering,* vol. 3, no. 4, pp. 628-636, 2017, doi: https://doi.org/10.1021/acsbiomaterials.7b00031.

[141] W. S. Pierpoint, "o-Quinones formed in plant extracts. Their reactions with amino acids and peptides," *Biochemical journal,* vol. 112, no. 5, pp. 609-616, 1969, doi: https://doi.org/10.1042/bj1120609.

[142] B. Singh, K. Suri, K. Shevkani, A. Kaur, A. Kaur, and N. Singh, "Enzymatic Browning of Fruit and Vegetables: A Review," *Enzymes in Food Technology,* pp. 63-78, 2018, doi: https://doi.org/10.1007/978-981-13-1933-4_4.

[143] J. R. Jeon *et al.*, "Laccase-catalysed polymeric dye synthesis from plant-derived phenols for potential application in hair dyeing: Enzymatic colourations driven by homo- or hetero-polymer synthesis," *Microbial Biotechnology,* vol. 3, no. 3, pp. 324-335, 2010, doi: https://doi.org/10.1111/j.1751-7915.2009.00153.x.

[144] J. Su, J. Fu, Q. Wang, C. Silva, and A. Cavaco-Paulo, "Laccase: a green catalyst for the biosynthesis of poly-phenols," *Critical Reviews in Biotechnology,* vol. 38, no. 2, pp. 294-307, 2018, doi: https://doi.org/10.1080/07388551.2017.1354353.

[145] G. Yabuta, Y. Koizumi, K. Namiki, M. Hida, and M. Namiki, "Structure of Green Pigment Formed by the Reaction of Caffeic Acid Esters (or Chlorogenic acid) with a Primary Amino Compound," *Bioscience, Biotechnology, and Biochemistry,* vol. 65, no. 10, pp. 2121-2130, 2001, doi: https://doi.org/10.1271/bbb.65.2121.

[146] T. Coultate and R. S. Blackburn, "Food colorants: their past, present and future," *Coloration Technology,* vol. 134, no. 3, pp. 165-186, 2018, doi: https://doi.org/10.1111/cote.12334.

[147] N. Martins, C. L. Roriz, P. Morales, L. Barros, and I. C. F. R. Ferreira, "Food colorants: Challenges, opportunities and current desires of agro-industries to ensure consumer expectations and regulatory practices," *Trends in Food Science & Technology,* vol. 52, pp. 1-15, 2016, doi: https://doi.org/10.1016/j.tifs.2016.03.009.

[148] A. Schieber, "Reactions of Quinones—Mechanisms, Structures, and Prospects for Food Research," *Journal of Agricultural and Food Chemistry,* vol. 66, no. 50, pp. 13051-13055, 2018, doi: https://doi.org/10.1021/acs.jafc.8b05215.

[149] F. Shahidi and P. Ambigaipalan, "Phenolics and polyphenolics in foods, beverages and spices: Antioxidant activity and health effects – A review," *Journal of Functional Foods,* vol. 18, pp. 820-897, 2015, doi: https://doi.org/10.1016/j.jff.2015.06.018.

[150] A. P. Periyasamy and J. Militky, *Sustainability in Textile Dyeing: Recent Developments* (Sustainability in the Textile and Apparel Industries: Production Process Sustainability). Cham: Cham: Springer International Publishing, 2020, pp. 37-79.

[151] L. He, V. L. L. So, S. Fan, and J. H. Xin, "Polyphenol-Assisted Natural Coloration on Various Synthetic Textile Materials," *Fibers and Polymers,* vol. 19, no. 7, pp. 1411-1419, 2018, doi: https://doi.org/10.1007/s12221-018-8581-x.

[152] Y. Lam, Y. Ho, L. He, X. Wang, and J. H. Xin, "Laccase-Catalyzed Biomimetic Coloration of Wool Fabrics with Phenols," *AATCC Journal of Research,* vol. 6, no. 3, pp. 41-44, 2019, doi: https://doi.org/10.14504/ajr.6.S1.9.

[153] W. Boerjan, J. Ralph, and M. Baucher, "Lignin Biosynthesis," *Annual Review of Plant Biology,* vol. 54, pp. 519-546, 2003, doi: https://doi.org/10.1146/annurev.arplant.54.031902.134938.

[154] H. El Gharras, "Polyphenols: food sources, properties and applications – a review," *International Journal of Food Science & Technology,* vol. 44, no. 12, pp. 2512-2518, 2009, doi: https://doi.org/10.1111/j.1365-2621.2009.02077.x.

[155] S. Bittner, "When quinones meet amino acids: chemical, physical and biological consequences," *Amino Acids,* vol. 30, no. 3, pp. 205-224, 2006, doi: https://doi.org/10.1007/s00726-005-0298-2.

[156] J. Velíšek, J. Davídek, and K. Cejpek, "Biosynthesis of food constituents: natural pigments. Part 1—a review," *Czech Journal of Food Sciences,* vol. 25, no. 6, pp. 291-315, 2007, doi: https://doi.org/10.17221/748-CJFS.

[157] W. M. Haynes, *CRC handbook of chemistry and physics*. CRC press, 2014.

[158] M. Fleck and A. M. Petrosyan, *Salts of Amino Acids: Crystallization, Structure and Properties*, 2014 ed. Cham: Cham: Springer International Publishing AG, 2014.

[159] N. F. Della Vecchia, R. Avolio, M. Alfè, M. E. Errico, A. Napolitano, and M. d'Ischia, "Building-Block Diversity in Polydopamine Underpins a Multifunctional Eumelanin-Type Platform Tunable Through a Quinone Control Point," *Advanced Functional*

Materials, vol. 23, no. 6, pp. 1331-1340, 2013, doi: https://doi.org/10.1002/adfm.201202127.

[160] N. F. Della Vecchia *et al.*, "Tris Buffer Modulates Polydopamine Growth, Aggregation, and Paramagnetic Properties," *Langmuir,* vol. 30, no. 32, pp. 9811-9818, 2014, doi: https://doi.org/10.1021/la501560z.

[161] S. Rohn, "Possibilities and limitations in the analysis of covalent interactions between phenolic compounds and proteins," *Food Research International,* vol. 65, pp. 13-19, 2014, doi: https://doi.org/10.1016/j.foodres.2014.05.042.

[162] C. Kallinich, S. Schefer, and S. Rohn, "Analysis of protein-phenolic compound modifications using electrochemistry coupled to mass spectrometry," *Molecules,* vol. 23, no. 2, p. 264, 2018, doi: https://doi.org/10.3390/molecules23020264.

[163] R. Pinnataip and B. P. Lee, "Oxidation Chemistry of Catechol Utilized in Designing Stimuli-Responsive Adhesives and Antipathogenic Biomaterials," *ACS Omega,* vol. 6, no. 8, pp. 5113-5118, 2021, doi: https://doi.org/10.1021/acsomega.1c00006.

[164] S. Razaviamri, K. Wang, B. Liu, and B. P. Lee, "Catechol-based antimicrobial polymers," *Molecules,* vol. 26, no. 3, p. 559, 2021, doi: https://doi.org/10.3390/molecules26030559.

[165] H. M. Rawel and S. Rohn, "Nature of hydroxycinnamate-protein interactions," *Phytochemistry Reviews,* vol. 9, no. 1, pp. 93-109, 2010, doi: https://doi.org/10.1007/s11101-009-9154-4.

[166] G. P. Maier, C. M. Bernt, and A. Butler, "Catechol oxidation: Considerations in the design of wet adhesive materials," *Biomaterials Science,* vol. 6, no. 2, pp. 332-339, 2018, doi: https://doi.org/10.1039/c7bm00884h.

[167] Z. Wang, S. Zhao, R. Song, W. Zhang, S. Zhang, and J. Li, "The synergy between natural polyphenol-inspired catechol moieties and plant protein-derived bio-adhesive

enhances the wet bonding strength," *Scientific Reports,* vol. 7, no. 1, pp. 9664-10, 2017, doi: https://doi.org/10.1038/s41598-017-10007-8.

[168] A. H. Hofman, I. A. van Hees, J. Yang, and M. Kamperman, "Bioinspired underwater adhesives by using the supramolecular toolbox," *Advanced Materials,* vol. 30, no. 19, p. 1704640, 2018.

[169] J. Yang, V. Saggiomo, A. H. Velders, M. Cohen Stuart, and M. Kamperman, "Reaction pathways in catechol/primary amine mixtures : A window on crosslinking chemistry," *PLoS One,* vol. 11, no. 12, pp. e0166490-e0166490, 2016, doi: https://doi.org/10.1371/journal.pone.0166490.

[170] A. V. T. Le, Y.-L. Su, and S.-H. Cheng, "A novel electrochemical assay for aspartame determination via nucleophilic reactions with caffeic acid ortho-quinone," *Electrochimica Acta,* vol. 300, pp. 67-76, 2019, doi: https://doi.org/10.1016/j.electacta.2019.01.020.

[171] P. Xu, H. Uyama, J. E. Whitten, S. Kobayashi, and D. L. Kaplan, "Peroxidase-Catalyzed in Situ Polymerization of Surface Orientated Caffeic Acid," *Journal of the American Chemical Society,* vol. 127, no. 33, pp. 11745-11753, 2005, doi: https://doi.org/10.1021/ja051637r.

[172] H. Liu and W. Yu, "Study of the structure transformation of wool fibers with Raman spectroscopy," *Journal of Applied Polymer Science,* vol. 103, no. 1, pp. 1-7, 2007, doi: https://doi.org/10.1002/app.23862.

[173] E. Filippidi *et al.*, "Toughening elastomers using mussel-inspired iron-catechol complexes," *Science,* vol. 358, no. 6362, pp. 502-505, 2017, doi: https://doi.org/10.1126/science.aao0350.

[174] R. Botta, A. Rajanikanth, and C. Bansal, "Surface Enhanced Raman Scattering studies of l-amino acids adsorbed on silver nanoclusters," *Chemical physics letters,* vol. 618, pp. 14-19, 2015, doi: https://doi.org/10.1016/j.cplett.2014.10.052.

[175] G. Balakrishnan, G. V. Barnett, S. R. Kar, and T. K. Das, "Detection and Identification of the Vibrational Markers for the Quantification of Methionine Oxidation in Therapeutic Proteins," *Analytical Chemistry,* vol. 90, no. 11, pp. 6959-6966, 2018, doi: https://doi.org/10.1021/acs.analchem.8b01238.

[176] P. Bazylewski, R. Divigalpitiya, and G. Fanchini, "In situ Raman spectroscopy distinguishes between reversible and irreversible thiol modifications in l-cysteine," *RSC Advances,* vol. 7, no. 5, pp. 2964-297, 2017, doi: https://doi.org/10.1039/c6ra25879d.

[177] R. Mauchauffé, M. Moreno-Couranjou, N. D. Boscher, A.-S. Duwez, and P. Choquet, "Liquid-Assisted Plasma-Enhanced Chemical Vapor Deposition of Catechol and Quinone-Functionalized Coatings: Insights into the Surface Chemistry and Morphology: Liquid-Assisted Plasma-Enhanced Chemical Vapor Deposition of Catechol," *Plasma Processes and Polymers,* vol. 13, no. 8, pp. 843-856, 2016, doi: https://doi.org/10.1002/ppap.201600002.

[178] G. Socrates, *Infrared and Raman characteristic group frequencies : tables and charts*, 3rd ed.. ed. Chichester, England: Chichester, England : Wiley, 2001.

[179] F. Gürer *et al.*, "Water-based carbodiimide mediated synthesis of polysaccharide-amino acid conjugates: Deprotection, charge and structural analysis," *Carbohydrate Polymers,* vol. 267, pp. 118226-118226, 2021, doi: https://doi.org/10.1016/j.carbpol.2021.118226.

[180] M. Kaisersberger-Vincek, S. Gorgieva, and V. Kokol, *Specific functionalization of wool with ε-poly-L-lysine (ε-PL) for antimicrobial properties* (Worldwide Research Efforts in the Fighting Against Microbial Pathogens). 2013, p. 239.

[181] A. Barth, "Infrared spectroscopy of proteins," *Biochimica et Biophysica Acta (BBA) - Bioenergetics,* vol. 1767, no. 9, pp. 1073-1101, 2007, doi: https://doi.org/10.1016/j.bbabio.2007.06.004.

[182] A. B. D. Nandiyanto, R. Oktiani, and R. Ragadhita, "How to read and interpret ftir spectroscope of organic material," *Indonesian Journal of Science and Technology,* vol. 4, no. 1, pp. 97-118, 2019, doi: https://doi.org/10.17509/ijost.v4i1.15806.

[183] R. L. Allen, *Colour chemistry*. Springer Science & Business Media, 2013.

[184] D. Kernell, *Colours and Colour Vision: An Introductory Survey*. Cambridge University Press, 2016.

[185] A. R. Choudhury, *Textile preparation and dyeing*. Science publishers, 2006.

[186] A. E. Ghaly, R. Ananthashankar, M. Alhattab, and V. V. Ramakrishnan, "Production, Characterization and Treatment of Textile Effluents: A Critical Review," *Journal of Chemical Engineering & Process Technology,* vol. 5, pp. 1-18, 2013, doi: https://doi.org/10.4172/2157-7048.1000182.

[187] R. V. Kandisa, K. N. Saibaba, K. B. Shaik, and R. Gopinath, "Dye removal by adsorption: a review," *Journal of Bioremediation and Biodegradation,* vol. 7, no. 6, 2016, doi: https://doi.org/10.4172/2155-6199.1000371.

[188] C. R. Holkar, A. J. Jadhav, D. V. Pinjari, N. M. Mahamuni, and A. B. Pandit, "A critical review on textile wastewater treatments: Possible approaches," *Journal of Environmental Management,* vol. 182, pp. 351-366, 2016, doi: https://doi.org/10.1016/j.jenvman.2016.07.090.

[189] H. Y. Zhu, R. Jiang, Y. Q. Fu, R. R. Li, J. Yao, and S. T. Jiang, "Novel multifunctional NiFe2O4/ZnO hybrids for dye removal by adsorption, photocatalysis and magnetic separation," *Applied Surface Science,* vol. 369, pp. 1-10, 2016, doi: https://doi.org/10.1016/j.apsusc.2016.02.025.

[190] J. Gómez-Pastora, S. Dominguez, E. Bringas, M. J. Rivero, I. Ortiz, and D. D. Dionysiou, "Review and perspectives on the use of magnetic nanophotocatalysts (MNPCs) in water treatment," *Chemical Engineering Journal,* vol. 310, pp. 407-427, 2017, doi: https://doi.org/10.1016/j.cej.2016.04.140.

[191] A. Sun, H. Chen, C. Song, F. Jiang, X. Wang, and Y. Fu, "Magnetic Bi25FeO40-graphene catalyst and its high visible-light photocatalytic performance," *RSC Advances,* 10.1039/C3RA22626C vol. 3, no. 13, pp. 4332-4340, 2013, doi: https://doi.org/10.1039/C3RA22626C.

[192] C. Li *et al.*, "Mussel-inspired synthesis of polydopamine-functionalized calcium carbonate as reusable adsorbents for heavy metal ions," *RSC Advances,* 10.1039/C4RA08193E vol. 4, no. 88, pp. 47848-47852, 2014, doi: https://doi.org/10.1039/C4RA08193E.

[193] M. F. R. Pereira, S. F. Soares, J. J. M. Órfão, and J. L. Figueiredo, "Adsorption of dyes on activated carbons: influence of surface chemical groups," *Carbon,* vol. 41, no. 4, pp. 811-821, 2003, doi: https://doi.org/10.1016/S0008-6223(02)00406-2.

[194] Y. Liu, Y. Zhao, W. Cheng, and T. Zhang, "Targeted reclaiming cationic dyes from dyeing wastewater with a dithiocarbamate-functionalized material through selective adsorption and efficient desorption," *Journal of Colloid and Interface Science,* vol. 579, pp. 766-777, 2020, doi: https://doi.org/10.1016/j.jcis.2020.06.083.

[195] S. Ranote, D. Kumar, S. Kumari, R. Kumar, G. S. Chauhan, and V. Joshi, "Green synthesis of Moringa oleifera gum-based bifunctional polyurethane foam braced with ash for rapid and efficient dye removal," *Chemical Engineering Journal,* vol. 361, pp. 1586-1596, 2019, doi: https://doi.org/10.1016/j.cej.2018.10.194.

[196] J. Ye, L. Jin, X. Zhao, X. Qian, and M. Dong, "Superior adsorption performance of metal-organic-frameworks derived magnetic cobalt-embedded carbon microrods for

triphenylmethane dyes," *Journal of Colloid and Interface Science,* vol. 536, pp. 483-492, 2019, doi: https://doi.org/10.1016/j.jcis.2018.10.073.

[197] G. Wu *et al.*, "Magnetic copper-based metal organic framework as an effective and recyclable adsorbent for removal of two fluoroquinolone antibiotics from aqueous solutions," *Journal of Colloid and Interface Science,* vol. 528, pp. 360-371, 2018.

[198] X. Huang, C. Xu, J. Ma, and F. Chen, "Ionothermal synthesis of Cu-doped Fe3O4 magnetic nanoparticles with enhanced peroxidase-like activity for organic wastewater treatment," *Advanced Powder Technology,* vol. 29, no. 3, pp. 796-803, 2018, doi: https://doi.org/10.1016/j.apt.2017.12.025.

[199] Y. Liu, K. Ai, and L. Lu, "Polydopamine and Its Derivative Materials: Synthesis and Promising Applications in Energy, Environmental, and Biomedical Fields," *Chemical Reviews,* vol. 114, no. 9, pp. 5057-5115, 2014, doi: https://doi.org/10.1021/cr400407a.

[200] A. Islam *et al.*, "Step towards the sustainable toxic dyes removal and recycling from aqueous solution- A comprehensive review," *Resources, Conservation and Recycling,* vol. 175, p. 105849, 2021, doi: https://doi.org/10.1016/j.resconrec.2021.105849.

[201] X. Qi, X. Tong, W. Pan, Q. Zeng, S. You, and J. Shen, "Recent advances in polysaccharide-based adsorbents for wastewater treatment," *Journal of Cleaner Production,* vol. 315, p. 128221, 2021, doi: https://doi.org/10.1016/j.jclepro.2021.128221.

[202] G. R. Mahdavinia, F. Bazmizeynabad, and B. Seyyedi, "kappa-Carrageenan beads as new adsorbent to remove crystal violet dye from water: adsorption kinetics and isotherm," *Desalination and Water Treatment,* vol. 53, no. 9, pp. 2529-2539, 2015, doi: https://doi.org/10.1080/19443994.2013.870741.

[203] D. Wen *et al.*, "Simple and Sensitive Colorimetric Detection of Dopamine Based on Assembly of Cyclodextrin-Modified Au Nanoparticles," *Small,* vol. 12, no. 18, pp. 2439-2442, 2016, doi: https://doi.org/10.1002/smll.201503874.

[204] Y. Huang *et al.*, "Synthesis of yolk/shell Fe3O4–polydopamine–graphene–Pt nanocomposite with high electrocatalytic activity for fuel cells," *Journal of Power Sources,* vol. 246, pp. 868-875, 2014.

[205] H. Gao, Y. Sun, J. Zhou, R. Xu, and H. Duan, "Mussel-Inspired Synthesis of Polydopamine-Functionalized Graphene Hydrogel as Reusable Adsorbents for Water Purification," *ACS Applied Materials & Interfaces,* vol. 5, no. 2, pp. 425-432, 2013, doi: https://doi.org/10.1021/am302500v.

[206] Y. Xie *et al.*, "Highly Regenerable Mussel-Inspired Fe3O4@Polydopamine-Ag Core–Shell Microspheres as Catalyst and Adsorbent for Methylene Blue Removal," *ACS Applied Materials & Interfaces,* vol. 6, no. 11, pp. 8845-8852, 2014, doi: https://doi.org/10.1021/am501632f.

[207] S. Kim, G.-h. Moon, G. Kim, U. Kang, H. Park, and W. Choi, "TiO2 complexed with dopamine-derived polymers and the visible light photocatalytic activities for water pollutants," *Journal of Catalysis,* vol. 346, pp. 92-100, 2017, doi: https://doi.org/10.1016/j.jcat.2016.11.027.

[208] N. Farnad, K. Farhadi, and N. H. Voelcker, "Polydopamine Nanoparticles as a New and Highly Selective Biosorbent for the Removal of Copper (II) Ions from Aqueous Solutions," *Water, Air, & Soil Pollution,* vol. 223, no. 6, pp. 3535-3544, 2012, doi: https://doi.org/10.1007/s11270-012-1131-7.

[209] Z. Dong, F. Zhang, D. Wang, X. Liu, and J. Jin, "Polydopamine-mediated surface-functionalization of graphene oxide for heavy metal ions removal," *Journal of Solid*

State Chemistry, vol. 224, pp. 88-93, 2015, doi: https://doi.org/10.1016/j.jssc.2014.06.030.

[210] A. Cai, X. Wang, A. Guo, and Y. Chang, "Mussel-inspired green synthesis of polydopamine-Ag-AgCl composites with efficient visible-light-driven photocatalytic activity," *Journal of Photochemistry and Photobiology B: Biology,* vol. 162, pp. 486-492, 2016, doi: https://doi.org/10.1016/j.jphotobiol.2016.07.020.

[211] Q. Ye, L. Liu, Z. Chen, and L. Hong, "Analysis of chlorophenols in environmental water using polydopamine-coated magnetic graphene as an extraction material coupled with high-performance liquid chromatography," *Journal of Separation Science,* vol. 39, no. 9, pp. 1684-1690, 2016, doi: https://doi.org/10.1002/jssc.201501283.

[212] X. Zhang *et al.*, "Efficient removal and highly selective adsorption of Hg2+ by polydopamine nanospheres with total recycle capacity," *Applied Surface Science,* vol. 314, pp. 166-173, 2014.

[213] K. Cui *et al.*, "Regenerable urchin-like Fe3O4@PDA-Ag hollow microspheres as catalyst and adsorbent for enhanced removal of organic dyes," *Journal of Hazardous Materials,* vol. 350, pp. 66-75, 2018, doi: https://doi.org/10.1016/j.jhazmat.2018.02.011.

[214] M. Feng, S. Yu, P. Wu, Z. Wang, S. Liu, and J. Fu, "Rapid, high-efficient and selective removal of cationic dyes from wastewater using hollow polydopamine microcapsules: Isotherm, kinetics, thermodynamics and mechanism," *Applied Surface Science,* vol. 542, p. 148633, 2021, doi: https://doi.org/10.1016/j.apsusc.2020.148633.

[215] J. Fu *et al.*, "Selective adsorption and separation of organic dyes from aqueous solution on polydopamine microspheres," *Journal of Colloid and Interface Science,* vol. 461, pp. 292-304, 2016.

[216] Q. Liu, B. Yu, W. Ye, and F. Zhou, "Highly Selective Uptake and Release of Charged Molecules by pH-Responsive Polydopamine Microcapsules," *Macromolecular Bioscience,* vol. 11, no. 9, pp. 1227-1234, 2011, doi: https://doi.org/10.1002/mabi.201100061.

[217] Z. Zhu *et al.*, "Ultrahigh adsorption capacity of anionic dyes with sharp selectivity through the cationic charged hybrid nanofibrous membranes," *Chemical Engineering Journal,* vol. 313, pp. 957-966, 2017.

[218] B. Mao, Q. An, B. Zhai, Z. Xiao, and S. Zhai, "Multifunctional hollow polydopamine-based composites (Fe3O4/PDA@Ag) for efficient degradation of organic dyes," *RSC Advances,* 10.1039/C6RA05954F vol. 6, no. 53, pp. 47761-47770, 2016, doi: https://doi.org/10.1039/C6RA05954F.

[219] H. Zhang, L. Y. Guo, J. Jiao, X. Xin, D. Sun, and S. Yuan, "Ionic Self-Assembly of Polyoxometalate–Dopamine Hybrid Nanoflowers with Excellent Catalytic Activity for Dyes," *ACS Sustainable Chemistry & Engineering,* vol. 5, no. 2, pp. 1358-1367, 2017, doi: https://doi.org/10.1021/acssuschemeng.6b01805.

[220] X. Qu, P. J. J. Alvarez, and Q. Li, "Applications of nanotechnology in water and wastewater treatment," *Water Research,* vol. 47, no. 12, pp. 3931-3946, 2013, doi: https://doi.org/10.1016/j.watres.2012.09.058.

[221] H. Hosseinzadeh, S. Zoroufi, and G. R. Mahdavinia, "Study on adsorption of cationic dye on novel kappa-carrageenan/poly(vinyl alcohol)/montmorillonite nanocomposite hydrogels," *Polymer Bulletin,* vol. 72, no. 6, pp. 1339-1363, 2015, doi: https://doi.org/10.1007/s00289-015-1340-5.

[222] G. Zeng *et al.*, "Application of dopamine-modified halloysite nanotubes/PVDF blend membranes for direct dyes removal from wastewater," *Chemical Engineering Journal,* vol. 323, pp. 572-583, 2017.

[223] Y. Long, L. Xiao, and Q. Cao, "Co-polymerization of catechol and polyethylenimine on magnetic nanoparticles for efficient selective removal of anionic dyes from water," *Powder Technology,* vol. 310, pp. 24-34, 2017, doi: https://doi.org/10.1016/j.powtec.2017.01.013.

[224] J. Yan, Y. Huang, Y. E. Miao, W. W. Tjiu, and T. Liu, "Polydopamine-coated electrospun poly(vinyl alcohol)/poly(acrylic acid) membranes as efficient dye adsorbent with good recyclability," *Journal of Hazardous Materials,* vol. 283, pp. 730-739, 2015, doi: https://doi.org/10.1016/j.jhazmat.2014.10.040.

[225] J. Manna, S. Akbayrak, and S. Özkar, "Palladium(0) nanoparticles supported on polydopamine coated CoFe2O4 as highly active, magnetically isolable and reusable catalyst for hydrogen generation from the hydrolysis of ammonia borane," *Applied Catalysis B: Environmental,* vol. 208, pp. 104-115, 2017, doi: https://doi.org/10.1016/j.apcatb.2017.02.037.

[226] X. Li, H. Lu, Y. Zhang, F. He, L. Jing, and X. He, "Fabrication of magnetic alginate beads with uniform dispersion of CoFe2O4 by the polydopamine surface functionalization for organic pollutants removal," *Applied Surface Science,* vol. 389, pp. 567-577, 2016, doi: https://doi.org/10.1016/j.apsusc.2016.07.162.

[227] R. M. Mohamed, A. Shawky, and I. A. Mkhalid, "Facile synthesis of MgO and Ni-MgO nanostructures with enhanced adsorption of methyl blue dye," *Journal of Physics and Chemistry of Solids,* vol. 101, pp. 50-57, 2017, doi: https://doi.org/10.1016/j.jpcs.2016.10.009.

[228] Y. Wang *et al.*, "Preparation of polydopamine coated Fe3O4 nanoparticles and their application for enrichment of polycyclic aromatic hydrocarbons from environmental water samples," *Journal of Chromatography A,* vol. 1283, pp. 20-26, 2013.

[229] R. Rakhshaee, "Rule of Fe0 nano-particles and biopolymer structures in kinds of the connected pairs to remove Acid Yellow 17 from aqueous solution: Simultaneous removal of dye in two paths and by four mechanisms," *Journal of Hazardous Materials,* vol. 197, pp. 144-152, 2011, doi: https://doi.org/10.1016/j.jhazmat.2011.09.067.

[230] X. Han, L. Zhang, and C. Li, "Preparation of polydopamine-functionalized graphene–Fe3O4 magnetic composites with high adsorption capacities," *RSC Advances,* 10.1039/C4RA04182H vol. 4, no. 58, pp. 30536-30541, 2014, doi: https://doi.org/10.1039/C4RA04182H.

[231] M. Munoz, Z. M. de Pedro, J. A. Casas, and J. J. Rodriguez, "Preparation of magnetite-based catalysts and their application in heterogeneous Fenton oxidation – A review," *Applied Catalysis B: Environmental,* vol. 176-177, pp. 249-265, 2015, doi: https://doi.org/10.1016/j.apcatb.2015.04.003.

[232] F. Chen, S. Xie, X. Huang, and X. Qiu, "Ionothermal synthesis of Fe3O4 magnetic nanoparticles as efficient heterogeneous Fenton-like catalysts for degradation of organic pollutants with H2O2," *Journal of Hazardous Materials,* vol. 322, pp. 152-162, 2017, doi: https://doi.org/10.1016/j.jhazmat.2016.02.073.

[233] H. J. Kim *et al.*, "Recyclable aqueous metal adsorbent: Synthesis and Cu(II) sorption characteristics of ternary nanocomposites of Fe3O4 nanoparticles@graphene–poly-N-phenylglycine nanofibers," *Journal of Hazardous Materials,* vol. 401, p. 123283, 2021, doi: https://doi.org/10.1016/j.jhazmat.2020.123283.

[234] M. H. Karimi, G. R. Mahdavinia, B. Massoumi, A. Baghban, and M. Saraei, "Ionically crosslinked magnetic chitosan/κ-carrageenan bioadsorbents for removal of anionic eriochrome black-T," *International Journal of Biological Macromolecules,* vol. 113, pp. 361-375, 2018, doi: https://doi.org/10.1016/j.ijbiomac.2018.02.102.

[235] R. A. Revia and M. Zhang, "Magnetite nanoparticles for cancer diagnosis, treatment, and treatment monitoring: recent advances," *Materials Today,* vol. 19, no. 3, pp. 157-168, 2016, doi: https://doi.org/10.1016/j.mattod.2015.08.022.

[236] S. Liu, B. Yu, S. Wang, Y. Shen, and H. Cong, "Preparation, surface functionalization and application of Fe3O4 magnetic nanoparticles," *Advances in Colloid and Interface Science,* vol. 281, p. 102165, 2020, doi: https://doi.org/10.1016/j.cis.2020.102165.

[237] Y. Yao, S. Miao, S. Liu, L. P. Ma, H. Sun, and S. Wang, "Synthesis, characterization, and adsorption properties of magnetic Fe3O4@graphene nanocomposite," *Chemical Engineering Journal,* vol. 184, pp. 326-332, 2012, doi: https://doi.org/10.1016/j.cej.2011.12.017.

[238] S. Zhang *et al.*, "Mussel-inspired polydopamine biopolymer decorated with magnetic nanoparticles for multiple pollutants removal," *Journal of Hazardous Materials,* vol. 270, pp. 27-34, 2014, doi: https://doi.org/10.1016/j.jhazmat.2014.01.039.

[239] Z. Zhou and R. Liu, "Fe3O4@polydopamine and derived Fe3O4@carbon core–shell nanoparticles: Comparison in adsorption for cationic and anionic dyes," *Colloids and Surfaces A: Physicochemical and Engineering Aspects,* vol. 522, pp. 260-265, 2017, doi: https://doi.org/10.1016/j.colsurfa.2017.02.063.

[240] B. Chen *et al.*, "A novel Fe3+-stabilized magnetic polydopamine composite for enhanced selective adsorption and separation of Methylene blue from complex wastewater," *Journal of Hazardous Materials,* vol. 392, p. 122263, 2020.

[241] C. Salazar-Camacho, M. Villalobos, M. d. l. L. Rivas-Sánchez, J. Arenas-Alatorre, J. Alcaraz-Cienfuegos, and M. E. Gutiérrez-Ruiz, "Characterization and surface reactivity of natural and synthetic magnetites," *Chemical Geology,* vol. 347, pp. 233-245, 2013, doi: https://doi.org/10.1016/j.chemgeo.2013.03.017.

[242] S. W. Bian, S. Liu, and L. Chang, "Synthesis of magnetically recyclable Fe3O4@polydopamine–Pt composites and their application in hydrogenation reactions," *Journal of Materials Science,* vol. 51, no. 7, pp. 3643-3649, 2016, doi: https://doi.org/10.1007/s10853-015-9688-3.

[243] R. Ge *et al.*, "Fe3O4@polydopamine Composite Theranostic Superparticles Employing Preassembled Fe3O4 Nanoparticles as the Core," *ACS Applied Materials & Interfaces,* vol. 8, no. 35, pp. 22942-22952, 2016, doi: https://doi.org/10.1021/acsami.6b07997.

[244] M. F. C. Andrade, A. L. A. Parussulo, C. G. C. M. Netto, L. H. Andrade, and H. E. Toma, "Lipase immobilized on polydopamine-coated magnetite nanoparticles for biodiesel production from soybean oil," *Biofuel Research Journal,* vol. 3, no. 2, pp. 403-409, 2016, doi: https://doi.org/10.18331/brj2016.3.2.5.

[245] Y. Yu, J. G. Shapter, R. Popelka-Filcoff, J. W. Bennett, and A. V. Ellis, "Copper removal using bio-inspired polydopamine coated natural zeolites," *Journal of Hazardous Materials,* vol. 273, pp. 174-182, 2014, doi: https://doi.org/10.1016/j.jhazmat.2014.03.048.

[246] P. An *et al.*, "A bio-inspired polydopamine approach to preparation of gold-coated Fe3O4 core-shell nanoparticles: Synthesis, characterization and mechanism," *Nano,* vol. 08, no. 06, p. 1350061, 2013, doi: https://doi.org/10.1142/s1793292013500616.

[247] Z. Huang and H. K. Lee, "Study and comparison of polydopamine and its derived carbon decorated nanoparticles in the magnetic solid-phase extraction of estrogens," *Journal of Chromatography A,* vol. 1414, pp. 41-50, 2015, doi: https://doi.org/10.1016/j.chroma.2015.08.039.

[248] Q. Fang, S. Duan, J. Zhang, J. Li, and K. C. F. Leung, "Dual shelled Fe3O4/polydopamine hollow microspheres as an effective Eu(iii) adsorbent," *Journal*

of Materials Chemistry A, https://doi.org/10.1039/C6TA09968H vol. 5, no. 6, pp. 2947-2958, 2017, doi: 10.1039/C6TA09968H.

[249] J. Fu *et al.*, "Adsorption of methylene blue by a high-efficiency adsorbent (polydopamine microspheres): kinetics, isotherm, thermodynamics and mechanism analysis," *Chemical Engineering Journal,* vol. 259, pp. 53-61, 2015.

[250] K. Gupta and O. P. Khatri, "Fast and efficient adsorptive removal of organic dyes and active pharmaceutical ingredient by microporous carbon: Effect of molecular size and charge," *Chemical Engineering Journal,* vol. 378, p. 122218, 2019, doi: https://doi.org/10.1016/j.cej.2019.122218.

[251] D. Kalderis *et al.*, "Adsorption of polluting substances on activated carbons prepared from rice husk and sugarcane bagasse," *Chemical Engineering Journal,* vol. 144, no. 1, pp. 42-50, 2008, doi: https://doi.org/10.1016/j.cej.2008.01.007.

[252] W. Xiong, Q. Zhao, X. Li, and L. Wang, "Multifunctional Plasmonic Co-Doped Fe2O3@polydopamine-Au for Adsorption, Photocatalysis, and SERS-based Sensing," *Particle & Particle Systems Characterization,* vol. 33, no. 9, pp. 602-609, 2016, doi: https://doi.org/10.1002/ppsc.201600085.

[253] B. Ali Sabri, S. Meenaloshini, N. M. Abreeza, and A. N. Abed, "A review study on coupling agents used as ceramic fillers modifiers for dental applications," *Materials Today: Proceedings,* 2021, doi: https://doi.org/10.1016/j.matpr.2021.06.340.

[254] Y. Xie, Y. Zheng, J. Fan, Y. Wang, L. Yue, and N. Zhang, "Novel Electronic–Ionic Hybrid Conductive Composites for Multifunctional Flexible Bioelectrode Based on in Situ Synthesis of Poly(dopamine) on Bacterial Cellulose," *ACS Applied Materials & Interfaces,* vol. 10, no. 26, pp. 22692-22702, 2018, doi: https://doi.org/10.1021/acsami.8b05345.

[255] L. Feng, K.-Y. Wang, J. Willman, and H.-C. Zhou, "Hierarchy in Metal–Organic Frameworks," *ACS Central Science,* vol. 6, no. 3, pp. 359-367, 2020, doi: https://doi.org/10.1021/acscentsci.0c00158.

[256] Z. Wang, D. Wang, S. Zhang, L. Hu, and J. Jin, "Interfacial Design of Mixed Matrix Membranes for Improved Gas Separation Performance," *Advanced Materials,* vol. 28, no. 17, pp. 3399-3405, 2016, doi: https://doi.org/10.1002/adma.201504982.

[257] P. Pandey *et al.*, "Metal-organic frameworks-based triboelectric nanogenerator powered visible light communication system for wireless human-machine interactions," *Chemical Engineering Journal,* vol. 452, p. 139209, 2023, doi: https://doi.org/10.1016/j.cej.2022.139209.

[258] H. You, X. Zhang, D. Zhu, C. Yang, P. Chammingkwan, and T. Taniike, "Advantages of polydopamine coating in the design of ZIF-8-filled thin-film nanocomposite (TFN) membranes for desalination," *Colloids and Surfaces A: Physicochemical and Engineering Aspects,* vol. 629, p. 127492, 2021, doi: https://doi.org/10.1016/j.colsurfa.2021.127492.

[259] L. Ma, S. Huang, S. He, Z. Wang, and Z. Cheng, "Polydopamine-coated downconversion nanoparticle as an efficient dual-modal near-infrared-II fluorescence and photoacoustic contrast agent for non-invasive visualization of gastrointestinal tract in vivo," *Biosensors and Bioelectronics,* vol. 151, p. 112000, 2020, doi: https://doi.org/10.1016/j.bios.2019.112000.

[260] N. Rahman and P. Varshney, "Assessment of ampicillin removal efficiency from aqueous solution by polydopamine/zirconium(iv) iodate: optimization by response surface methodology," *RSC Advances,* https://doi.org/10.1039/D0RA02061C vol. 10, no. 34, pp. 20322-20337, 2020, doi: 10.1039/D0RA02061C.

[261] S. Qian and K. Sheng, "PLA toughened by bamboo cellulose nanowhiskers: Role of silane compatibilization on the PLA bionanocomposite properties," *Composites Science and Technology,* vol. 148, pp. 59-69, 2017, doi: https://doi.org/10.1016/j.compscitech.2017.05.020.

[262] H. Diao, Y. Si, A. Zhu, L. Ji, and H. Shi, "Surface modified nano-hydroxyapatite/poly(lactide acid) composite and its osteocyte compatibility," *Materials Science and Engineering: C,* vol. 32, no. 7, pp. 1796-1801, 2012, doi: https://doi.org/10.1016/j.msec.2012.04.065.

[263] L. Huang *et al.*, "Structural analyses of the bound rubber in silica-filled silicone rubber nanocomposites reveal mechanisms of filler-rubber interaction," *Composites Science and Technology,* vol. 233, p. 109905, 2023, doi: https://doi.org/10.1016/j.compscitech.2022.109905.

[264] Z. Chu, T. Zhao, L. Li, J. Fan, and Y. Qin, "Characterization of Antimicrobial Poly (Lactic Acid)/Nano-Composite Films with Silver and Zinc Oxide Nanoparticles," *Materials*, vol. 10, no. 6, doi: https://doi.org/10.3390/ma10060659.

[265] Y. Nie, J. Yang, Z. Liu, Z. Zhou, Y. Ming, and T. Hao, "Precursor formation and crystal nucleation in stretched polyethylene/carbon nanotube nanocomposites," *Polymer,* vol. 239, p. 124438, 2022, doi: https://doi.org/10.1016/j.polymer.2021.124438.

[266] E. Torino, R. Aruta, T. Sibillano, C. Giannini, and P. A. Netti, "Synthesis of semicrystalline nanocapsular structures obtained by Thermally Induced Phase Separation in nanoconfinement," *Scientific Reports,* vol. 6, no. 1, p. 32727, 2016, doi: https://doi.org/10.1038/srep32727.

[267] K. Molnar, J. Moczo, M. Murariu, P. Dubois, and B. Pukanszky, "Factors affecting the properties of PLA/CaSO4 composites: homogeneity and interactions," *Express*

Polymer Letters, vol. 3, no. 1, pp. 49-61, 2009, doi: https://doi.org/10.3144/expresspolymlett.2009.8.

[268] M. Taheri *et al.*, "Stability of ZIF-8 nanopowders in bacterial culture media and its implication for antibacterial properties," *Chemical Engineering Journal,* vol. 413, p. 127511, 2021, doi: https://doi.org/10.1016/j.cej.2020.127511.

[269] Y. Tu, C. Lei, F. Deng, Y. Chen, Y. Wang, and Z. Zhang, "Core–shell ZIF-8@polydopamine nanoparticles obtained by mitigating the polydopamine coating induced self-etching of MOFs: prototypical metal ion reservoirs for sticking to and killing bacteria," *New Journal of Chemistry,* 10.1039/D1NJ00461A vol. 45, no. 19, pp. 8701-8713, 2021, doi: https://doi.org/10.1039/D1NJ00461A.